Stony Brook University

A tale of two lipids: A role for compartmentalized generation of PIP_2 in *Yersinia* infection, & Characterization of a small molecule inhibitor of PA generation by Phospholipase D enzyme family members

A Dissertation Presented

by

Wenjuan Su

to

The Graduate School
In Partial fulfillment of the
Requirements
for the Degree of

Doctor of Philosophy

in

Molecular and Cellular Pharmacology

Stony Brook University

May 2009

Stony Brook University

The Graduate School

Wenjuan Su

We, the dissertation committee for the above candidate for the Doctor of Philosophy degree, hereby recommend the acceptance of this dissertation.

Michael A. Frohman, M.D., Ph.D.
Dissertation Director
Professor
Department of Pharmacological Sciences

James B. Bliska, Ph.D.
Chairperson of the Defense
Professor
Department of Molecular Genetics & Microbiology

Jeffrey Pessin, Ph.D.
Professor
Department of Molecular Pharmacology, Albert Einstein College of Medicine

Howard Crawford, Ph.D.
Associate Professor
Department of Pharmacological Sciences

Nicholas Carpino, Ph.D.
Assistant Professor
Department of Molecular Genetics & Microbiology

This dissertation is accepted by the Graduate School.

Lawrence Martin
Dean of the Graduate School

Abstract of the Dissertation

A tale of two lipids: A role for compartmentalized generation of PIP_2 in *Yersinia* infection, & Characterization of a small molecule inhibitor of PA generation by Phospholipase D enzyme family members

by

Wenjuan Su

Doctor of Philosophy

in

Molecular and Cellular Pharmacology

Stony Brook University

2009

Generation of the lipid phosphatidylinositol-4,5-bisphosphate (PIP_2) by PI4P-5-kinase (PIP5K) isoforms is critical for many cell biological processes triggered by signaling events. I found that PIP5K$\alpha^{-/-}$ mice exhibit diminished resistance to infection by *Yersinia pseudotuberculosis*, a model agent for pathogenic gram-negative bacteria. The susceptibility ensues from inadequately suppressed systemic bacterial replication at late infective stages concomitant with reduced serum IFNγ, a CD4 T-cell-produced cytokine that is key in the host response. Mechanistically underlying this outcome, the loss of PIP5Kα decreases macrophage phagocytosis when synergistically combined with action

of YopE, a *Yersinia*-produced toxin that lowers PIP_2 levels by deactivating Rac1, a key stimulator for all PIP5Ks. Moreover, MHC II cell-surface expression is lowered on macrophages and dendritic cells, as a result of *cis*-Golgi sequestration. Taken together, my finding reveals a PIP5Kα requirement in innate and adaptive immune responses for pathogens that subvert host defenses dependent on generation of PIP_2**.**

The signaling enzyme Phospholipase D (PLD) and the lipid second messenger it generates, phosphatidic acid (PA), are implicated in many cell biological processes including Ras activation, cell spreading, stress fiber formation, chemotaxis, and membrane vesicle trafficking. PLD production of PA is inhibited by the primary alcohol 1-butanol, which has thus been widely employed to identify PLD/PA-driven processes. However, 1-butanol does not always effectively reduce PA accumulation, and its use may result in PLD-independent deleterious effects. Consequently, identification of potent specific small molecule PLD inhibitors would be an important advance for the field. I examine one such here, denoted "FIPI", which was identified recently in an in vitro chemical screen for PLD2 inhibitors, and show that it rapidly blocks in vivo PA production with sub-nM potency. Moreover, FIPI inhibits PLD regulation of F-actin cytoskeleton reorganization, cell spreading, and chemotaxis, indicating potential utility for it as a therapeutic for autoimmunity and cancer metastasis.

This work is dedicated to my family.

Table of Contents

List of Abbreviations

ARF OR

ARF	ADP-ribosylation factor
APC	Antigen presenting cell
BMDM	Bone marrow-derived macrophage
BMDC	Bone marrow-derived dendritic cell
DAG	Diacylglycerol
FACS	Fluorescence-activated cell sorter
FAK	Focal adhension kinase
FYB	Fyn-binding protein
GAP	GTPase-activating proteins
GDI	GDP-dissociation inhibitors
GFP	Green fluorescent protein
GEF	Nucleotide-exchange factors
IFNγ	Inteferon γ
IPTG	Isopropyl-β-D-thiogalactopyranoside
Lyso-PA	Lysophosphatidic acid
M	Microfold
MHC	Major histocompatibility class
MLNs	Mesenteric lymph nodes
mTOR	Mammalian target of rapamycin
PA	Phosphatidic acid
PAP	Phosphatidic acid phosphatase

PC	Phosphatidylcholine
PH	Plekstrin homology
PI	Phosphatidylinositol
PI3K	Phosphoinositide 3-kinase
$PI4,5P_2$ or PIP_2	Phosphatidylinositol 4,5 bisphosphate
PIP4K	Phosphatidylinositol 5-phosphate 4-kinase
PIP5K	Phosphatidylinositol 4-phosphate 5-kinase
PKC	Protein kinase C
PLC	Phospholipase C
PLD	Phospholipase D
PM	Plasma membrane
PMA	Phorbol myristate acetate
PP	Peyer's patches
PX	Phox homology
RNAi	RNA interference
TNFα	Tumor necrosis factor-alpha
TLR	Toll-like receptor
Yop	Yersinia outer protein

List of Figures

Chapter 1

Chapter 2

Chapter 3

Acknowledgements

First of all, I would like to thank my advisor, Dr. Michael Frohman, for his support and encouragement. He gave me a lot of leeway in doing experiments. I can't remember how many times I showed the negative results to him, but he always sees the positive sides and encourages me to move forward. I do learn to be patient and optimistic in not only academic, but also real life.

I also want to thank current and former Frohman lab members for help me carry out my thesis project. Without their help, I would not accomplish my project. Especially, Dr. Guangwei Du was a great teacher and friend. We had a lot of thoughtful discussions, which benefits me even in the future. All other members (Winnie, Phyllis, Mary, Akua, Yeku, Yelena, Alex, Krishna, Xiaoxue, Qun, Qin, Junzhu, Liz, Xiao, Ping, Gary) are also cordially achnowledged. They made my graduate student life more joyful.

I am indebted to Yue Zhang, a postdoctor in Dr. James Bliska's lab. She taught me every experiment of Yersinia, and put a lot of input into PIP5K project. Without her help, there is no way to finish my Yersinia project.

I am grateful to my committee members: Drs. James Bliska, Howard Crawford, Jeffrey Pessin, and Nicholas Carpino. Their support and suggestions topped off my project.

I appreciate the help form all the pharm staff and students who make our program like a big family. Thank you all!

I can't thank enough my beer buddies. They got me to forget the loneliness inflicted on me living in a foreign country. Hongling Zhao, Yan Song, Xiuquan Shi, Ruixue Wang, Yiwei Gao, Drs, Jie Wang, Hui Pan and Eugene lee. Thank you, guys!

I gratefully acknowledge professor in Fudan university and Shanghai institute for biological sciences, China: Drs. Lan Ma, Gang Pei, and Lin Lu. They open the door for me to biomedical research, in which I will pursue my career.

Finally, I deeply appreciate the unyielding love and support form my families, specially my parents and husband, without them I am not sure I would get where I am now.

Chapter 1

Introduction

1. 1 Objective and specific aims

The overall objective of this thesis is to study the function of two lipid-modifying enzymes: phosphatidylinositol 4-phosphate 5-kinase α and phospholipase D (PLD).

PIP5K, the major enzyme responsible for the generation of PIP_2, has three isoforms designated α, β, and γ. PIP5K and PIP_2 have been implicated in many cellular processes including vesicle trafficking, exocytosis, cell motility, and cytoskeleton reorganization (Santarius et al., 2006). PIP5Kβ was reported to be involved in Fcγ receptor-mediated phagocytosis (Coppolino et al., 2002). Overexpression of the catalytically inactive mutant of PIP5Kβ diminished PIP_2 production and the F-actin accumulation at the phagosomal cup, resulting in decreased phagocytosis. PIP5Kα and β also localize to the phagosomal cup during the uptake of *Yersinia (Y.) pseudotuberculosis* (Wong and Isberg, 2003), which is a gram-negative enteropathogenic bacterium. In COS cells, overexpression of PIP5Kα can bypass the inhibition of Rac1 activity by the bacterial toxin YopE, a Rho GAP protein. However, the role of PIP5K in the uptake of *Y. pseudotuberculosis* in professional phagocytes such as macrophages has not been clarified, and the physiological role of PIP5Kα in host defense is largely unknown.

PIP5Kα knockout mice were generated by our collaborator, and they found that PIP5Kα negatively regulates anaphylaxis caused by FcεRI-mediated responses of mast

cells (Sasaki et al., 2005). Taking advantage of this mouse model, the first part of my thesis was to examine the physiological role of PIP5Kα in *Y. pseudotuberculosis* infection.

The second lipid-modifying enzyme studied here is phospholipase D (PLD). Mammalian PLD1 and PLD2 perform a transphosphatidylation reaction using water to hydrolyze phosphatidylcholine (PC) to generate PA, which is a key signaling lipid. PLD has been shown to be involved in many biological processes and diseases including phagocytosis, chemotaxis and inflammatory diseases; exocytosis, insulin secretion; survival, metastasis and tumorigenesis (Huang and Frohman, 2007). Thus, PLD is an attractive therapeutic target. Several inhibitors of PLD activity have been described including 1-butanol, ceramide (Vitale et al., 2001), neomycin (Huang et al., 1999), and natural products (Garcia et al., 2008), but these compounds work indirectly to inhibit PLD activity, or have many other effects on signaling pathways that complicate their use and interpretation. Identification of small molecule inhibitor is a big advance in the field. Such one, denoted "FIPI", was characterized in the second part of my thesis.

The specific aims of this thesis were (1) to examine the role of PIP5Kα in the uptake of *Y. pseudotuberculosis* using bone marrow-derived macrophages (BMDMs) from wild type (wt) and PIP5K$\alpha^{-/-}$ mice infected with wt bacteria or Yop inactive mutants; (2) to determine the physiological role of PIP5Kα in host defense against *Y. pseudotuberculosis* using oral infection mouse model; (3) to dissect the cellular mechanism of how PIP5Kα acts as a protective factor in host defense using the cell culture system; and (4) to characterize pharmacological properties of the small molecule PLD inhibitor FIPI and identify its potential applications.

1. 2 An overview of phosphatidylinositol 4-phosphate 5-kinase (PIP5K)

PIP_2 has a long established role as a precursor of signaling molecules including inositol 1,4,5-triphosphate ($InsP_3$) and diaglycerol (DAG) generated after hydrolysis of PIP_2 by phospholipases, and PIP_3 generated by the phosphorylation of PIP_2 by phosphoinositide 3-kinases (PI3K) (Watt et al., 2002). PIP_2 is now recognized to play more direct roles as a key signaling and targeting lipid in regulation of diverse cellular activities, including gating of ion channels (Hilgemann and Ball, 1996; Suh and Hille, 2005), exocytosis (Aikawa and Martin, 2003; Gong et al., 2005), cytoskeleton reorganization, cell motility (Golub and Caroni, 2005; Insall and Weiner, 2001), vesicular trafficking (Downes et al., 2005), and apoptosis (Halstead et al., 2006; Mejillano et al., 2001).

PIP_2 is particularly abundant at the plasma membrane (PM) and proposed to be a PM marker, distinguishing the PM from other organelles that are highly enriched in other types of phosphoinositides (Di Paolo and De Camilli, 2006; Roth, 2004). At the PM, PIP_2 is the hub for the docking of multi-components of signaling pathways and the regulation of cytoskeleton dynamics. By doing so, PIP_2 becomes a master regulator in receptor-related signaling. In addition, it also appears as smaller pools in intracellular membranes including the Golgi, endosomes and the endoplasmic reticulum (Watt et al., 2002). Except that PIP_2 may be important for the maintenance of Golgi integrity, the role of PIP_2 at those organelles is far less studied.

PIP_2 is generated from phosphatidylinositol monophosphates (PIPs) by two distinct enzymes: the phosphatidylinositol 4-phosphate 5 kinases (PIP5Ks) and the

phosphatidylinositol 5-phosphate 4 kinases (PIP4Ks). These two types of PIP kinases recognize different substrates: PI4P versus PI5P. As PI4P is much more abundant than PI5P (Toker and Cantley, 1997), PIP5Ks are likely to be the major source of PIP_2, which has been confirmed by pulse-labeling studies (Stephens et al., 1991). PIP5K catalyzes the phosphorylation of PI4P at the D5 position of the inositol ring to generate PIP_2. To date, three mammalian PIP5K isoforms, α, β, and γ, and three splicing variants of the γ isoforms, γ635, γ661, and γ 687, have been identified (Giudici et al., 2004). It is important to note that human and mouse PIP5K have different nomenclature: mPIP5Kα is hPIP5Kβ; mPIP5Kβ is hPIP5Kα.

Although PIP5K isoforms share virtually identical activation loops, they have specific and distinct intracellular localizations (Doughman et al., 2003b). PIP5Kγ661, which specifically interacts with a component of focal adhesion assembly, locates at the focal adhesion (Di Paolo et al., 2002; Ling et al., 2002). However, the subcellular distribution of the other two isoforms is controversial. Overexpressed PIP5Kα and β localize in the cytosol in HeLa cells (Honda et al., 1999). Endogenous hPIP5Kα (mPIP5Kβ) locates in the nuclei and cytosol while hPIP5Kβ(mPIP5Kα) mainly locates to vesicular structure in the perinuclear region (Doughman et al., 2003a)). Furthermore, PIP5Kα and β appear to translocate to the limited area of the plasma membrane when cells are activated (Coppolino et al., 2002; Doughman et al., 2003b; Honda et al., 1999), which suggests that the intracellular location of PIP5K and local production of PIP_2 by PIP5K is dynamically regulated by upstream signaling pathways.

There is now overwhelming evidence suggesting that some pools of PIP_2 are generated in a spatially and temporally regulated manner (Brown et al., 2001; Critchley,

2005). In response to upstream signaling stimulation, PIP5K activity can be regulated by small GTPases, phosphatic acid and phosphorylation (Doughman et al., 2003a). Among these, small G-proteins as well as their regulators are likely to be important factors determining the localization of PIP5K and regulating their activities (Santarius et al., 2006). The super-family of small G-protein can be classified into five subfamilies: Ras, Rho, Arf (ADP-ribosylation factor), Rab and Ran. They are shuttled between membranes and cytosol, and act as molecular switches to spatially and temporally modulate a variety of cellular functions through diverse signaling networks. Their ability to modulate downstream signaling process depends on the tight regulation of their activation and inhibition through interactions with regulators including guanine nucleotide-exchange factors (GEFs), GTPase-activating proteins (GAPs), as well as GDP-dissociation inhibitors (GDIs).

Individual PIP5K isoforms have been identified as downstream effectors of small G-protein to generate PIP_2 at specific cellular sites. Rho and Rac have been shown to physically interact with PIP5K regardless of whether they are in active, GTP-bound form or not (Chatah and Abrams, 2001). However, only GTP-bound form of RhoA, Rac1, and Arf6 has the capacity to activate PIP5K. Both Rac and Rho's GTP forms have been shown to mediate translocation and activation of PIP5Kα upon thrombin receptor activation (Yang et al., 2004). Under some circumstances, different small G-proteins coordinate together to manipulate localization and activity of PIP5K. In COS cells challenged with *Y. pseudotuberculosis*, Rac1 recruits PIP5Kα to nascent phagosomal cup and then Arf6 activates PIP5Kα there (Wong and Isberg, 2003).

The majority of studies of PIP5K were done in cell culture systems; however, the significance of PIP_2/PIP5K in vivo has not been well studied. Recently, with isoform-specific knockout mice, the physiological role of each isoform of PIP5K has begun to be defined. PIP5Kγ is the major isoform in the brain. Mice lacking the PIP5Kγ gene are postnatal lethal due to synapse transmission defects. PIP5K$\alpha^{-/-}$ mice show higher allergic reaction and histamine release upon Fcε receptor activation, suggesting that PIP5Kα is a negative regulator of anaphylaxis. Platelets lacking PIP5Kβ exhibited impaired aggregation accompanied by disaggregation and failed to form arterial thrombi properly in vivo due to the deficiency in PIP_2 synthesis and IP_3 formation (Wang et al., 2008). The physiological role of PIP5K will be further clarified by using these isoform-specific knockout mice.

1. 3 An overview of host defense against *Yersinia*

Yersinia is a gram-negative extracellular bacterium, and three *Yersinia* species including *Y. pseudotuberculosis, Y. endocolitica and Y. pestis* are pathogens for humans. *Y. pseudotuberculosis* and *Y. enterocolitica* are food-borne enteropathogenic bacteria and typically cause self-limiting infections restricted to the intestinal tract and intestinal lymphoid system such as Peyer's patches (PPs) and mesenteric lymph nodes (MLNs) (Carniel, 2002). In certain predisposed patients (e. g. with iron overload states), a systemic infection with focal abscess formation can develop (Abbott et al., 1986). A similar disease appears in an oral mouse infection model, which is widely used to study the pathogensis of enteropathogenic *Yersiniae* and host defense against them. *Y. pestis*

displays a different mode of transmission by either a flea vector or the aerosol route, and causes plague, an often fatal disease (Brubaker, 2003).

In several animal models of intestinal infection e.g., rodent or pig, the enteropathogenic *Yersinia* initially infects terminal ileum and cecum. Bacteria begin to colonize PPs within several hours. The bacteria specifically associate with microfold (M) cells, which are located in the follicle-associated epithelia. Invasin expressed by *Yersinia* interacts with β1 integrin, resulting in efficient bacterial attachment and entry into M cells (Viboud and Bliska, 2005). Once internalized by M cells, *Yersinia* is transported across the epithelial barrier and enters PPs. Underneath the follicle-associated epithelia, there are dendritic cells, macrophages, and lymphocytes. The possibility has been proposed that internalized bacteria are transported within phagocytes such as macrophages or dendritic cells to MLNs. Highly virulent stains of enteropathogenic *Yersinia* also spread systemically to colonize in spleen and liver, which can cause lethal infections in rodents. The route of this dissemination is not clear. One possibility is via the blood stream since this dissemination appears to bypass colonization of the PPs. This process may involve phagocytes that uptake bacteria in the intestine and carry them to spleen and liver through blood stream. In PPs, MLNs, spleen, or liver, the bacteria replicate extracellularly and form microabscesses. Within these lesions, the bacteria form microcolonies and are resistant to phagocytosis.

When faced with a bacterial pathogen such as *Y. pseudotuberculosis*, the mammalian host raises a series of defense responses involving both the innate and adaptive immune system. During early stage of infection, innate host defenses such as polymorphonuclear leukocytes (PMNs), macrophages, and natural killer (NK) cells control *Yersinia* infection

(Autenrieth and Firsching, 1996; Carter et al., 1979; Kerschen et al., 2004; Lian et al., 1987). Macrophages and neutrophils, professional phagocytes, directly attack the invading pathogen, mediate secretion of pro-inflammatory cytokines and mount a protective inflammatory response. Eventually, however, a strong adaptive immune response is needed to overcome *Yersinia* infection. Specific antibodies (Igwe et al., 1999; Vogel et al., 1993) and IFNγ-producing $CD4^+$ and $CD8^+$ T cells (Autenrieth et al., 1994; Autenrieth et al., 1992; Autenrieth et al., 1993) are known to mediate protection against *Yersinia* infection, and this has been shown in adoptive transfer experiments (Autenrieth et al., 1992; Falgarone et al., 1999).

On the other hand, to overcome host defense mechanisms, *Yersiniae* translocate a set of Yops into immune cells by a type III secretion system (T3SS) to inhibit the innate and adaptive immune responses. The major anti-host determinants are encoded by a 70-kb virulence plasmid (pYV), including protein microinjection apparatus T3SS as well as six translocated effector proteins (YopH, YopO/YpkA, YopP/J, YopE, YopM, and YopT) (Fig 1. 2) (Heesemann et al., 2006; Viboud and Bliska, 2005). At least 4 of them (YopE, YopH, YopT, and YopO/YpkA are involved in inhibiting phagoyctosis of *Yersiniae* by disrupting cytoskeleton (Bliska and Black, 1995; Fallman et al., 1995; Rosqvist et al., 1990). YopE is a GTPase-activating protein that targets mainly on Rac GTPase, thereby affecting the actin cytoskeleton reorganization (Aepfelbacher and Heesemann, 2001; Black and Bliska, 2000; Rosqvist et al., 1991), which results in inhibition of phagocytosis. Additionally, YopE functions to counteract pro-inflammatory cytokine production (Schotte et al., 2004). YopH is a phosphotyrosine phosphatase (Zhang et al., 1992) that dephosphorylates focal adhesion kinase (Fak), paxillin, Fyn-binding protein

(FYB), and p130, therefore disrupting focal adhesions (Andersson et al., 1996; Black et al., 1998; Hamid et al., 1999; Persson et al., 1997) and suppressing the production of reactive oxygen intermediates by macrophages and PMNs (Bliska and Black, 1995; Persson et al., 1999). In addition to playing a part in bacterial evasion, YopH also contributes to subvent the adaptive immune response by impairing T- and B-cell activation (Alonso et al., 2004; Yao et al., 1999). YopT is a cysterine protease that preferentially inactivates RhoA GTPase by cleavage of the C-terminal geranylgeranyl-cyteine residue (Shao et al., 2002; Zumbihl et al., 1999). Besides paralyzing phagocytosis, Yops also inhibit the pro-inflammatory response elicited by infected cells. For example, YopJ (YopP in *Y. entercolitica*) inhibits TNFα and IL-8 release mainly by inhibiting the NFκB dissociation from IκB and NFκB translocation to the nucleus (Boland and Cornelis, 1998; Denecker et al., 2001; Denecker et al., 2002; Orth et al., 1999; Palmer et al., 1998; Schesser et al., 1998). Additionally, YopJ inhibits at least three MAP kinase pathways (ERK1/2, JNK1, and p38) that are involved in the immune response against *Yersinia*. Inhibition of MAPK and NFκB pathways by YopJ contribute to the ability of *Yersinia* to induce apoptosis of macrophages and dendritic cells (Erfurth et al., 2004; Mills et al., 1997; Monack et al., 1998).

Besides the cellular role of Yops, the role of Yops on the virulence of *Yersiniae* has also been extensively studied in the mouse infection model. A YopH mutant of *Y. pseudotuberculosis* specially fails to colonize the mesenteric lymph nodes, but YopE and YopO mutants showed only minor defects in persistence in intestinal and lymph tissues while most of mice recovered from infection (Logsdon and Mecsas, 2003). YopT itself is not required for virulence, but it can promote virulence in the absence of YopE (Viboud

et al., 2006). YpkA and YopJ make minor contributions to virulence in the oral mouse infection model (Galyov et al., 1994)

1. 4 An overview of the phospholipase D (PLD) superfamily

PLD was defined in 1947 by Hanahan and Chaikoff in carrot extracts as a phospholipids-specific phosphodiesterase that hydrolyzed phosphatidylcholine (PtdCho) to generate phosphatidic acid (PA or PtdOH) and choline. More generally, PLD is now viewed as a transphosphatidylase (Fig. 1. 3) that can use water for hydrolysis or can use glycerol or short-chain primary alcohols such as ethanol or 1-butanol to generate phosphatidylalcohol products. Phosphatidylalcohols are not normally found in biological membranes, are relatively inert with respect to the functions mediated by PtdOH, and are relatively metabolically stable in comparison to PtdOH. Hence, eliciting phosphatidyl-butanol (Ptd-but) formation by exposing cells to low levels of 1-butanol has become widely used as a convenient means to record and assay PLD activity. Moreover, addition of high levels of alcohol has been used as a means to divert PLD away from producing PtdOH, and thus as way to inhibit PLD-mediated pathways, with the caveat that the amounts of alcohol required to fully block production of PtdOH by PLDalso affect some other vital signaling pathways such as production of phosphoinositides (Skippen et al., 2002b), promotion of adipocyte differentiation (Emoto et al., 2000), and modulation of p42/44 mitogen-activated protein kinase signaling in hepatocytes (Aroor et al., 2002; Pannequin et al., 2007).

Members of the PLD superfamily that extends from virus, bacteria to human are defined by the presence of a HKD catalytic site (formally known as $HxK(x)_4D(x)_6GSxN$). Although the classic definition of the family involves hydrolysis of

PtdCho to generate PtdOH and choline, some of the family members possess quite divergent activities (Liscovitch et al., 1985), including ones that use cardiolipin (Choi et al., 2006a) or other phospholipids as substrates, or use the phosphatidyltransferase capacity to synthesize new lipids (cardiolipin synthase and phosphatidylserine synthase (Koonin, 1996; Ponting and Kerr, 1996; Sung et al., 1997b). The superfamily also includes endonucleases (Nuc) that use the phospodiesterase activity to cleave the backbone of DNA (Zhao et al., 1997), pox virus envelope proteins and their mammalian counterparts that are required for virion formation through an unknown biochemical mechanism (Sung et al., 1997b), and the protein Tdp1, which resolves stalled Topoisomerase-DNA complexes involving covalent links between the protein and the DNA by again using the phosphodiesterase activity to sever them (Interthal et al., 2001).

In addition to the catalytic motif, other common structural domains are found in eukaryotic PLD proteins (Frohman et al., 1999). PX domain has been reported to bind to PtdIns(3,4,5)P_3 as determined by the association of PLD1 with lipid rafts, which facilitates transit of the enzyme to endosomes after its translocation to the plasma membrane upon agonist stimulation (Du et al., 2003). PH domains can bind PtdIns (4,5)P_2, and the PLD1 PH domain has been reported to exhibit binding to phospholipids; however, as described below, the stimulation of PLD by PtdIns(4,5)P_2 is mediated by a different region of the protein, and deletion of the PH domain does not impair its intrinsic enzymatic activity (Sung et al., 1999a; Sung et al., 1999b). PX domains are found in many signaling molecules and mediate protein-protein interactions or binding to phosphatidylinositol phosphates (Xu et al., 2001). In other assays, affinity for PtdIns(5)P (Du et al., 2003) and binding to the EGF receptor (Lee et al., 2006) have also been

observed. The PX domain may play a role to facilitate internalization of PLD1 from the plasma membrane (Du et al., 2003). PLD1 and PLD2 activation are highly dependent on PtdIns(4,5)P_2. The activation requires a sequence of conserved basic and aromatic amino acids. Such a polybasic motif mediates the interaction of this and other proteins with negatively charged lipids (Morris, 2007; Stace and Ktistakis, 2006). The affinity for PtdIns(4,5)P_2 may additionally facilitate the translocation of PLD to the plasma membrane surface (Du et al., 2003).

Activation of classical mammalian PLDs in cells is triggered by a wide range of stimuli that signal through G-protein coupled receptors and receptor tyrosine kinases (Besterman et al., 1986; Bocckino et al., 1987; Daniel et al., 1986; Oude Weernink et al., 2007; Pai et al., 1988). Although there are reports suggesting that PLD can in some cases interact directly with the receptors (Lee et al., 2006) or G-proteins (Preininger et al., 2006), in general the activation mechanism is thought to be downstream of protein kinase C (PKC) activation and mobilization of small GTPases of the Rho and Arf families (Brown et al., 1995; Brown et al., 1993; Jenkins and Frohman, 2005; McDermott et al., 2004). However, exactly how PLD activation by these cytosolic factors is coordinated with receptor stimulation is complex, and it remains unclear despite extensive efforts by many groups.

PA, the product of PLD, is an important second messenger and functions as a signal transducer, lipid anchor, and fusogenic lipid. In addition to acting as an intracellular messenger, PLD-generated PA can also undergo conversion to other bioactive lipids. For example, PA dephosphorylation by phosphatidic acid phosphohydrolases, is a significant route for generation of diacylglycerol (DAG) in stimulated cells (Brindley and

Waggoner, 1996; Sciorra and Morris, 1999). PA can also be deacylated by phospholipase A to form the cell surface receptor active compound lysoPA, and PA may be an important source of arachidonic acid for the synthesis of prostaglandins and leukotrenes.

Mammalian PLD and its product PA are now widely recognized as key signaling molecules that have been implicated in a number of cellular processes including Golgi budding, cell spreading, mitochondria dynamics, facilitating exocytic trafficking, vesicle fusion to target membrane, EGFR endocytosis (Jenkins and Frohman, 2005). Recently, more evidence implicates the role of PLD in tumorigenesis. Elevated PLD activity is found in many types of human cancer including breast, colon, gastric, and kidney (Foster DA, 2007). PLD2 point mutations and deletion are found in breast cancer (Wood LD et al., 2007). Increased PLD activity can provide an alternative survival signal via activating mTOR, which is parallel to PI3-kinase/Akt pathway (Chen et al., 2005; Chen et al., 2003). PLD2 is recently revealed to play an unexpected role in Ras activation in response to EGF stimulation (Zhao et al., 2007), in which the PLD-generated PA acts upstream of Ras by recruiting its immediate activator, Sos, to translocate to the plasma membrane. Moreover, the ability of the MDA-MB-231 cells to migrate and invade matrigel is dependent on PLD and mTOR (Zheng et al., 2006), suggesting that PLD contributes to cell migration and invasiveness. These observations reinforce that PLD is a promising target and inhibiting PLD activity is clinically attractive.

Fig. 1. 1. The regulation of PIP5K by small GTPases.
Upon stimulation of cell surface receptors, GTP-bound small GTPases can regulate the subcellular localization of PIP5K and activate it to generate PIP_2 locally. Regulation of PIP5K by Arf and Rho family GTPases is mainly involved in the regulation of vesicle trafficking and cytoskeleton reorganization. PIP_2 can activate ARF-GAP to accelerate inactivation of Arf, which indicates a negative feedback.

Fig.1.1

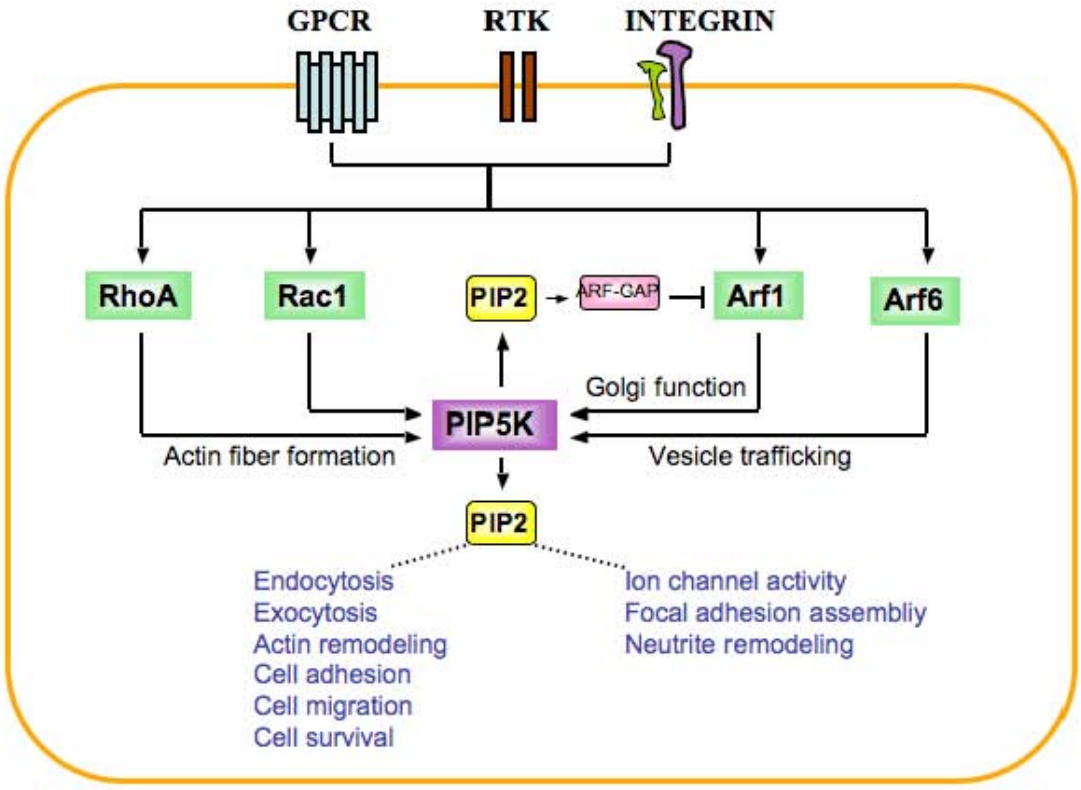
GPCR
RTK
INTEGRIN
RhoA
Rac1
PIP2
ARF-GAP
Arf1
Arf6
Golgi function
PIP5K
Actin fiber formation
Vesicle trafficking
PIP2
Endocytosis
Exocytosis
Actin remodeling
Cell adhesion
Cell migration
Cell survival
Ion channel activity
Focal adhesion assembliy
Neutrite remodeling

Fig. 1. 2. The anti-defense role of Yops (Heesemann et al., 2006)

Signaling elicited by *Yersinia* infection is most likely initiated by αβ1 integrins and TLR-2 and -4. As shown, Yop effectors inhibited three major signaling pathways at different steps. YopH, a protein phosphatase, blocks the focal adhesion complex (FAC) formation. αβ1 integrin- and TLR-2-activation also leads to activation of the GTPase Rho and Rac, which can be inactivated by YopE, a GAP protein, or the cysteine protease YopT that cleaves the C-terminal geranylgeranylated cysteine methyl ester. Inactivation of Rho and Rac abrogates the cytoskeleton rearrangement required for phagocytosis, cell migration and the oxidative burst. YopP (YopJ in *Y. pseudotuberculosis*) binds to MAP kinase and IκB kinase β, and thus blocks the MAPK- and NFκB-signal transduction pathways, leading to downregulating the inflammatory and anti-apoptosis responses.

Fig. 1. 2.

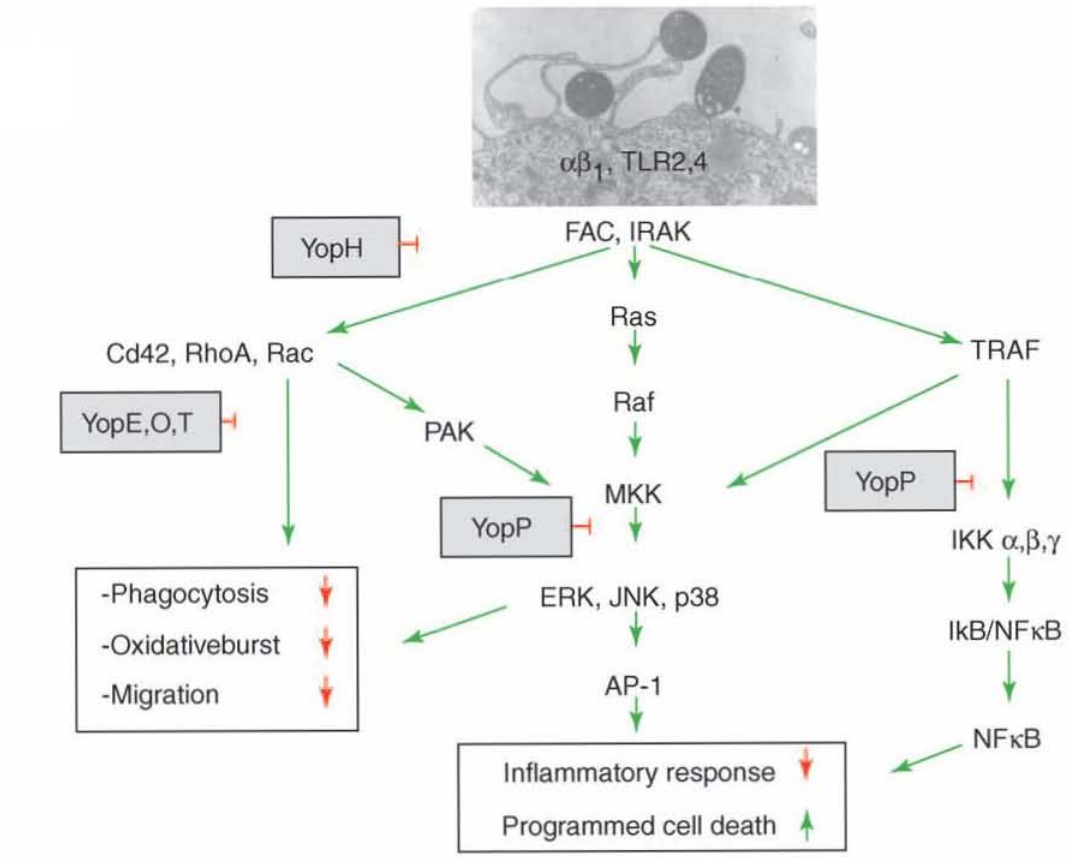

Adapted from Curr. Opin. MIcrobiol. 2006

Fig. 1. 3. Phospholipid metabolism by PLD (Jenkins and Frohman, 2005).
Phospholipase D (PLD) hydrolyzes the phosphodiester bond between the choline head group and lipid backbone of phosphatidylcholine (PC) to release the pleiotropic lipid phosphatidic acid (PA). PA can be further converted to lyso-phospatidic acid (Lyso-PA) by phospholipase A or to diacylglycerol (DAG) by phosphatidic acid phosphatase. Lyso-PA and DAG can also be metabolized to PA by lyso-phosphatidic acid acyltransferase (LPAAT) and diacylglycerol kinase, respectively.

Fig. 1. 3

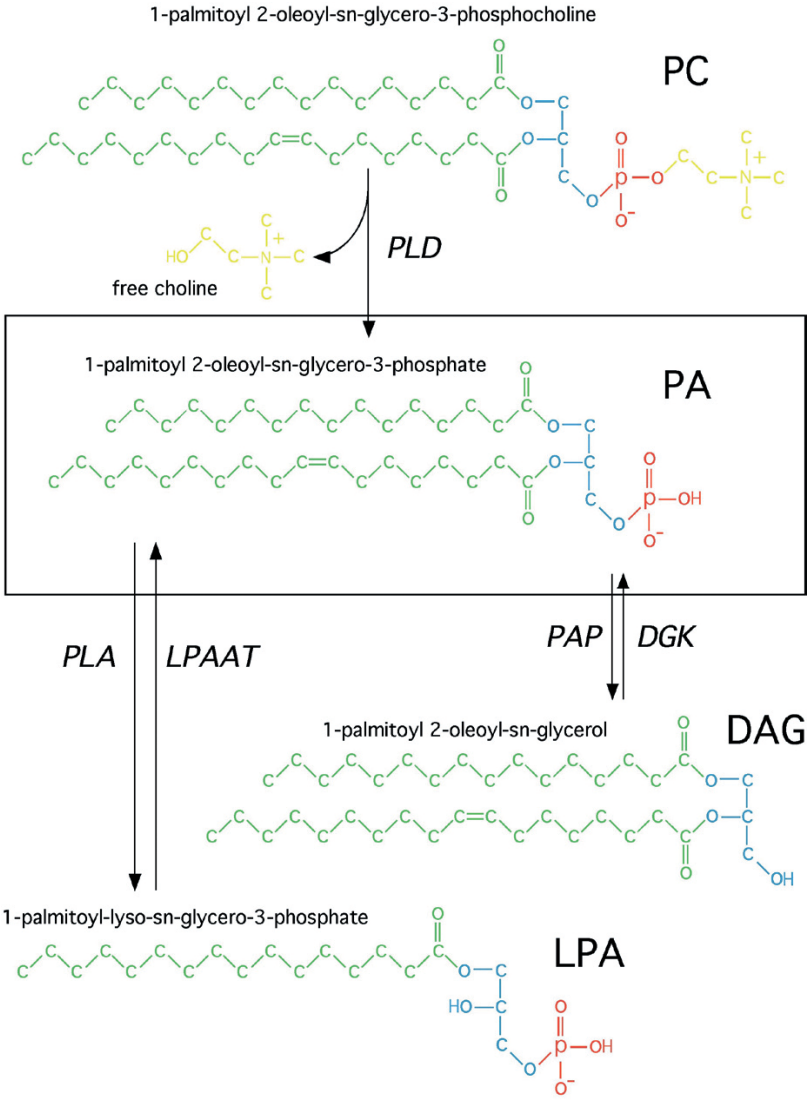

Adapted from Cell. Mol. Life Sic. 2005

Chapter 2

The role of PIP5Kα in *Y. pseudotuberculosis* infection

The majority of this chapter has been submitted. Most data are generated by W. Su with the help from Y. Zhang, J. Bliska, and P. Mena. PIP5K$\alpha^{-/-}$ mouse was a generous gift from Y. Kanaho.

2. 1 Summary

Phagocytosis is important in innate immune defense and also plays a vital role in the initiation of the adaptive immune response. Phosphatidylinositol 4-phosphate 5-kinase (PIP5K), the major enzyme responsible for phosphatidylinositol(4,5)P_2 (PIP_2) production, has been showed to be involved in many cell biological processes including phagocytosis. Here, I describe the involvement of the α isoform of PIP5K in host defense against *Y. pseudotuberculosis*. PIP5K$\alpha^{-/-}$ macrophages show reduced phagocytosis of *Y. pseudotuberculosis* and this reduction depends on Rac1 inactivation by the bacterial toxin YopE. PIP5K$\alpha^{-/-}$ mice are more sensitive to *Y. pseudotuberculosis* infection and also have lower serum levels of the cytokine interferon γ (IFNγ) during later stage of infection, with concomitantly higher bacterial splenic colonization levels. Unexpectedly, PIP5K$\alpha^{-/-}$ dendritic cells and macrophages have defects on the surface expression of MHC class II molecules, suggesting that in PIP5K$\alpha^{-/-}$ mice, the $CD4^+$ T cells may not be fully activated due to insufficient antigen presentation. Furthermore, the immunostaining results show that the defect in MHC class II presentation is at least partially caused by a trafficking problem. Contrast to what is in wt BMDMs, MHC class II is accumulated in

the *cis*-Golgi network, and inefficiently goes to the *trans*-Golgi network in PIP5K$\alpha^{-/-}$ BMDMs. Taken together, our findings reveal that a superficially redundant capacity for PIP_2 generation by multiple PIP5K isoforms is in fact a necessity for innate and adaptive immune responses in the face of bacterial invasion mechanisms that subvert host defenses.

2. 1 Introduction

Infection by *Y. pseudotuberculosis,* a gram-negative pathogen, typically occurs through consuming contaminated food products. The infection is frequently characterized by self-limited local proliferation of the bacteria in the small intestine and the associated Peyer's patches and mesenteric lymph nodes (MLNs), resulting in intestinal inflammation that can be misdiagnosed as appendicitis (Naktin and Beavis, 1999). However, enteric *Yersinia* can also disseminate systemically in patients with hemochromatosis (El-Maraghi and Mair, 1979). Host innate immune responses mediated by neutrophils, macrophages and Natural Killer (NK) cells constitute the initial line of defense. However, an adaptive immune response involving T-cell activation and production of the cytokine IFNγ is ultimately required for clearance of disseminated *Yersinia* (Autenrieth and Heesemann, 1992; Parent et al., 2006).

Phagocytosis is a key step of the innate host defense against bacterial infection. Neutrophils constitute the primary host defense cell responsible for the phagocytosis, but macrophages also play a vital role. Uptake of *Y. pseudotuberculosis* by epithelial cells is mediated by direct or indirect interaction of the bacteria with β1 integrin; the phagocytic event then proceeds via a signaling pathway that involves many cellular components including the small GTPase Rac1 (Alrutz et al., 2001; Black and Bliska, 2000; Wong and Isberg, 2005a), which triggers changes in the actin cytoskeleton, secretion, and gene transcription through different downstream effectors. Once bound to the macrophage surface, however, *Y. pseudotuberculosis* attempts to block internalization by injecting a set of proteins known as YopE, T and H into the macrophage. YopE and YopT block or restrict Rac1 function, respectively (Wong and Isberg, 2005b). YopE, which is thought to

be the more powerful factor (Viboud et al., 2006), functions as a GTPase-activating protein to inactivate Rac1-GTP, converting it to Rac1-GDP (Black and Bliska, 2000).

One of the key effector functions of activated Rac1 is to recruit the enzyme Type I phosphatidylinositol 4-phosphate 5-kinase (PIP5K) to sites of phagocytosis and stimulate it to generate the lipid phosphatidylinositol (4,5)P_2 (PIP_2) (Santarius et al., 2006). PIP_2 facilitates many cellular processes including phagocytosis (Botelho et al., 2000; Pizarro-Cerda and Cossart, 2004; Scott et al., 2005; Wong and Isberg, 2003), Toll-like receptor signaling (Kagan and Medzhitov, 2006), nucleation of actin filaments (Niggli, 2005), and regulated exocytosis (Haucke and Di Paolo, 2007).

The PIP5K enzyme family consists of three different isoforms, α, β, and γ (Doughman et al., 2003a). The mouse and human α and β isoforms are named reciprocally. Mouse PIP5Kβ (human PIP5Kα) has been reported to regulate Fcγ receptor-mediated phagocytosis by producing PIP_2 on the phagosomal cup to trigger local actin remodeling (Coppolino et al., 2002), as demonstrated using overexpression of a kinase-dead isoform to competitively inhibit the wild-type endogenous isoform (this inactive isoform most likely competitively inhibits both the α and β isoforms due to sequence similarity). Mouse PIP5Kα (human PIP5Kβ) also localizes to the phagosomal cup and overexpression of it can bypass the inhibition of *Y. pseudotuberculosis* uptake by bacterial toxin YopE(Wong and Isberg, 2003). Study of the α and β isoforms in other systems has suggested that there may be partial overlap in their function, since both localize to the plasma membrane (Padron et al., 2003) and stimulate actin comet tails when overexpressed (Rozelle et al., 2000).

PIP5K enzyme activity can also be recruited and stimulated by the small GTPase ARF6 (Honda et al., 1999), and the inhibition of *Y. pseudotuberculosis* uptake caused by YopE inhibition of Rac1 can be bypassed by increasing the expression level of ARF6 or mouse PIP5Kα. It has been proposed that Rac1 is primarily responsible for the recruitment of PIP5Kα to the phagocytic cup and ARF6 primarily responsible for the activation of PIP5Kα based on overexpression studies (Wong and Isberg, 2003), but the exact and potentially overlapping roles of the GTPases remains incompletely defined.

Taken together, these findings suggest a process defined by some level of redundancy, in that there are three PIP5K isoforms (α, β and γ) that can generate PIP_2 at the phagosomal cup during *Y. pseudotuberculosis* internalization, and two pathways (ARF6 and Rac1) through which the PIP5Ks can potentially be recruited and stimulated.

In this report, we examine the host response to *Y. pseudotuberculosis* infection using mice deficient in PIP5Kα (human PIP5Kβ). Mast cells in PIP5Kα-deficient mice exhibit only modest (<10%) decreases in cellular PIP_2 levels, but exhibit anaphylaxis secondary to exaggerated levels of cytokine release after Fcε receptor cross-linking (Sasaki et al., 2005), caused potentially by increases in Fcε receptor signaling or by decreased levels of cortical actin. Extending the earlier reports that employed overexpression of dominant-negative kinase-dead isoforms to competitively inhibit both PIP5Kα and PIP5Kβ simultaneously, we demonstrate here that isolated PIP5Kα-deficiency suffices to decrease *Y. pseudotuberculosis* phagocytosis by macrophages, but only when the bacteria expresses the YopE toxin that inactivates Rac1, providing new insights in the nature of redundancy in this process. Moreover, we report that the PIP5Ka-deficient mice exhibit

increased deep tissue dissemination and mortality when infected with *Y. pseudotuberculosis*. Based on these and other findings, we suggest that the decreased phagocytosis-mediated innate immune response in combination with decreased cell surface expression of MHC Class II proteins on macrophages and dendritic cells leads to a failure during the adaptive immune response to adequately stimulate T-cells to secrete the cytokine Interferon-γ (IFNγ), which is vital in the host response against systemic *Yersinia* proliferation (Autenrieth and Heesemann, 1992; Parent et al., 2006).

2. 2 Material and method

Genotyping

1 cm long sections of tails were cut from wt and PIP5K$\alpha^{-/-}$ mice, and boiled in 0.5 ml of 0.05 M NaOH for 20 min. Remove the sample from the heat and neutralized by adding 50 μl of a solution of 1M Tris-HCl (pH=8), and 10 mM EDTA. Vortex to mix. 1 μl of supernatant was used as the template in a 20 μl PCR reaction with the following primers:

Wt forward, 5'-TCACTGTGTCAATGTGCCTTTAC;

Neo forward, 5'-CCTACCGGTGGATGTGGAATGTG;

Neo reverse, 5'-ACACAGGCAAATGAATCTGTGC.

Bacterial strains and culture conditions.

All *Y. pseudotuberculosis* strains are derived from 32777 (Simonet and Falkow, 1992). Wild-type (*Yersinia*), virulence plasmid-cured (Yop^{null}), multiple Yop mutant YopJTEH (encoding catalytic inactive YopJ, T, E, H, and is also named as mJTEH) were described before (Zhang et al., 2008). Individual Yop-inactive mutants, $YopT^{ina}$, $YopE^{ina}$, $YopH^{ina}$ were constructed similarly as $YopJTEH^{ina}$. Where indicated, these strains also carry the plasmid p67GFP3.1 (Pujol and Bliska, 2003). To induce expression of green fluorescent protein (GFP), 0.5 mM isopropyl-β-D-thiogalactopyranoside (IPTG) was included wherever indicated. To prepare bacteria for infection of tissue cultured cells, overnight bacterial culture were diluted to an OD_{600} of 0.1 in Luria-Bertani (LB) broth supplemented with 2.5 mM $CaCl_2$ and shaken at 37°C for a 2 h. To maximally induce the expression of Yops before bacteria contacting with the cells, overnight cultures were diluted to OD_{600} of 0.1 in LB broth containing 20 mM $MgCl_2$ and 20 mM sodium oxalate and shaken at 26°C for 1 h followed by 2 h at 37°C. To determine the percentage of

phagocytosis, bacteria were washed once and resuspended in pre-warmed HBSS and used to infect macrophages at a multiplicity of infection (MOI) of 20. The plates were centrifuged at 200g for 5 min to facilitate contact of the bacteria with the macrophages and then incubated at 37°C for 20 min. To infect mice, overnight culture grown at 26°C were washed and re-suspend in phosphate-buffered saline (PBS) at $5X10^8$ colony forming unite (CFU)/ml.

Infection of mouse

Female wild-type (wt) and PIP5K$\alpha^{-/-}$ mice of 8-10 weeks age, as has been described before (Sasaki et al., 2005), were fasted for 16 h, then inoculated intragastrically with 200 μl of bacterial culture through a 20 gauge-feeding needle. Mice were provided with food and water ad libitum thereafter. At indicated time post infection, or when death was imminent, mice were euthanized by CO_2 asphyxiation. When indicated, blood was collected through cardiac puncture, and separated into serum after centrifugation in Z-Gel Micro tubes (SARSTEDT). Where indicated, mouse spleens and/or mesenteric lymph nodes (MLNs) were dissected aseptically, weighed and homogenized in 4.5 ml of sterile PBS or dispersed to separate into cell suspension in Dulbecco's Modified Eagle Medium (DMEM). Serial dilutions were plated on LB agar to determine bacterial colonization. All animal procedures were approved by an institutional review board.

Culture of Bone marrow-derived macrophages and dendritic cells

Bone marrow-derived macrophages (BMDMs) were prepared as previously described (Zhang et al., 2005). Briefly, the bone marrow cells isolated from two femurs were seeded into 100-mm-diameter Petri dishes at 5×10^6 cells/plate in DMEM with high glucose supplemented with 20% heat-inactive fetal bovine serum (FBS, Hyclone), 30%

L-cell-conditioned medium, 2mM $_L$-glutamine, and 1 mM sodium pyruvate. After 5 days of incubation at 37°C in an atmosphere of 5% CO_2 and one change of fresh medium, the cells were collected in cold PBS, suspend in BMM-low medium (the same as above except with 10% FBS and 15% L-cell-conditioned medium). Infection was carried out in BMM-low medium. Rac1 inhibitor NSC23766 was used to pre-treat cells for 4 hours before and during infection at the concentration of 100 μM in water. Bone marrow-derived dendritic cells were prepared as has been described (Lutz et al., 1999). 2×10^6 Bone marrow cells were incubated in RPMI-1640 medium containing 2 mM L-glutamine, 1% sodium pyruvate, 50 μM β-mercaptoethanol, 10% FBS and 20 ng/ml GM-CSF (R&D) for 7 days with two changes of the same medium. All tissue culture reagents were purchased from Invitrogen unless otherwise specified.

Reverse transcription and polymerase chain reaction (PCR)

Total RNA was isolated from wt and PIP5K$\alpha^{-/-}$ BMDMs using RNeasy (QIAGENE), and reversely transcripted to DNA by using Transcriptor First Strand cDNA Synthesis Kit (Roche). The following primers were used in the PCR reactions, PIP5Kα: forward, 5'-AAGTGTGTTCCTCCCCAGTG, reverse, 5'-GCCCATAGAATTTTGGCAGA; PIP5Kβ: for, 5'-CTTCTATGCTGAGCGGTTCC, reverse, 5'-TGCTCAGTGGGTGAACTCG; PIP5Kγ: forward, 5'-CATCCAAGAAAGGACGTGGT, reverse, 5'-GGCTCCACCTGCACAGTTAT.

Immunofluorescence microscopy

Phagocytosis assay was performed as described previously (Zhang et al., 2008). Before and during infection, the bacteria were induced to express GFP with IPTG. After infection of BMDMs, the monolayer was fixed with 4% paraformaldehyde in PBS at

room temperature. Non-internalized and partially internalized bacteria were identified after immunolabeling with rabbit anti-*Yersinia* serum SB349 (1:1000) followed by Alexa Fluor 647-conjugated goat anti-rabbit antibody (1:5000) (Molecular Probes) without permeabilization. Percentage of uptake was defined as the number of internalized bacteria relative to the total number of cell-associated bacteria. To visualize the surface expression of MHC class II molecules from BMDMs, IFNγ treated cells were fixed and stained with anti-MHC II antibody from Santa Cruz (1:50) (sc-593222) and anti-rat secondary antibody conjugated with AlexaFluor 488 (1:500). When indicated, permeabilization was done by incubating with 0.1% Triton X-100 in PBS. *Cis*-Golgi marker anti-GM130 (1:50), and *trans*-Golgi network marker anti-TGN38 (1:50) were from Santa Cruz. Other antibodies were from Cell Signaling.

Measurement of Cytokine levels

Macrophages (2.5 x 10^5/ml) were infected in 24-well plates. 2 h post-infection, medium was collected after centrifugation for 5 min at 200 x *g*. The cytokine levels were measured by cytokine antibody array (Raybio. Cat. No. AAM-CYT-2-8). TNF-α concentrations in post-infection sera were measured with Quantikine Mouse TNF-α Immunoassay (R&D Systems) following the manufacturer's instructions. IFN-γ concentrations were determined with mouse IFNγ MAX set Deluxe kit (BioLegend).

Western blot analysis

Macrophages (1 x 10^6 cells/well) were infected in 6-well plates. Cell lysates were prepared by boiling in 1x Laemmli sample buffer and were resolved with 10% sodium dodecyl sulfate-polyacrylamide gel electrophoresis. For checking MHC class II level, cells were lyzed by RIPA buffer and short spin at 5000× rpm for 5 min. The supernatants

were diluted by 2xSDS-urea sample buffer. Western blotting with commercial primary antibodies was performed as suggested by the suppliers. Anti-phospho-ERK, anti-total ERK, and anti-α tubulin were from Sigma. Anti-MHC II antibody were from Santa Cruz. Other antibodies were from Cell Signaling. Secondary antibodies used were conjugated with Alexa Fluor 680 (Molecular Probe) or IRDye 800 (Rockland). Signals were collected using an Odyssey VI scanner (Li-Cor Biosciences).

Peritoneal neutrophil isolation and bacterial killing

8-10 weeks-old wt and PIP5K$^{-/-}$ mice were i. p. injected with 3% thioglycollate. 4 hours later, HBSS was used to wash peritoneum three times, and fluid was collected in Falcon tube followed by centrifugation at 1000×rpm for 5 min. Cell pellets were washed by PBS twice by centrifugation, and then 5×10^5 cells per ml were resuspended in DMEM with 10% FBS and plated in a12-well plate. Infection was performed as described above. Briefly, cells were incubated with bacteria at MOI=20 for 1 hour and half. The same amount of bacteria incubated in the well without cells were used as control. After incubation, adding 1ml of HBSS containing 0.1% of TritonX-100 lysed cells. 100 ul of lysate was taken to do the serial dilution, and then plated in the LB agar to determine the baterial number.

Flow cytometry

Cell suspension was prepared from un-infected or infected spleens. Infected samples were treated with Penn/Strep for 20 min on ice. Then red blood cells were lysed with 144 mM of ammonium chloride (pH7.4). After washing in DMEM, single splenocyte suspension was prepared by passing through a 70 μm Cell Strainer (BD Falcon). To assay for neutrophil/monocyte and T cell content, one million splenocytes were resuspend in

fluorescence-activated cell sorter (FACS) buffer (0.2% bovine serum albumin and 0.02% NaN_3 in PBS) and incubated with anti-mouse CD16/CD32 (FcγIII/II Receptor) clone 2.4G2 (BD Pharmingen). Then the cells were labeled at 4°C for 30 min with R-phycoerythrin (PE) anti-mouse Ly-6G/Ly-6C (Gr-1, clone RB6-8C5) or Alexa Fluor488 anti-mouse CD3ε (Clone 145-2C11). The cells were washed twice with FACS buffer after centrifugation and fixed with 1% formalin in PBS. At least 10,000 events were acquired using a BD FACSCaliber. Data were analyzed with CellQuest and Winlist.

To assay MHC II surface expression, BMDCs, or BMDMs treated with IFNγ or vehicle for 24 hours were collected in ice-cold PBS. Cells were labeled with Alexa Fluor647-conjugated anti-mouse I-A/I-E (clone M5/114.15.2), BMDCs were co-stained with Alexa Fluor488-conjugated hamster anti-CD11c (clone N418). Samples were analyzed without fixing and dead cells were excluded after staining with 1ug/ ml propidium iodide (PI). Isotype-matched antibodies were used in all cases to control for nonspecific binding. Antibodies were from BioLegend unless specified.

2. 4 Results

Macrophages derived from PIP5Kα$^{-/-}$ mice exhibit a phagocytosis defect upon Y. pseudotuberculosis infection.

PIP5K has been reported to play a role in phagocytosis, and macrophages are important phagocytes in innate immunity. To examine whether the selective elimination of PIP5Kα impacts in the phagocytosis process, I examined *Y. pseudotuberculosis* uptake by bone marrow-derived macrophages (BMDMs) as experimental model system. To make sure there is no compensation from other isoforms of PIP5K, the transcription levels of PIP5Kα, β and γ were examined using reverse transcription followed by PCR. In PIP5Kα$^{-/-}$ BMDMs, there was no PIP5Kα message detected, but PIP5Kβ and γ showed similar expression levels in comparison with those in wt BMDMs (Fig. 2. 1A).

In uptake assays, BMDMs isolated from wt and PIP5Kα$^{-/-}$ mice were incubated with GFP-expressing wt *Yersinia* or Yop^{null} *Yersinia* at a MOI of 20 for 20 minutes and fixed. Bacteria on the outer surface of the macrophages were identified by labeling them with anti-*Y. pseudotuberculosis* antibody, as shown in blue in Fig. 2. 1B, whereas the phagocytosed bacteria remained unlabeled by the antibody and hence appear green. Phagocytic index was calculated as a ratio of the number of internalized bacteria to the total number of bacteria taken up or still externally bound. Binding of wt and Yop^{null} bacteria to wt and PIP5Kα$^{-/-}$ macrophages was indistinguishable (Fig. 2. 1C, bottom); however, differences were observed in phagocytosis rates (Fig. 2. 1C, upper). For wt macrophages, approximately 50% of the wt *Yersinia* were internalized and 50% remained on the surface. This ratio reflects Yop-mediated resistance to the internalization process, since for the Yop^{null} *Yersinia*, 80% of the bacteria bound were internalized in the same

time-frame. Macrophages from PIP5K$\alpha^{-/-}$ mice phagocytosed 30% less wt *Yersinia* than wt macrophages ($p< 0.01$). However, the PIP5K$\alpha^{-/-}$ and wt macrophages phagocytosed similar amounts of the Yop^{null} *Yersinia*. These data suggested a setting of cryptic redundancy - that PIP5Kα is required only when the *Yersinia* are actively resisting phagocytosis using their Yop toxin system. To pursue this observation further, the *Yersinia* were cultured under conditions that lead to super-induction of the Yop proteins. In this setting, binding of the bacteria to the wt and PIP5K$\alpha^{-/-}$ macrophages remained similar (Fig. 2. 1D), but the deficit in phagocytosis was even more pronounced (Fig. 2.1D, upper), with the PIP5K$\alpha^{-/-}$ macrophages internalizing even fewer bacteria, and less than 50% of that engulfed by wt macrophages ($p< 0.01$). In contrast, similar rates of phagocytosis in wt and PIP5K$\alpha^{-/-}$ macrophages were observed for a *Yersina* strain bearing a virulence plasmid that encoded catalytically-inactive mutants of Yops J, H, E, and T (mJHET), the four Yops that target phagocytosis as part of their mechanism of action, thus identifying one or more of them as the factor that synergizes with PIP5Kα deficiency to decrease uptake.

PIP5Kα is required for efficient uptake of Y. pseudotuberculosis when Rac1 activity is inhibited.

As shown in the previous section, the requirement for PIP5Kα in phagocytosis manifests only when *Yersinia* Yop toxin proteins cripple macrophage function in parallel. There are multiple Yop proteins that individually target many different host response steps (Viboud and Bliska, 2005). To identify the Yop protein that uncovers the

requirement for PIP5Kα in phagocytosis, I tested the efficiency of uptake of Yop mutant strains that individually express catalytically-inactive alleles of YopE, YopH, or YopT respectively. Binding of the bacteria to macrophages was unaltered; however, differences in phagocytosis were observed (Fig.2.2A). As above, the PIP5K$\alpha^{-/-}$ macrophages exhibited a 35-45% defect in phagocytosis of wt *Yersinia* relative to wt macrophages, and this difference persisted in the absence of active YopT and YopH, even though the overall rates of phagocytosis modestly rose for macrophages from both mouse genotypes. However, the mutant bacterial strain lacking active YopE (YopE^{ina}) was taken up by PIP5K$\alpha^{-/-}$ macrophages just as efficiently as it was by wt macrophages (Fig. 2.2A), and with approximately the same efficiency as when all of the Yops were absent (Fig. 2.1C). These results identify YopE, a GAP protein that triggers Rac1 deactivation, as the key signaling pathway component.

To confirm this finding, we employed NSC23766, a chemical inhibitor of Rac1, to pre-treat wt and PIP5K$\alpha^{-/-}$ macrophages, and measured the uptake efficiency using the mutant strain lacking active YopE. As above, both wt and PIP5K$\alpha^{-/-}$ macrophages exhibited efficient uptake of the bacteria in the absence of the inhibitor (Fig. 2.2B). In the presence of the inhibitor, however, PIP5K$\alpha^{-/-}$ macrophages phagocytosed 30% less bacteria than wt macrophages, consistent with our previous observations.

Taken together, these results demonstrate that PIP5Kα is important for *Y. pseudotuberculosis* uptake in the setting of Rac1 inhibition.

PIP5Kα deficiency does not alter signaling pathways or release of pro-inflammatory cytokines and factors by macrophages.

Besides acting as professional phagocytes, macrophages also play critical roles in mounting immune responses such as producing pro-inflammatory cytokines. To assess whether lacking of PIP5Kα results in other defects on the function of macrophages, BMDMs from wt and PIP5K$\alpha^{-/-}$ mice were exposed to *Y. pseudotuberculosis,* and MAPK and NFκB activation were examined as shown in Fig. 2. 3A. For uninfected cells of either genotype, the levels of phosphorylation of JNK, p38, and ERK were undetectable, and the level of NFκB's inhibitor, IκB, was high, signifying low levels of NFκB activity (Fig. 2. 3A; quantitation shown in B and C). infection with wt *Yersinia* for 20 min triggered transient phosphorylation of JNK, p38, and ERK, and NFκB activation (as monitored by IκB down-regulation) in wt BMDM cells. Activation was also assessed in response to mutant *Y. pseudotuberculosis* cured of its virulence plasmid and thus lacking the ability to express Yop proteins (Yop^{null}); these bacteria lack the ability to suppress JNK, p38, and ERK activation, and even higher levels of phosphorylation (and greater levels of IkB degradation) were seen in response to bacterial infection. No significant difference was observed in MAPK phosphoylation and NFκB activation between wt and PIP5K$\alpha^{-/-}$ macrophages, suggesting that the intrinsic signaling pathways triggered by *Yersinia* mainly via activation of the Toll-like receptors (TLR)-2 and 4 is intact in PIP5K$\alpha^{-/-}$ macrophages.

PIP5Kα deficiency was reported to increase degranulation and cytokine production after Fcε receptor cross-linking in mast cells. To examine pro-inflammtory factors secretion by macrophages, I used an array approach to measure those cytokines and

factors known to be released by stimulated macrophages (Fig. 2. 3D). No statistically significant difference was observed. These data suggest that the release of proinflammatory and bactericidial factors by macrophages in PIP5K$\alpha^{-/-}$ mice is similar to that of wt mice.

PIP5Kα does not affect the function of neutrophils during Y. pseudotuberculosis infection.

Neutrophils mount the initial defense mechanism against *Y. pseudotuberculosis* by engulfing them or by releasing antimicrobial factors via degranulation. PIP5Kα deficiency has been reported to promote degranulation by mast cells (Sasaki et al., 2005), suggesting that it could affect this process in neutrophils. To test whether PIP5Kα-deficiency affects the killing ability of neutrophils, I isolated thioglycollate-elicited neutrophils from the peritoneal fluid of wt and PIP5K$\alpha^{-/-}$ mice and incubated them with *Y. pseudotuberculosis*. On average, 22% of the bacteria were killed by wt neutrophils, and similar results were obtained from the PIP5K$\alpha^{-/-}$ neutrophils (Fig. 2. 4A).

Intact killing ability does not necessarily mean that the PIP5K$\alpha^{-/-}$ neutrophils are completely functional. A key characteristic of neutrophils involves their ability to follow chemotactic cues to sites of inflammation to gain proximity to pathogens. To examine neutrophil chemotaxis and recruitment to the spleen during the infection process, we isolated splenocytes from the infected mice and performed FACS analysis to quantitate the number of neutrophils recruited to spleens upon *Y. pseudotuberculosis* challenge. Statistically similar numbers of neutrophils ($Gr1^+$ cells) were recruited to the spleens of

wt and PIP5K$\alpha^{-/-}$ mice at both day 3 and day 6 after infection (Fig. 2. 4B). Taken together, these data indicate that neutrophil recruitment is normal in PIP5K$\alpha^{-/-}$ mice in the setting of infection and that the neutrophils appear to function normally.

PIP5K$\alpha^{-/-}$ mice exhibit increased susceptibility to Y. pseudotuberculosis infection.

Oral inoculation of mice with *Y. pseudotuberculosis* results in lethality in a dose-dependent manner. Infection with *Y. pseudotuberculosis* lacking the YopE toxin greatly reduces the mortality rate (Black and Bliska, 2000; Viboud et al., 2006), indicating a critical role for activated Rac1 in resistance to pathogenesis. My previous data show that PIP5Kα has an an irreplaceable role in the phagocytosis of *Y. pseudotuberculosis* when bacterial toxin YopE is present. To test if PIP5Kα plays a real role in *Y. pseudotuberculosis* infection *in vivo*, age-matched PIP5K$\alpha^{-/-}$ mice and wild-type (wt) mice were administered *Y. pseudotuberculosis* orally at a dose of 5×10^8 CFU/ mouse and monitored for 21 days.

As anticipated at this dose of infection, the wt mice exhibited significant but limited mortality, with 15% of the mice dying between 8-10 days post infection (Fig. 2. 5A). The PIP5K$\alpha^{-/-}$ mice, however, exhibited substantially greater susceptibility to the infection, with mortality beginning at day 3 and continuing on throughout the period of observation, ultimately reaching 65% by day 20. Thus, PIP5Kα plays a protective role in *Y. pseudotuberculosis* infection that is not fully compensated for by the remaining isoforms, PIP5Kβ and γ.

Increased numbers of bacteria in the spleens of PIP5K$\alpha^{-/-}$ mice by day 6 post infection.

Dissemination to deep tissues such as the spleen and then explosive local proliferation is the primary mechanism via which death ensues for animals infected by *Y. pseudotuberculosis* (Carter, 1975; Naktin and Beavis, 1999). To examine the rate and extent of deep tissue invasion in the PIP5K$\alpha^{-/-}$ mice as a potential cause for their accelerated and exaggerated mortality, spleens were isolated from wt and PIP5K$\alpha^{-/-}$ mice at days 3 and 6 after infection as above. At day 3, slightly elevated but not statistically different numbers of *Y. pseudotuberculosis* were found in the spleens of PIP5K$\alpha^{-/-}$ mice in comparison to the spleens of wt mice (Fig. 2. 5B, $p=0.63$). The difference was dramatic though by day 6 post infection, when 25-fold more *Y. pseudotuberculosis* was found in the PIP5K$\alpha^{-/-}$ spleens than in the wt spleens (8.9×10^5 versus 3.4×10^4 CFU/spleen, $p<0.01$), indicating either that more bacteria were disseminating into the PIP5K$\alpha^{-/-}$ deep tissues from the intestinal tract, or that the PIP5K$\alpha^{-/-}$ mice were exhibiting defective bacterial clearance in the spleen. Regardless, this finding provides an explanation for the increased mortality observed for the PIP5K$\alpha^{-/-}$ mice.

Oral ingestion of *Y. pseudotuberculosis* at sufficient doses leads to bacterial infiltration of the Peyer's patches within 24 hours in wt mice. The Peyer's patches are frequently unable to contain the infection, resulting in bacterial invasion of the MLN, the final and key barrier to preventing deep tissue dissemination (Carter, 1975). To test the possibility that the increased number of bacteria in the spleens of the PIP5K$\alpha^{-/-}$ mice at day 6 post infection ensued from overwhelming bacterial proliferation in the MLN, the number of bacteria in the MLN was examined. No significant difference was found between the wt and PIP5K$\alpha^{-/-}$ mice at either day 3 or 6 (Fig. 2. 5C). These data indicate that *Y. pseudotuberculosis* spread to and replicate in the MLN of wt and PIP5K$\alpha^{-/-}$ mice

at comparable rates, suggesting that differences in invasion of the Peyer's patches, spread to the MLN, and local proliferation there do not underlie the profound increase in deep tissue dissemination displayed by the PIP5K$\alpha^{-/-}$ mice.

Diminished IFNγ level in infected PIP5K$\alpha^{-/-}$ mice.

TNFα and IFNγ are two key cytokines protecting host against *Y. pseudotuberculosis* infection. Mice inoculated with *Yersinia* respond in the early, innate, phase of the infection by producing the cytokine TNFα, which is critical for host survival (Autenrieth and Heesemann, 1992; Parent et al., 2006). Low levels of the cytokine IFNγ that stimulates macrophages to upregulate MHC II expression, are also released by NK cells, enabling efficient presentation of antigens to $CD4^+$-T-cells and activation of the adaptive immune response. The stimulated $CD4^+$-T-cells then release large amounts of IFNγ, which is critical for preventing overwhelming bacterial proliferation and death, as has been demonstrated by neutralizing the IFNγ during on-going infections (Autenrieth and Heesemann, 1992; Parent et al., 2006). In the murine oral infection model, the serum concentrations of TNFα and IFNγ form a linear relationship with bacterial colonization levels in the spleens following logarithmic transformation (Y. Zhang, unpublished observations). To examine whether PIP5K$\alpha^{-/-}$ mice have normal levels of TNFα and IFNγ in response to *Y. pseudotuberculosis* infection, I collected serum on day 3 and 6 post-infection for wt and PIP5K$\alpha^{-/-}$ mice and plotted serum levels of TNFα and IFNγ in relationship to the level of bacterial infection (Fig. 2. 6A and B). On day3, the plots of log [serum TNFα]-logCFU of wt and PIP5K$\alpha^{-/-}$ essentially overlaps. On day6, the slopes of the lines remain the same, yet the y- intercepts increased, suggesting that cells

secreting more TNFα, or more cells or cell types participating in TNFα secretion at the later stage of infection. In any case, TNFα release increased in proportion to bacterial infection, but did so to similar extents in wt and PIP5Kα$^{-/-}$ mice; thus a defect in TNFα release in response to bacterial loading is not readily apparent.

The linear relationship between log[serum IFNγ] and logCFU, however, indicates that PIP5K$^{-/-}$ mice may be deficient in mounting a pro-inflammatory response against *Yersinia*. At day 3, IFNγ levels were increased above the undetectable levels observed in control mice, but were still relatively low. The two lines derived from wt and PIP5Kα$^{-/-}$ mice are similar with a pooled slope of 0.21(Fig. 2. 6B), indicating that initially, IFNγ was produced similarly in both mouse types. From day3 to day6, in wt group, the IFNγ levels had risen by 20-fold on average and the slope of the line increased from 0.21 to 0.52 ($p=0.038$), consistent with the hypothesis that the cells of the adaptive immunity, e. g., T cells are more effective than the cells of innate immunity such as NK cells in IFNγ secretion. The rates of increase in IFNγ levels in wt and PIP5Kα$^{-/-}$ mice in proportion to bacterial load were almost identical (slopes of the lines shown in Fig. 2. 6B, $p=0.95$), signifying a similarly proportionate response by both genotypes, which also indicates that once activated, T cells in PIP5Kα$^{-/-}$ mice secret IFNγ as efficiently as that of wt. However, the y-intercepts of the lines were significantly different ($p<0.05$), revealing that at any given level of bacterial load, IFNγ release in PIP5Kα$^{-/-}$ mice is approximately 3-times less than that in wt mice. This finding of diminished IFNγ release in the face of mounting bacterial sepsis provides a reasonable basis for the observed more frequent

mortality of the PIP5K$\alpha^{-/-}$ mice (Fig. 2. 5A), and suggested that there were fewer T-cells responding to the infection or that the T-cells were responding less well.

T cell contents of spleens were similar between wt and PIP5K$\alpha^{-/-}$ mice.

T cells are the major source of IFNγ upon bacterial infection. T cells can be classified into two types: $CD4^+$ that is a marker for T helper cells; and $CD8^+$ cells that are cytotoxic T cells. CD3 is a part of the T cell receptor complex, often used as a pan-T cell marker. To check whether the T cell content is normal in PIP5K$\alpha^{-/-}$ spleens, splenocytes were isolated, and T cells were detected by anti-CD3, anti-CD4, and anti-CD8 antibodies. No obvious difference was observed between wt and PIP5K$\alpha^{-/-}$ mice (Fig. 2.7A). Slightly more $CD8^+$ cells were found in PIP5K$\alpha^{-/-}$ spleens (12.8%) than wt (10.3%), but the difference was not statistically significant.

In some circumstances, T cells are activated or recruited to affected tissues upon bacterial infection. To test this possibility, spleens were isolated from infected wt and PIP5K$\alpha^{-/-}$ mice. T cells were labeled by anti-CD3, and analyzed by flow cytometry. Similar numbers of CD3-positive cells were observed in wt and PIP5K$\alpha^{-/-}$ spleens on day3 or day6 post-infection (Fig. 2. 7B). Further dissecting each T cell population by labeling $CD4^+$ and $CD8^+$ cells found similar T cell contents in wt or PIP5K$\alpha^{-/-}$ spleens at day6 after infection (Fig. 2. 7C). These data suggest that there is no defect in T cell content in PIP5K$\alpha^{-/-}$ mice either before or after infection. It is interesting to notice that *Y. pseudotuberculosis* infection did not cause any obvious T cell recruitment while the percentage of T cells in infected spleens is actually lower than that in uninfected spleens

(29% versus 17.4% in wt mice), suggesting either *Yersinia* inhibits T cell recruitment or other immune cells are recruited into spleen leading to increased total cell number. Overall, these data rule out the possibility that fewer T cells responding to infection cause lower IFNγ in PIP5K$^{-/-}$ mice.

Lower levels of MHC class II on the surface of the antigen presenting cells (APCs) of PIP5Kα$^{-/-}$ mice.

Antigen presentation is a key step to link innate and adaptive immunity and activate T cells. Defective antigen presentation could be another possibility for poor T cell responses in PIP5Kα$^{-/-}$ mice. Major histocompatibility complex class II (MHC II) molecules are expressed in antigen presenting cells (APCs) i. e. dendritic cells (DCs) and macrophages, and responsible for presenting proteins such as those found on bacteria. Therefore, we set out to determine the levels of MHC class II molecules on the surface of BMDCs or BMDMs. In vitro differentiation of wt bone marrow cells with granulocyte/macrophage-colony stimulation factors (GM-CSF) for 7 days results in MHC class II molecules expressed in 70% of CD11c^{+} cells, in contrast, only 44% of CD11c^{+} cells from PIP5Kα$^{-/-}$ mice express MHC class II molecules (Fig. 2. 8A), and this difference in percentage is statistically significant ($p<0.05$)(Fig. 2. 8B). This finding suggests that PIP5Kα plays a part in antigen presentation, an unexpected novel function of PIP5Kα.

To further confirm the MHC II presentation defect in PIP5Kα$^{-/-}$ cells, I also examined the MHC class II level on the surface of BMDMs. They normally express low level of

MHC Class II on their surface (Fig. 2. 8C). After 24 hours of exposure to IFNγ, however, wt macrophages increased their surface level expression of MHC Class II by approximately 35-fold. A smaller increase in expression of approximately 20-fold was observed for the PIP5K$\alpha^{-/-}$ macrophages (Fig. 2. 8C). On average, the MHC class II signal on the surface of PIP5K$\alpha^{-/-}$ BMDMs is 37% lower than that of wt cells (Fig. 2. 8D).

The IFNγ signaling pathway proceeds via STAT phosphorylation and triggers transcriptional upregulation of both MHC II and other response components including iNOS, to produce NO. No differences in STAT phosphorylation in response to IFNγ were observed for PIP5K$\alpha^{-/-}$ macrophages in comparison to wt macrophages, and iNOS upregulation was similar between the genotypes as well (Fig. 8E). These data indicate that the IFNγ signaling pathway is intact in PIP5K$\alpha^{-/-}$ macrophages and that downstream target transcriptional responses appear to be normal.

Collectively, these results demonstrate that these two major types of APCs from PIP5K$\alpha^{-/-}$ mice are defective for surface expression of MHC class II molecules. With lower levels of MHC class II molecules on the surface of the APCs, the $CD4^+$ T cell response in PIP5K$\alpha^{-/-}$ mice is rendered less effective, thereby providing an explanation for the decreased serum levels of IFNγ in PIP5K$\alpha^{-/-}$ mice during a later stage of *Y. pseudtotuberculosis* infection.

PIP5Kα may affect the translocation of MHC class II to the plasma membrane.

To address how PIP5Kα affects the surface expression level of MHC II, confocal immunofluorescent examination of the macrophage cells was then performed. Anti-MHC Class II staining of non-permeabilized wt BMDMs revealed a strong pattern of cell-surface expression (Fig. 2. 9A). Consistent with the FACS analysis shown in Fig. 8B, a marked reduction in cell-surface MHC Class II protein was observed for PIP5Kα$^{-/-}$ BMDMs (Fig. 2. 9B). When the immunostaining was performed on permeabilized BMDMs, cytosolic, vesicular-appearing, localization of MHC II was noted for both the wt (Fig. 2.9C) and PIP5Kα$^{-/-}$ (Fig. 2. 9D) cells, suggesting that the lack of plasma membrane localization in PIP5Kα$^{-/-}$ BMDMs ensued from an alteration in MHC II trafficking and distribution rather than changes in transcription. Confirming this observation, western blot analysis of MHC II revealed a modest but not substantial decrease in total MHC in the PIP5Kα$^{-/-}$ BMDMs in comparison to the wt BMDMs (Fig. 2. 9E).

MHC Class II proteins are synthesized in the endoplasmic reticulum (ER), become glycosylated in the Golgi, and then cycle between the plasma membrane, endosome recycling compartments, and lysosomes to acquire processed antigen for presentation to T-cells. Marker analysis was used to determine the nature of the MHC II altered localization. Analysis of wt BMDMs revealed extensive co-localization of the cytosolic vesicular MHC II immunostaining with GM130, a *cis*-Golgi resident protein (Fig. 2. 10A), and possibly a small amount of co-localization with TGN38 (Fig. 2. 10C), a marker for the *trans*-Golgi. A high degree of co-localization of MHC II with GM130 was also observed for PIP5Kα$^{-/-}$ BMDMs (Fig. 2. 10B), but little or no co-localization was observed with TGN38 (Fig. 2. 10D). Significant amounts of co-localization were not

observed in either genotype with EEA1, a marker for early endosomes, or LAMP-1, a marker for lysosomes (Fig. 2. 10E and F). These findings indicate that MHC Class II proteins either decrease their rate of exiting the *cis*-Golgi compartment in PIP5K$\alpha^{-/-}$ BMDM, or that their rate of turnover is dramatically increased upon exit once they proceed to begin cycling between the plasma membrane and the endosome and lysosome compartments.

Taken together, this work reveals expected and unexpected roles of PIP5Kα in host defense again *Y. pseudotuberculosis*: phagocytosis and MHC II presentation. Both of them may contribute to the phenotype shown in PIP5K$\alpha^{-/-}$ mice.

2. 4 Discussion

The PIP5K lipid kinases play regulatory roles in many signal transduction-mediated cell biological processes by producing the pleiotropic signaling lipid PIP_2. PIP_2 can be generated from several types of enzyme families in addition to the PIP5Ks, and there are three PIP5Ks with considerable sequence conservation; hence it is only relatively recently, with the availability of knockout animals, that the roles uniquely performed by each source of PIP_2 generation have begun to be defined.

Initial studies have suggested that the individual enzymes perform at least some isoform-specific functions through regulating subcellular compartmental production of PIP_2. Disruption of PIP5Kγ hinders both fusion of secretory vesicles into the plasma membrane during regulated exocytosis and their recycling via endocytosis, resulting in early post-natal lethality due to diminished release of synaptic neurotransmitters (Di Paolo et al., 2004). In contrast, disruption of the mouse PIP5Kα isoform is not lethal, and in fact results in increased regulated exocytosis by mast cells (Sasaki et al., 2005), potentially secondarily to exaggerated signaling through IgE receptors and / or because the cortical actin cytoskeleton network that serves in part to restrict exocytosis (Vitale et al., 2001) in mast cells is only partially intact in the absence of the pool of PIP_2 generated by PIP5Kα. In this study, we examine the potential role of PIP5Kα in bacterial infection using *Y. pseudotuberculosis* as our model system. We show that PIP5Kα is important in the host response against *Yersina*, but only a subset of the many potential roles for PIP_2 generation in this setting appear to be affected by the disruption. More specifically, we uncover a requirement for PIP5Kα in macrophage phagocytosis in the context of a bacterial toxin that blunts PIP_2 production, in the expression of surface MHC II by

macrophages and DC cells, and in the production of IFNγ by T-cells, although the latter may ensue from the first two consequences.

As reported previously (Coppolino et al., 2002; Wong and Isberg, 2003), PIP5Kα and β accumulate at nascent phagosomes during uptake of bacteria and IgG-coated beads, and overexpression of kinase-dead versions of either isoform impairs phagocytosis, most likely through blocking the action of both PIP5Kα and β simultaneously. We show here that under artificially favorable circumstances, i.e. uptake of crippled *Yersina* lacking the ability to express the Yop proteins that help the bacteria to resist phagocytosis, PIP5Kα is dispensable for the phagocytic process. However, *Yersinia* normally express these proteins, which convert the bacteria from ones incapable of causing pathogenesis, to ones associated with significant morbidity and mortality. YopE in particular disables Rac1, which has many downstream effectors. However, the observation that the decreased phagocytosis in the presence of YopE can be bypassed by overexpression of PIP5Kα or ARF6 in Cos1 cells suggests that it is activation of PIP5K that is the critical downstream effector pathway hampered when *Yersina* YopE targets Rac1. We show here that disruption of PIP5Ka combined with inactivation of Rac1 by YopE decreases phagocytosis substantially further, indicating that activation only of PIP5Kβ by ARF6 alone is even less capable of providing sufficient PIP_2 for efficient *Yersina* uptake to occur. This observation provides insight into both the unique and redundant mechanisms concerning PIP_2 production during phagocytosis and the mechanisms underlying resistance to bacterial deep tissue invasion. Mobilization of PIP5Kβ by ARF6 and Rac1 suffices to provide the PIP_2 required for the phagocytic process under benign circumstances, but in the setting of bacterial toxins that cripple the stimulatory input from

Rac1, enzymatic contribution from PIP5Kα becomes requisite. It will be interesting to see if a similar outcome is observed for PIP5Kβ knockout and combined α/β knockout mice.

In the course of these studies, we failed to observe obvious changes in the actin cytoskeleton of macrophages in the PIP5K$\alpha^{-/-}$ mice (data not shown), in contrast to what we reported previously for mast cells undergoing degranulation (Sasaki et al., 2005). However, it should be noted that the highly elegant studies that have been documented on actin rearrangement at the phagosomal cup have been conducted using very large IgG-coated latex beads that become phagocytosed slowly (Botelho et al., 2000), which exaggerates the actin accumulation and makes possible its visualization. *Yersinia* bacteria are ~ 1% the size of these beads and are phagocytosed quickly, making it impractical to image actin accumulation during an individual uptake event. Although we have no direct evidence for it, it is nonetheless possible that disorganization of the actin cytoskeleton at the phagosomal cup is the effector pathway downstream of the PIP_2 deficiency that hinders uptake. It should also be noted that the signaling pathways associated with phagocytosis and the phagocytic process itself differ according to the initial binding event. For example, the pathways triggered by binding of IgG-coated beads to Fc receptors are different in part from those triggered by *Yersinia* binding to β1 integrin, in particular in potential with respect to steps involving needs for synthesis of PIP_2 (Pizarro-Cerda and Cossart, 2004).

We also examined signaling pathways known to be activated by binding of *Yersinia* to the macrophage surface via β1-integrin and ensuing LPS stimulation. Again in contrast to what we previously reported for mast cells stimulated by cross-linking of IgE

receptors, we did not see exaggerated levels of signal transduction or exaggerated levels of regulated exocytosis. This finding suggests that the signaling outcome to compartment-specific deficiencies in PIP_2 will depend on the specific signaling network under examination. Consistent with the prior report on mast cell recruitment in allergic settings, we did not see alterations in chemotaxis under the infectious stimulatory setting examined here. PIP_2 production by PIP5K has been well described as having a role in chemotaxis, but it may be necessary to examine the PIP5Kβ knockout or the double knockout mice to provide explanation for the lack of effect we observed here.

Decreased bacterial uptake in itself suffices to explain the increased mortality observed in the PIP5K$\alpha^{-/-}$ mice. To illustrate this point, *Yersina* lacking active YopE are not capable of causing pathogenesis even at very high levels of inoculation (Black and Bliska, 2000), whereas the 40% decrease in phagocytosis caused by active YopE expression triggers a pathogenic outcome at sufficiently high levels of inoculation. The further 30% decrease in phagocytic rate that we observe here for the PIP5K$\alpha^{-/-}$ macrophages would be anticipated to accelerate bacterial replication, converting a survival inoculation into a lethal one. Nonetheless, the host response is more complex than the innate immune component of phagocytosis alone: two cytokines, TNFα and IFNγ, have been identified as being critical in the resistance to *Yersinia* deep tissue dissemination and proliferation in the setting of significant but subpathogenic levels of inoculation. Neutralization of these cytokines leads to uncontrolled bacterial replication and subsequent death (Autenrieth and Heesemann, 1992). The levels of TNFα release appeared normal, but IFNγ release was decreased, despite normal T-cell recruitment to the spleen. We can not rule out the possibility that the PIP5K$\alpha^{-/-}$ T-cells have a defect in

regulated exocytosis of IFNγ. However, such a mechanism is not suggested by our prior report on mast cells performing regulated exocytosis, and thus we favor the hypothesis that the T-cells are being inadequately stimulated by the macrophages and dendritic cells, since decreased phagocytic uptake of the bacteria would lead to decreased antigen presentation, and this in combination with decreased cell-surface MHC class II expression by the macrophages and dendritic cells could lead to the proportional but blunted T-cell response at every level of bacterial infection. Taken together, these findings describe a disruption in the PIP5K$\alpha^{-/-}$ mice of progression from the innate immune response to the adaptive one during *Yersina* infection.

The blunted cell surface MHC II expression of proteins on PIP5K$\alpha^{-/-}$ macrophages and dendritic cells was unexpected. It will be interesting to explore the mechanism underlying this response, which could involve a novel role for PIP_2 synthesis in egress of MHC II proteins from the *cis*-Golgi, or a novel role related to rates of MHC II turnover during cycling between the plasma membrane and compartments in which it acquires processed peptides.

The shift in ratio of bacteria bound to the outer surface of the macrophages versus being internalized may have an additional consequence. The route of enteropathogen dissemination into deep tissues is not well understood (Barnes et al., 2006) - the two main hypotheses are that the bacteria travel either as free agents to the deep tissues, or that they are carried to the deep tissues by macrophages and related cells. It is possible that the PIP5K$\alpha^{-/-}$ macrophages act as cargo carriers to the distal tissues for bound but un-phagocytosed bacteria that subsequently detach and replicate locally.

Finally, in preliminary studies, we have observed that the PIP5K$\alpha^{-/-}$ mice appear *less* susceptible to infection by *Listeria monocytogene*, a gram-positive pathogen that lacks Yop proteins and replicates intracellularly. This finding suggests that the requirement for PIP5Kα may depend on the invasive nature of the infectious organism.

Fig. 2. 1. PIP5Kα$^{-/-}$ macrophages phagocytose fewer Y. pseudotuberculossis in comparison to wild-type BMDM.

A) RNA was extract from macrophages derived from wt or PIP5Kα$^{-/-}$ mice, and levels of PIP5Kα, β, and γ message were detected by reverse transcription followed with PCR. B) BMDMs were incubated with GFP-expressing *Y. pseudotuberculosis* or its virulence plasmid-cured derivative (Yop^{null}) at a MOI of 20 for 20min and then washed with PBS and fixed. Bacteria bound to the surface of the macrophages were labeled using anti-*Y. pseudotuberculosis* and appear blue. F-actin staining using rhodamine-phalloidin was used to visualize macrophage actin (red). C) Bacterial uptake (phagocytic index) was determined for each experiment using the following calculation: %uptake = [internalized *Yersinia* (green color) / total *Yersinia* (internal *Yersinia* + extracellular *Yersinia* (blue)]. Bacterial binding was defined as the total number of cell-associated bacteria (internal + external) relative to the number of macrophages. D) Wt and mutant (expressing inactive alleles of Yops J, H, E, and T) *Y. pseudotuberculosis* denoted mJTEH were cultured in low calcium and high magnesium to up-regulate Yop expression and incubated with BMDM at a MOI of 20. The phagocytic index was determined as above. Data are expressed as the mean percentage obtained from three independent experiments. Significance of results was determined by unpaired Student's test. **, $P < 0.01$.

Fig. 2. 1.

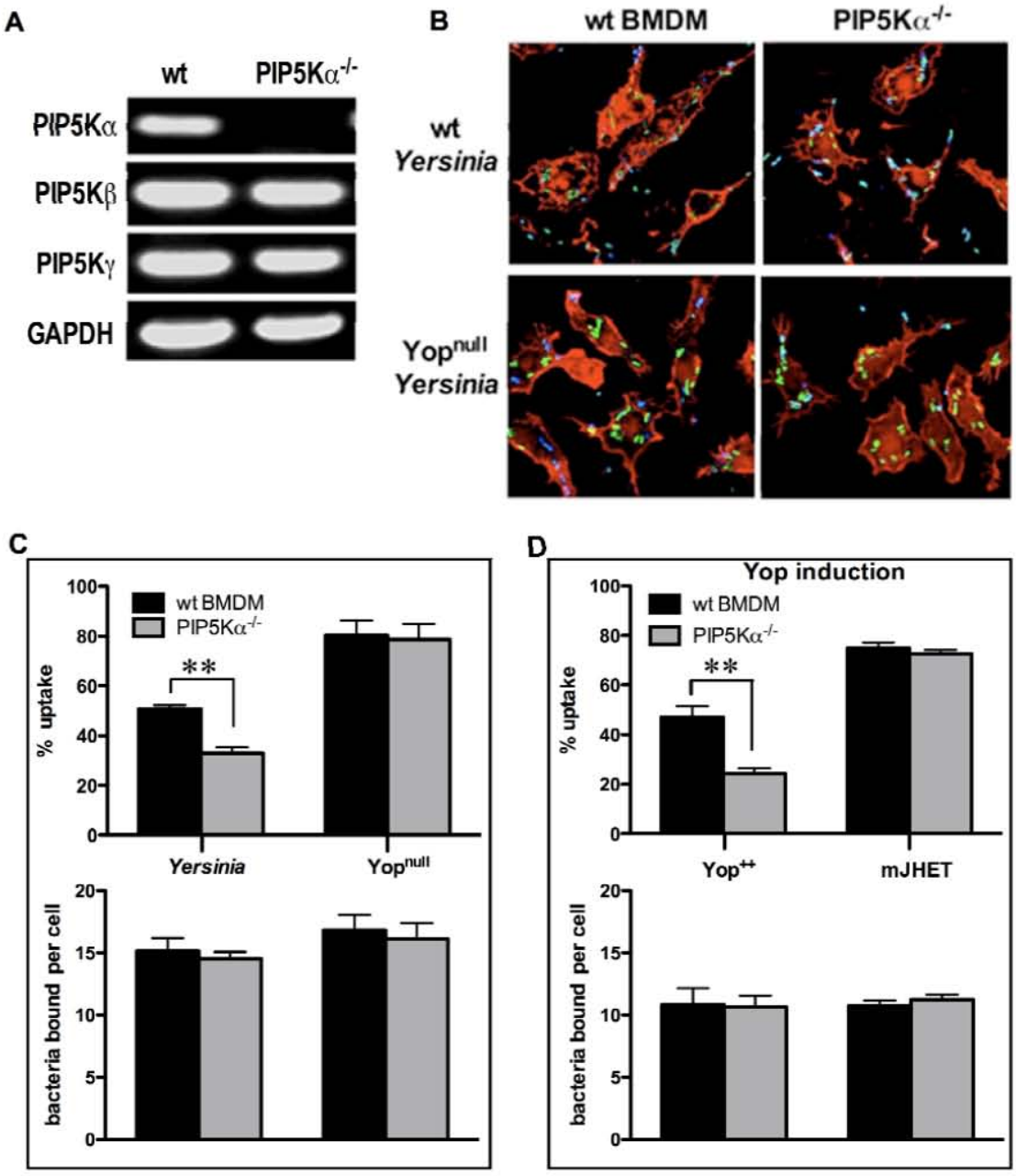
A
wt
PIP5Kα-/-
PIP5Kα
PIP5Kβ
PIP5Kγ
GAPDH
B
wt BMDM
PIP5Kα-/-
wt Yersinia
Yopnull Yersinia
C
wt BMDM
PIP5Kα-/-
% uptake
**
Yersinia
Yopnull
bacteria bound per cell
D
Yop induction
wt BMDM
PIP5Kα-/-
% uptake
**
Yop++
mJHET
bacteria bound per cell

Fig. 2. 2. Deficiency in PIP5Kα results in decreased Y. pseudotuberculosis uptake when Rac1 is inhibited. A) Macrophages derived from wt or PIP5K$\alpha^{-/-}$ mice were incubated with wt *Y. pseudotuberculosis* or with *Y. pseudotuberculosis* which the genes encoding YopE, YopT or YopH genes had been mutated to eliminate their catalytic activity, and the phagocytic index determined as above. The lower panel shows the bacterial binding per cell. B) Macrophages were pre-treated with vehicle or the Rac1 inhibitor NSC23766 (100 μM) for 4 hours and then incubated with the YopE catalytic-inactive mutant *Yersinia* (YopE^{ina}) to assess uptake. *, $P < 0.01$. Data are mean ± SD from triplicate experiments.

Fig. 2. 2.

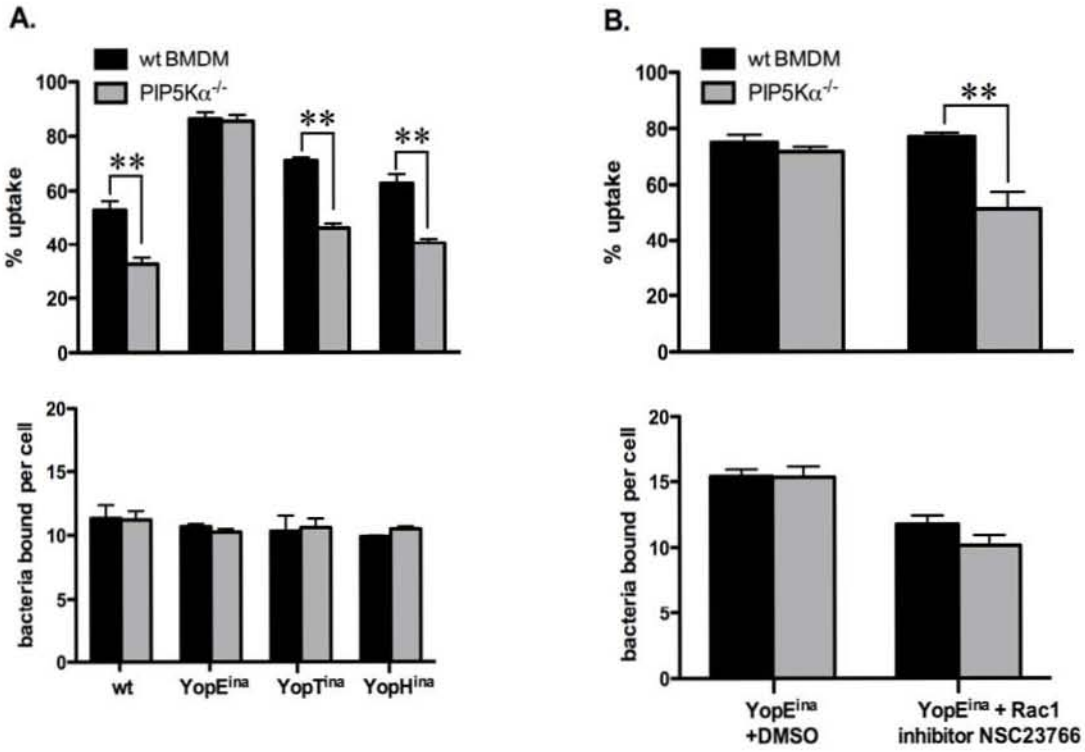
A.
wt BMDM
PIP5Kα-/-
% uptake
100
80
60
40
20
0
**
**
**
bacteria bound per cell
20
15
10
5
0
wt
YopEina
YopTina
YopHina
B.
wt BMDM
PIP5Kα-/-
% uptake
100
80
60
40
20
0
**
bacteria bound per cell
20
15
10
5
0
YopEina +DMSO
YopEina + Rac1 inhibitor NSC23766

Fig. 2. 3. Normal signaling responses and cytokine production by PIP5Kα$^{-/-}$ macrophages.

A) BMDMs from wt or PIP5Kα$^{-/-}$ mice were exposed to wild-type or Yop^{null} *Y. pseudotuberculosis* at a MOI of 20 for the indicated times. The cells were lysed and analyzed by immunobloting for ERK, phosphorylated ERK, p38, phosphorylated p38, JNK, phosphorylated JNK, and IκB. α-tubulin was used as a loading control. A very subtle decrease in phosphorylation is observed in knockout BMDMs in response to *Yersinia* exposure at 20min (lane 3) in comparison to wt BMDM (lane 4) in the representative experiment shown; however, this difference was not reproduced in two other experiments performed (not shown). B and C) Quantitation of ERK and IκB on western blots (n=3 experiments). (D) PIP5Kα$^{-/-}$ and wt BMDMs were incubated with wt *Y. pseudotuberculosis* for 20 min, and the supernatant was collected 4 hours after infection. Cytokine levels were measured using cytokine antibody arrays from RayBiotech. Data were analyzed using Raybio antibody array analysis tool.

Fig. 2. 3.

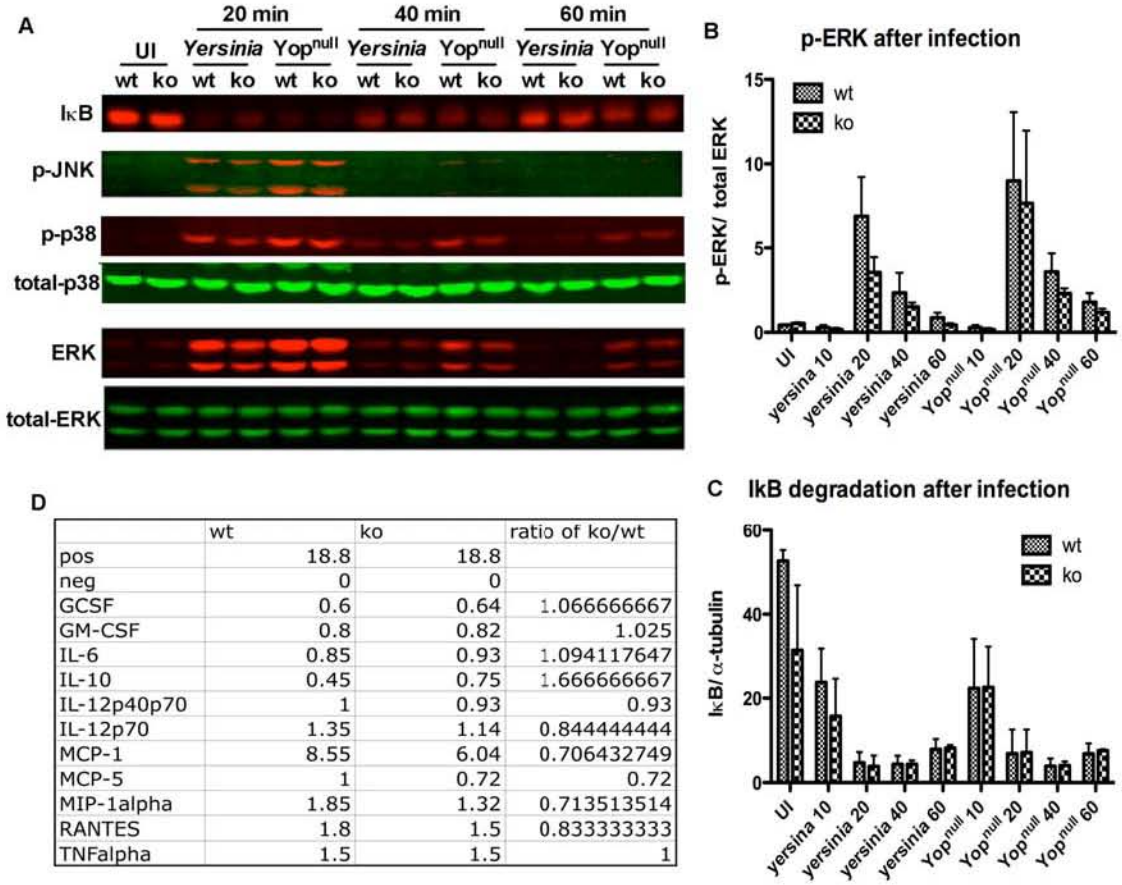

	wt	ko	ratio of ko/wt
pos	18.8	18.8	
neg	0	0	
GCSF	0.6	0.64	1.066666667
GM-CSF	0.8	0.82	1.025
IL-6	0.85	0.93	1.094117647
IL-10	0.45	0.75	1.666666667
IL-12p40p70	1	0.93	0.93
IL-12p70	1.35	1.14	0.844444444
MCP-1	8.55	6.04	0.706432749
MCP-5	1	0.72	0.72
MIP-1alpha	1.85	1.32	0.713513514
RANTES	1.8	1.5	0.833333333
TNFalpha	1.5	1.5	1

Fig. 2. 4. Neutrophil recruitment and bacterial killing is unaltered in PIP5K$\alpha^{-/-}$ mice. A) Thioglycollate-elicited neutrophils from wt or PIP5K$\alpha^{-/-}$ mice were incubated with wt *Y. pseudotuberculosis* at a multiplicity of infection (MOI) of 20 for 1.5 hours. Viable bacteria were quantitated using serial dilution plating. Average of three independent experiments is presented. B) Splenocytes isolated from wt (circles) or PIP5K$\alpha^{-/-}$ (open squares) mice innoculated with 5×10^8 CFU of wt *Y. pseudotuberculosis* /mouse were analyzed at day 3 or 6 after infection by FACS analysis using anti-Gr1 to label neutrophils.

Fig. 2. 4.

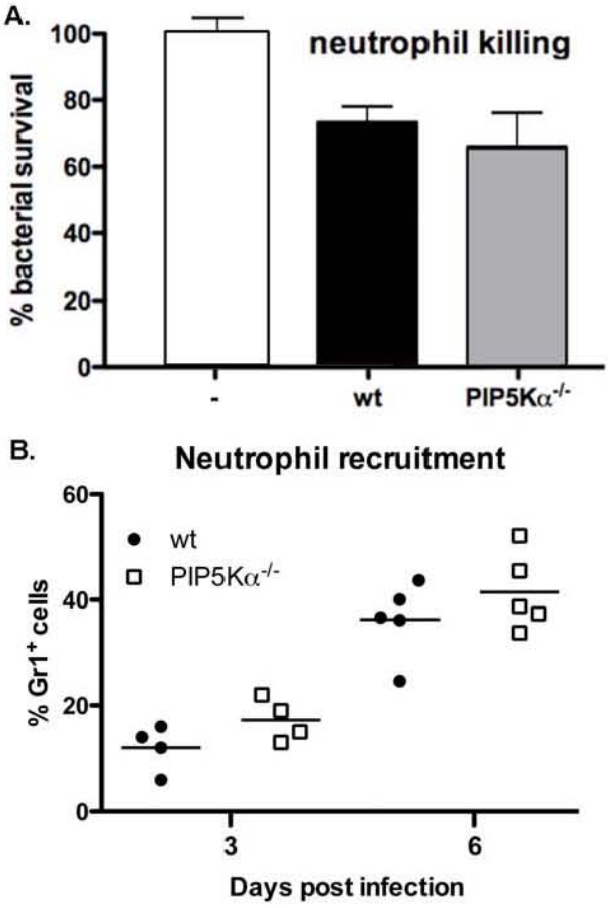
A.
neutrophil killing
% bacterial survival
100
80
60
40
20
0
-
wt
PIP5Kα-/-
B.
Neutrophil recruitment
% Gr1+ cells
60
40
20
0
wt
PIP5Kα-/-
3
6
Days post infection

Fig. 2. 5. PIP5Kα$^{-/-}$ mice exhibit elevated susceptibility to Y. pseudotuberculosis infection.

A) Age-matched female wt mice (filled circles; n=20) and PIP5Kα$^{-/-}$ mice (open squares; n=18) were orogastrically inoculated with 5×10^8 CFU of wt *Y. pseudotuberculosis* (strain IP32777) /mouse and monitored for 21 days. The data displayed are the aggregate of three independent experiments, each of which yielded similar outcomes. The difference between the curves is statistically significant, *P= 0.0009* (Logrank test). B&C) Age-matched female wt mice (circles) and PIP5K$^{-/-}$ mice (squares) were infected as A. The mice were sacrificed 3 or 6 days post-infection and the mesenteric lymph nodes (MLN) (C) and spleens (B) homogenized and plated in serial dilution to quantitate bacterial load. Symbols represent the $\log_{10}$CFU/ tissue from individual mice. Data shown are the summary of 2-3 independent experiments at each time point.

Fig. 2. 5.

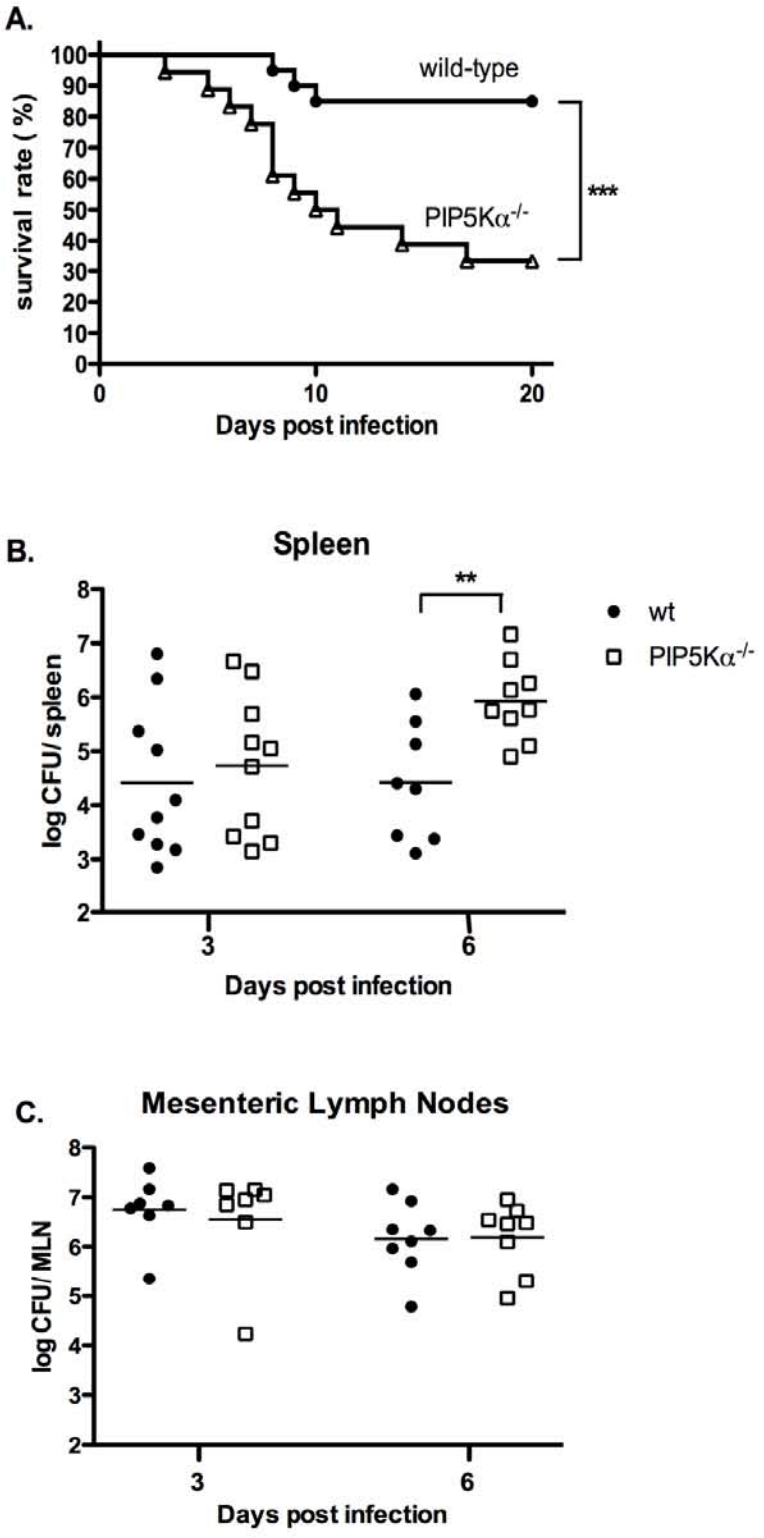
A.
survival rate (%)
100
90
80
70
60
50
40
30
20
10
0
0
10
20
Days post infection
wild-type
PIP5Kα-/-
***
B.
Spleen
log CFU/ spleen
8
7
6
5
4
3
2
3
6
Days post infection
**
wt
PIP5Kα-/-
C.
Mesenteric Lymph Nodes
log CFU/ MLN
8
7
6
5
4
3
2
3
6
Days post infection

Fig. 2. 6 IFNγ levels are suppressed in infected PIP5Ka$^{-/-}$ mice.

PIP5K$\alpha^{-/-}$ and wt mice were orally infected with 5×10^{8} CFU of *Y. pseudotuberculosis* /mouse. At days 3 and 6 after infection, sera were collected, and the spleens were dissected to quantify bacterial load after homogenization and serial dilution. Serum TNFα(A) or IFNγ(B) levels in pg/ml were measured by ELISA and are plotted in relationship to the levels of bacterial colonization in the spleens after logarithmic transformation.

Fig. 2. 6.

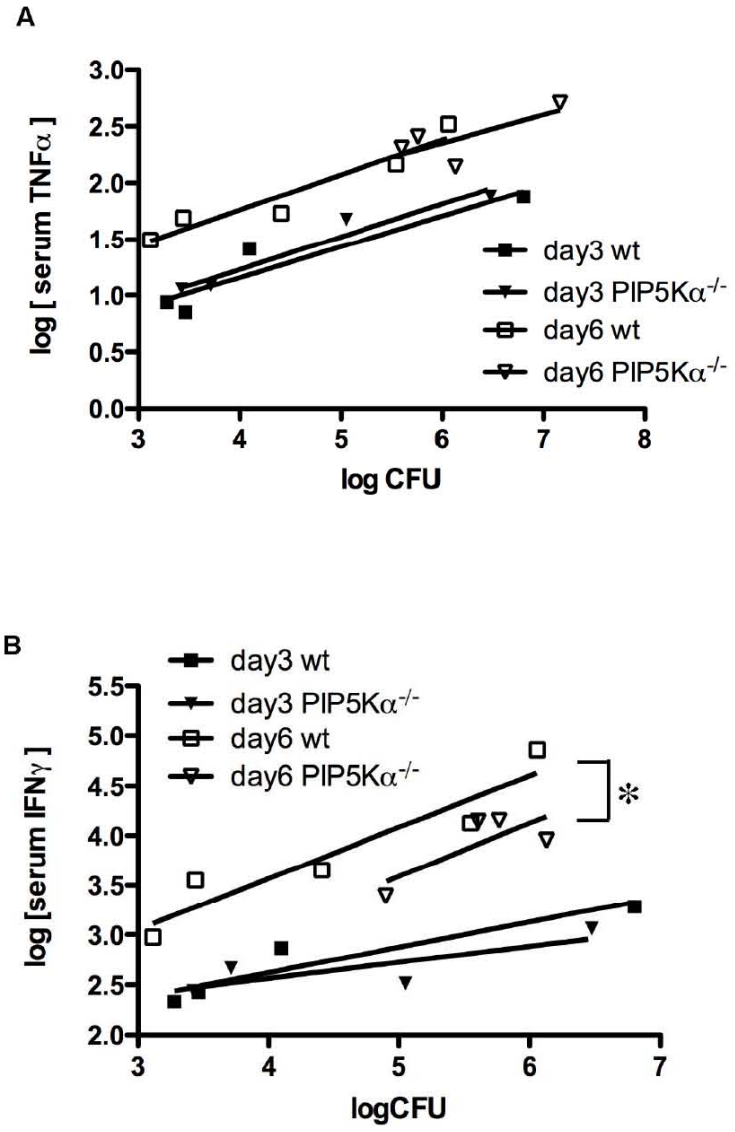
A
log [serum TNFα]
3.0
2.5
2.0
1.5
1.0
0.5
0.0
3
4
5
6
7
8
log CFU
day3 wt
day3 PIP5Kα-/-
day6 wt
day6 PIP5Kα-/-
B
log [serum IFNγ]
5.5
5.0
4.5
4.0
3.5
3.0
2.5
2.0
3
4
5
6
7
logCFU
day3 wt
day3 PIP5Kα-/-
day6 wt
day6 PIP5Kα-/-
*

Fig. 2. 7. T cell populations in spleens of wt and PIP5K$\alpha^{-/-}$ mice.

Single cell suspensions were made from spleens, and stained by anti-CD4, anti-CD8, and anti-CD3 antibodies followed by FACS analysis. A). % $CD4^+$ or $CD8^+$ T cells in spleens of uninfected mice. B). % $CD3^+$ cells in spleens on day 3 or day 6 post infection. C). % $CD4^+$ or $CD8^+$ T cells in spleens on day6 post infection.

Fig. 2. 7.

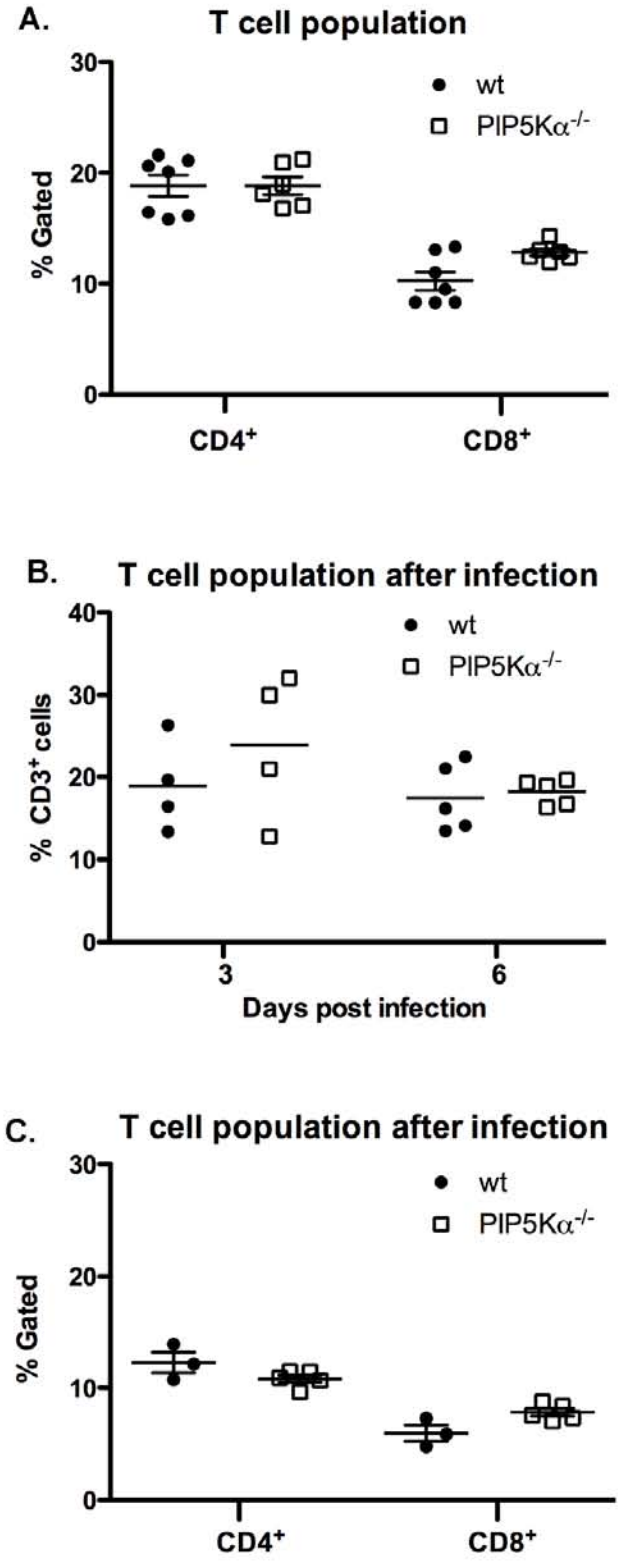
A.
T cell population
wt
PIP5Kα-/-
% Gated
30
20
10
0
CD4+
CD8+
B.
T cell population after infection
wt
PIP5Kα-/-
% CD3+ cells
40
30
20
10
0
3
6
Days post infection
C.
T cell population after infection
wt
PIP5Kα-/-
% Gated
30
20
10
0
CD4+
CD8+

Fig. 2. 8. Lower MHC class II levels on the surface of APCs from PIP5K$\alpha^{-/-}$ mice as compared to wt.

A) Bone marrow cells from wt and PIP5K$\alpha^{-/-}$ mice were treated in vitro with GM-CSF for 7 days and then were stained with FITC conjugated anti-CD11c and AlexaFluor647 conjugated anti-I-A/I-E (MHC class II) antibodies. Live cells were gated to be PI-negative in flow cytometry analysis. A representative image is shown. B) The percentage of MHC II class II positive cells among all the CD11c-positive cell is plotted. Data shown are the mean and SEM of three independent experiments, p value is determined by paired t-test after log transformation. C) Bone marrow derived macrophages (BMDMs) were treated with IFNγ or vehicle for 24 hours and stained by AlexaFluor647 anti-MHC II. PI was used to exclude cell death events. Representative image of FACS analysis is shown. D) The geometric means of fluorescent intensity. Data shown are the mean and SEM of three independent experiments. P values were determined by 2-way ANOVA. E) wt and PIP5K$\alpha^{-/-}$ BMDMs were incubated with 100 U/ml of IFNγ for the indicated time, and lysed with 1x Laemmli sample buffer. Phosphorylation of stat-1 at Y701 or S727 was analyzed by immunoblotting using specific antibodies. Total stat1 and α-tubulin were also used as loading controls.

Fig. 2. 8.

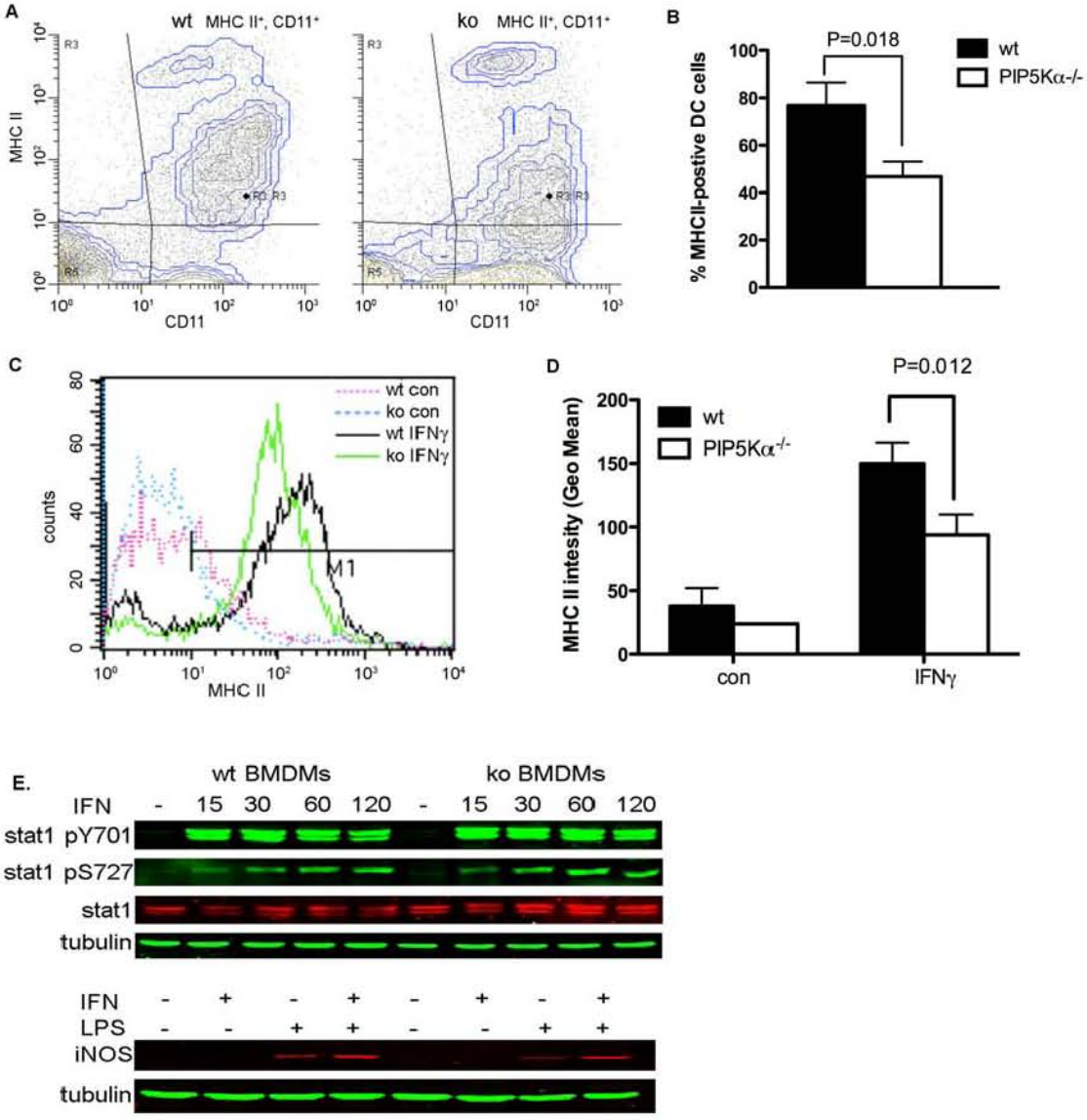
A
wt MHC II+, CD11+
ko MHC II+, CD11+
MHC II
CD11
B
P=0.018
wt
PIP5Kα-/-
% MHCII-postive DC cells
C
wt con
ko con
wt IFNγ
ko IFNγ
counts
M1
MHC II
D
P=0.012
wt
PIP5Kα-/-
MHC II intesity (Geo Mean)
con
IFNγ
E.
wt BMDMs
ko BMDMs
IFN - 15 30 60 120 - 15 30 60 120
stat1 pY701
stat1 pS727
stat1
tubulin
IFN
LPS
iNOS
tubulin

Fig. 2. 9. PIP5Kα regulates MHC II levels on the surface of APC in post-translational steps.

IFNγ-treated BMDMs from wt (A) or PIP5K$\alpha^{-/-}$ (B) mice were immunolabeled with anti-MHC II antibody and AlexaFluor488 conjugated secondary antibody without permeabilization to label surface MHC II, or permeailized with 0.1% Triton X-100 to detect cytosolic MHC II (C and D). Results shown are the representative of two independent experiments. E) Wt and PIP5K$\alpha^{-/-}$ BMDMs were treated with 100 U/ml for 24 hours, and then MHC class II expression levels were measured by western blotting.

Fig. 2. 9.

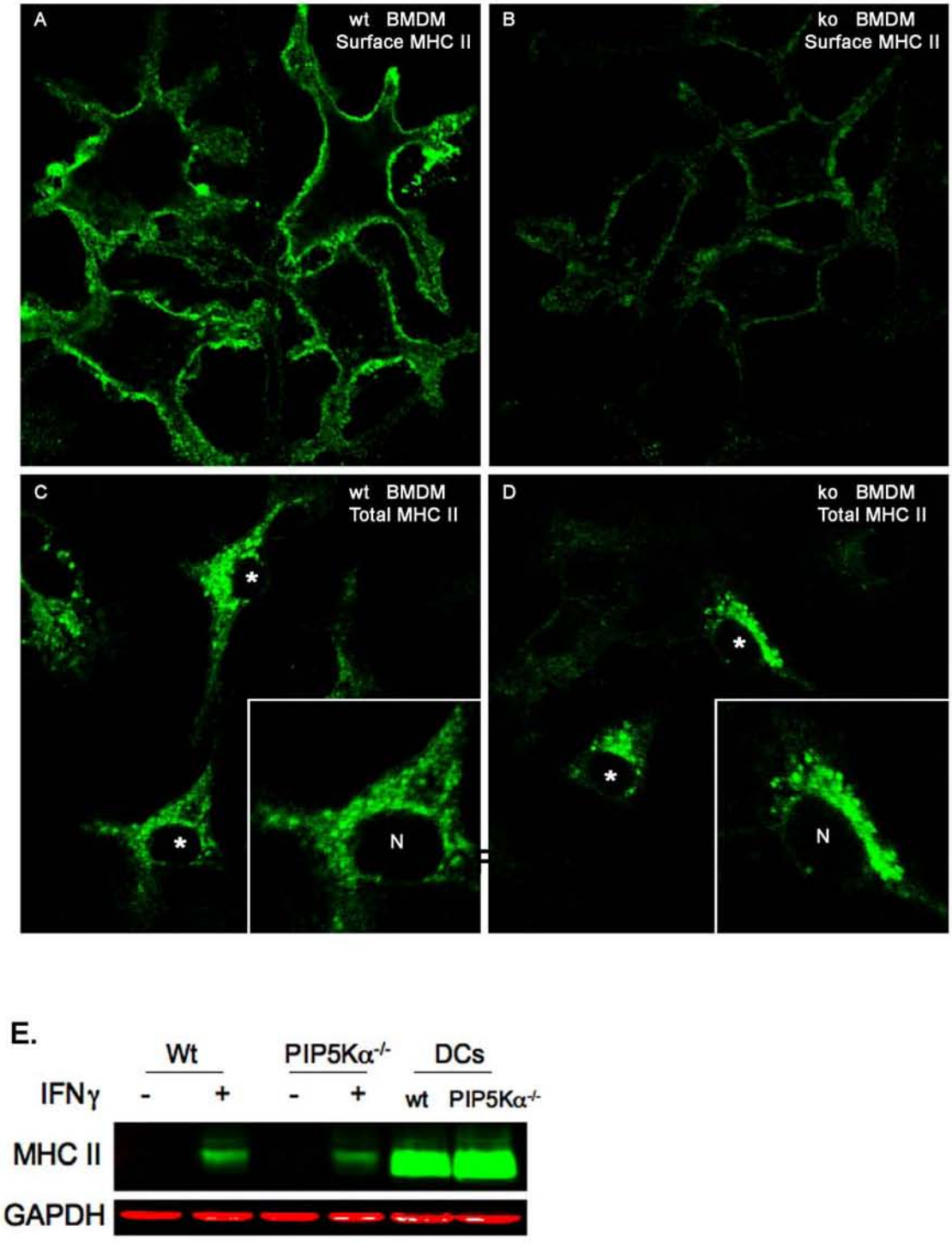
A
wt BMDM
Surface MHC II
B
ko BMDM
Surface MHC II
C
wt BMDM
Total MHC II
D
ko BMDM
Total MHC II
*
N
E.
Wt
PIP5Kα-/-
DCs
IFNγ
-
+
-
+
wt
PIP5Kα-/-
MHC II
GAPDH

Fig. 2. 10. MHC II in PIP5K$\alpha^{-/-}$ macrophages localizes to the cis-Golgi.

Wt (A, C) and PIP5K$\alpha^{-/-}$ (B, D) BMDMs were treated with IFNγ or vehicle for 24 hours, fixed, permeabilized using 0.1% Triton X-100, and stained by anti-MHC II and anti-GM130 (A, B) or anti-TGN38 (C, D), anti-EEA1(E), and anti-LAMP1(F). Representative cells are shown.

Fig. 2. 10.

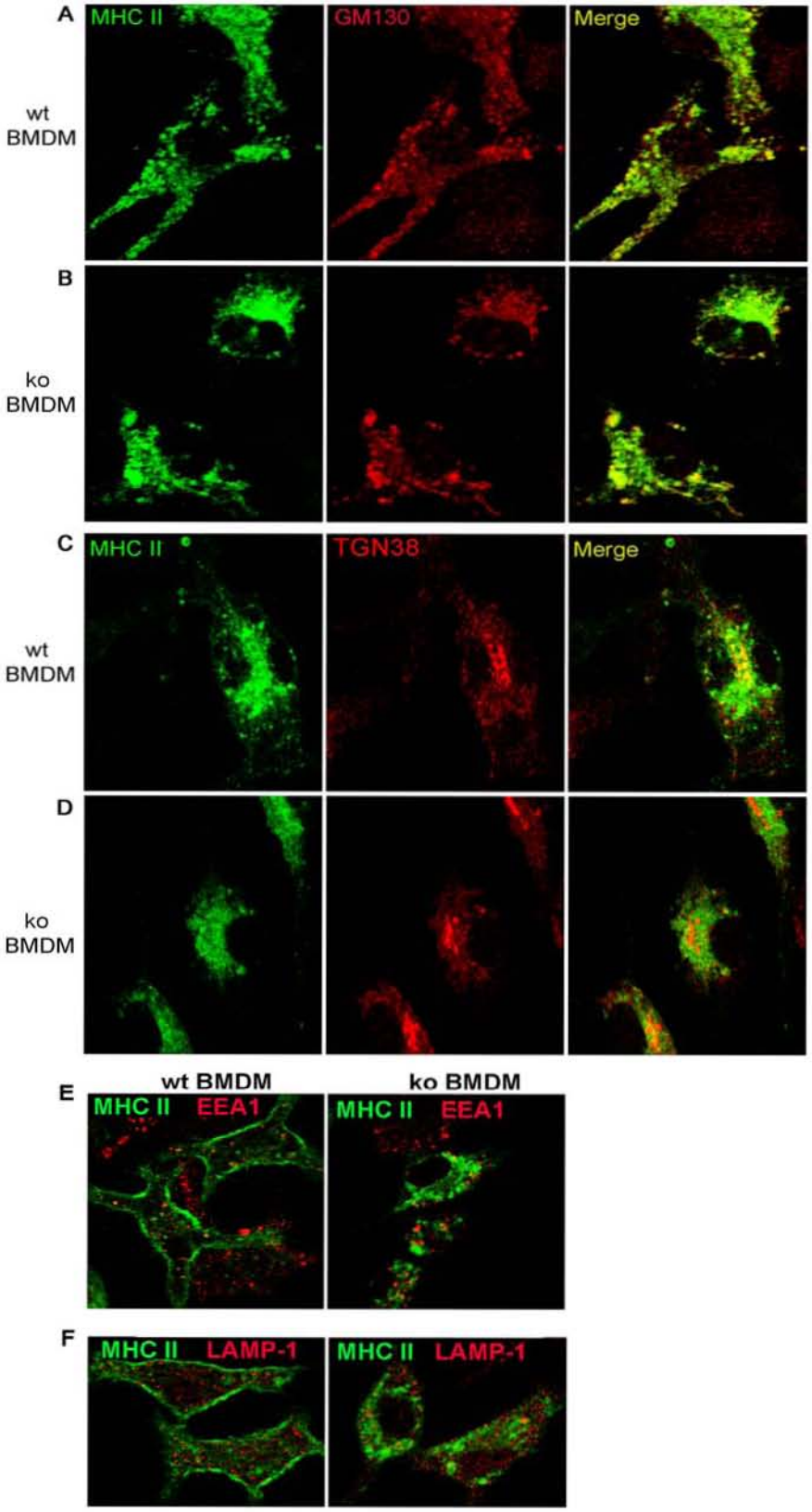
A
MHC II
GM130
Merge
wt
BMDM
B
ko
BMDM
C
MHC II
TGN38
Merge
wt
BMDM
D
ko
BMDM
E
wt BMDM
ko BMDM
MHC II
EEA1
MHC II
EEA1
F
MHC II
LAMP-1
MHC II
LAMP-1

Chapter3

Characterize the small molecule inhibitor of PLD, FIPI

The majority of this chapter is adapted from the paper published on Molecular Pharmacology. Fig.3.8 is adapted from Nishikimi et al., 2009.

3.1 Summary

The signaling enzyme Phospholipase D (PLD) and its product phosphatidic acid (PA), a lipid second messenger, are implicated in many cell biological processes including Ras activation, vesicle trafficking and endocytosis, cytoskeleton reorganization, cell migration and chemotaxis. Several PLD inhibitors such as 1-butanol have been described by far, however, they either work indirectly or do not effectively reduce PA accumulation. Thus, their use may result in PLD-independent deleterious effects. Consequently, identification of potent specific small molecule PLD inhibitors would be an important advance for the field. We examine one here, denoted "FIPI", which was identified recently in an *in vitro* chemical screen for PLD2 inhibitors, and show that it blocks *in vivo* PA production with sub-nM potency. Our data also demonstrate that FIPI inhibits PLD activity within 30 min, and its inhibitory effect is partially reversible. Surprisingly, several biological processes such as insulin secretion, which are blocked by 1-butanol, are not affected by FIPI, suggesting the need for re-evaluation of proposed roles for PLD. However, FIPI does inhibit PLD regulation of F-actin cytoskeleton

reorganization, cell spreading, and chemotaxis, indicating potential utility for it as a therapeutic for autoimmunity and cancer metastasis.

3.2 Introduction

The PLD superfamily extends from viruses and bacteria to humans (Jenkins and Frohman, 2005). Mammalian PLDs have been shown to be involved in many cell biological processes including Golgi budding (Chen et al., 1997; Yang et al., 2008), Ras activation (Mor et al., 2007; Zhao et al., 2007), mitochondrial dynamics (Choi et al., 2006b), cell spreading (Du and Frohman, 2008), F-actin stress fiber formation (Cross et al., 1996; Kam and Exton, 2001), and dynamin-driven EGFR endocytosis (Lee et al., 2006). Classic members of the superfamily, such as PLD1 and PLD2 in humans, perform a transphosphatidylation reaction using water to hydrolyze phosphatidylcholine (PC) to generate PA. More divergent family members can use other lipids or even DNA as substrates, or perform synthetic reactions by fusing lipids via a primary hydroxyl group using the transphosphatidylation mechanism (Sung et al., 1997a). Primary alcohols, such as 1-butanol, are used preferentially over water by classic PLDs, and cause PLD to generate phosphatidyl (Ptd)-alcohol instead of PA. The presence of as little as 0.1% butanol in cell culture media has been shown to inhibit many of the cell biological processes listed above, from which it has been inferred that these events are driven by PLD (reviewed in McDermott et al., 2004).

PA's mechanism of action is complex. It can function as a membrane anchor to recruit and/or activate proteins that encode specific PA-binding domains, can exert biophysical effects on membranes when the concentration is increased locally since it is a negatively-charged lipid, or can be converted to other bioactive lipids such as diacylglycerol (DAG) or lysoPA. Ptd-Butanol (Ptd-But) is thought to be unable to recruit or activate target proteins, to affect membrane structure, or to be able to serve as a

substrate to generate DAG or LysoPA. Nonetheless, despite 1-butanol's widespread utilization over the past 20 years, concerns have been raised as to whether it fully blocks PA production at the concentrations used (Skippen et al., 2002a), and whether butanol and Ptd-But have other effects on cells that extend beyond inhibiting PA production (reviewed in Huang et al., 2005; Huang and Frohman, 2007). Furthermore, cellular levels of PA are dictated by convergent synthetic and degradative enzymes that, in addition to the PLD pathway, include *de novo* synthesis by acylation of glycerol 3-phosphate and phosphorylation of diacylglycerol, and dephosphorylation catalyzed by membrane-bound and soluble phosphatases. Effects of primary alcohols on these enzymes are largely unexplored.

Several other inhibitors of PLD activity have been described including ceramide (Vitale et al., 2001), neomycin (Huang et al., 1999), and natural products (Garcia et al., 2008), but these compounds either sequester the requisite PLD co-factor Ptd-Inositol 4,5-bisphosphate (PIP_2), work indirectly to inhibit PLD activity, or have many other effects on signaling pathways that complicate their use and interpretation (reviewed in Jenkins and Frohman, 2005). Recently, a small molecule screen to identify inhibitors of human PLD2 using an *in vitro* biochemical assay identified halopemide, a dopamine receptor antagonist, as a modest inhibitor of PLD2 activity, and the analog 5-Fluoro-2-indolyl des-chlorohalopemide (denoted here, "FIPI") as being even more potent (Monovich et al., 2007). We show here that FIPI is a potent *in vivo* inhibitor of both PLD1 and PLD2, setting the stage for a new era of exploration and validation of cell biological roles for mammalian PLD. We provide evidence that supports several proposed functions for

PLD, but also demonstrate a lack of support for others, raising questions about prior studies that relied on primary alcohol-mediated inhibition to define *in vivo* PLD function.

3. 3 Materials and methods

PLD Inhibitor

5-Fluoro-2-indolyl des-clorohalopemide (FIPI) and benzyloxycarbonyl-des-chlorohalopemide were synthesized and described (compounds 4k and 4g from Monovich et al., 2007) and purified by preparative HPLC (YMC S5 ODS column, 20 x 100 mm, Waters, Inc.) using a gradient of 20% aqueous methanol to 100% methanol with 0.1% trifluoroacetic acid. The compounds were confirmed to have the correct structure by proton NMR and electrospray ionization mass spectrometer and they gave single, symmetrical peaks on HPLC analysis.

Cell culture and transfection

Tetracycline (Tet)-inducible Chinese hamster ovary (CHO) stable cells expressing wild-type PLD1 and PLD2 were generated using the T-Rex system (Du et al., 2004; Su et al., 2006) and cultured in F-12 medium containing 10% Tet-free fetal bovine serum (FBS) from Clontech. Recombinant protein expression was induced by adding 1 μg/ml doxcycline (Dox) for 16-24 hours. Miferpristone-inducible 3T3 cells expressing Flag-tagged MitoPLD were generated using the GeneSwitch system and MitoPLD induced by addition of 1 nM miferpristone for 16-24 hours. Bone marrow-derived macrophages (BMDM) were isolated from mice as previously described (Zhang et al., 2005). Min6 cells were cultured in DMEM supplemented with 10% FBS, 1% 2-mercaptoethanol, L-Glutamate and Pen/Strep. Other cell lines were cultured in DMEM containing 10% FBS. For transfection, cells were grown on coverslips in 24-well plates and transfected with 0.5 μg DNA per well using LipofectAMINE Plus. Six hours post-transfection, the media

were replaced with fresh growth medium and the cells incubated a further 24 hours before used for other assays.

PLD activity assay

The *in vitro* PLD activity assay was performed using an *in vitro* head-group release assay as previously described (Morris et al., 1997). *In vivo* PLD activities were determined using transphosphatidylation to measure the accumulation of phosphatidylbutanol in intact cells (Hammond et al., 1995; Morris et al., 1997). CHO cells were incubated with 2 μCi/ml [3H]palmitic acid as well as 1 μM doxycycline used for induction of PLD1 and PLD2 expression for 24 hours. Induction of PLD2 expression usually increases activity about 10 folds, however induction of PLD1 just increases activity 1.5 to 2 fold because its activation involve some co-factor such as PKC. Thus, PMA is used to mainly activate PLD1. For PLD2 activity dose curve, CHO cells were incubated with different concentrations of FIPI (diluted from a 7.5 mM stock concentration in DMSO) or medium containing a matching concentration of DMSO for 30 min before addition of 0.3% 1-butanol for another 30 min. Un-induced cells were used as control. For PLD1 and endogenous activity dose curve, 100nM of PMA was added with 0.3% of 1-butanol. PLD1 cells or un-induced cells were used as basal control respectively. For time course study, cells were preincubated with 100 nM of FIPI for 5, 10, 15, or 30 min followed by a 10 min incubation with 0.3% 1-butanol. For recovery experiments, cells were incubated with 2 μCi/ml [3H]palmitic acid, and then switched to fresh growth medium containing 50 μg/ml cyclohexamide. 30 min later, one set of cells were treated with 100 nM FIPI for 30 min followed by three washes with PBS and addition of fresh growth medium containing cyclohemimide. The cells were incubated for

1 hour or 8 hours. During the last 30 minutes, FIPI was added to a second set of cells, following which all of the sets of cells were assayed for PLD activity.

Immunofluorescent staining

Cells were fixed with 4% paraformaldehyde for 10 min followed by permeabilization with 0.1% Trition X-100. HA-tagged PLD1 and PLD2 proteins were detected by a monoclonal antibody (3F10) followed by secondary antibodies conjugated with Alexa 488. F-actin was stained by phalloidin conjugated with Rhodamine. Other proteins were GFP-tagged and visualized with green fluorescence. For glucose-stimulation assays, the cells were cultured in low glucose buffer or stimulated with high glucose for 30 min in the presence of 750 nM FIPI or DMSO. Images were taken using a Leica TCS SP2 spectral laser scanning confocal microscope with the Leica DMIRE2 inverted platform (Leica Microsystems, Heidelberg, Germany). Fluorescence intensity quantification was performed using Image J software (NIH; http://rsb.info.nih.gov/ij/).

Western blotting

Cells were lysed in 1x Laemmli sample buffer, and resolved by 10% SDS-PAGE. The blots were blocked with 1% casein in Tris-buffered saline (TBS). Western blotting with anti-phospho-ERK and total ERK (Sigma) and other primary antibodies (Cell signaling) was performed as suggested by the suppliers. The blots were developed using secondary antibodies conjugated with Alexa 680 or IRDye 800 (Rockland). Fluorescent signals were detected with an Odyssey infrared imaging system from LI-COR Biosciences.

Cell spreading

Cell spreading assays were performed as described previously (Du and Frohman, 2008). In brief, CHO cells were suspended by trypsinization, rested in the incubator for 2 hr, plated on fibronectin-coated coverslips for the indicated times, and fixed in 4% paraformaldehyde before processing for immunofluorescent staining.

Insulin secretion and quantification

Min6 cells cultured in 24 well plates were washed twice in KRBH (KCl: 4.74 mmol/L, NaCl: 125 mmol/L, $NaHCO_3$: 5 mmol/L, $MgSO_4$: 1.2 mmol/L, $CaCl_2$: 1 mmol/L, HEPES: 25 mmol/L, KH_2PO_4: 1.2 mmol/L, 2.5 mM glucose) buffer supplemented with 0.1% BSA. All wells were subsequently pre-incubated in Low glucose KRBH (2.5 mM glucose) buffer for 60 min. The buffer was then completely aspirated and fresh low glucose (control), or low glucose containing 75 nM or 750 nM FIPI inhibitor was added for an additional 30 min. After this preincubation period, fresh low glucose KRBH, high glucose KRBH (20 mM glucose) or high glucose KRBH buffer containing 75 nM or 750 nM FIPI inhibitor was added. After 60 min, all samples were collected and the cells were lysed in ethanol/acid (70% ethanol and 0.18 M HCL) and assayed for total insulin. Secreted and total insulin was measured using an ultra sensitive ELISA kit (Mercodia: 10115010) and BioRad plate reader.

Cell migration assay

HL-60 cells were induced to differentiate to dHL-60 with 1.75% DMSO to achieve the expression of the neutrophil phenotype (Lehman et al., 2006). dHL-60 were resuspended at 10^6 / ml in chemotaxis buffer (RPMI+ 0.5% BSA), and treated with 750 nM FIPI or DMSO for 1 hour. 200 μl were placed in the inserts of transwell plates that were separated from the lower wells by a 6.5-mm diameter, 5 μm pore membrane. 500 μl

of 10 nM fMLP in chemotaxis buffer was added into the lower wells of transwell plate. The transwell plates were incubated for 1 hour at 37°C. The number of cell that migrated to the lower wells was calculated by placing 10 μl aliquots on a hemocytometer and counting 4 fields. Each experiment was repeated at least 4 times.

3.4 Results

FIPI is a potent inhibitor of classical mammalian PLD

FIPI was reported to exhibit a 50% inhibitory concentration (IC_{50}) of 20 nM against PLD2 using an unpublished *in vitro* biochemical assay (Monovich et al., 2007). Using a well-established assay system, we have previously described biochemical characterization of recombinant PLD1 and PLD2 (Colley et al., 1997; Hammond et al., 1995; Hammond et al., 1997). When separated from cytoplasmic factors, PLD1 requires provision of a stimulator such as ARF or Rho small GTPases, or Protein Kinase C (PKC), whereas PLD2 exhibits constitutive activity, as shown in Fig. 3. 1A ("no DMSO" and "0" FIPI concentration). FIPI inhibited both PLD1 and PLD2 in a dose-dependent manner, with 50% loss of activity observed at approximately 25 nM. Thus, consistent with Monovich *et. al* (Monovich et al., 2007), FIPI is a potent concentration-dependent PLD2 inhibitor, and we show here that it inhibits PLD1 equally well under standard *in vitro* assay conditions.

We next examined FIPI potency *in vivo*, making use of CHO cell lines that inducibly overexpress PLD1 and PLD2 (Du et al., 2004; Su et al., 2006). PLD2-overexpressing cell lines exhibit high levels of activity under resting conditions, whereas PLD1-overexpressing cell lines require stimulation to trigger PLD1 activation (e.g. using PMA to activate endogenous PKC). FIPI was added into the cell culture media 1 hour prior to performing the PLD assay and was found to be a potent inhibitor of PLD2 with an IC_{50} of 10 nM (Fig. 3. 2B). PLD1 was inhibited even more strongly (IC_{50} = 1 nM), and parental cells stimulated with PMA to activate endogenous PLD1 and/or PLD2 exhibited half-maximal inhibition at 0.5 nM. Thus, FIPI efficiently crosses cell membranes and inhibits

PLD1 and PLD2 action on their endogenous substrate in the cytoplasmic environment. We also assayed a second analog, benzyloxycarbonyl-des-chlorohalopemide, which was reported to be much less potent against PLD2 in the *in vitro* assay (Monovich et al., 2007). We found that it displayed an IC_{50} of approximately 250 nM against PLD2 in the *in vivo* assay, confirming the essential structure-function relationship reported, although the degree of the difference in efficacy was less than described for the *in vitro* assay. These results also indicate that FIPI inhibits both the hydrolytic and transphosphatidylation activities of PLD1 and PLD2.

The classic PLD assay consists of adding 1-butanol to cells and measuring the production of Ptd-But (e.g. Fig. 3. 1B). To visualize PA production subcellularly, we employed a fluorescent PA sensor consisting of EGFP fused to a 40-amino acid PA-binding domain from the yeast Spo20 protein (Zeniou-Meyer et al., 2007). In resting cells, the majority of the sensor localizes to the nucleus (Fig. 3. 1C). In cells overexpressing PLD2, the sensor translocates in part to the plasma membrane and to intracellular membrane vesicles, presumably endosomes, which is where PLD2 resides (Du et al., 2004; Roth, 2004); however, no localization of the sensor was observed at these sites after addition of FIPI to the PLD2-overexpressing cells, indicating a lack of generation of PA by PLD2.

Finally, we examined FIPI action on MitoPLD, a highly divergent mammalian PLD superfamily member that hydrolyzes the lipid cardiolipin to generate PA (Choi et al., 2006b). In wild-type cells, mitochondria exist as both isolated small organelles and an extended tubular network (Fig. 3. 1D). Upon induction of MitoPLD overexpression, the mitochondria aggregate into a single peri-nuclear cluster (arrow) in a PA-dependent

manner. FIPI had no effect on this process, indicating that it does not block the catalytic activity of this related but distant family member. We also examined whether FIPI blocks yeast sporulation, a process known to be dependent on the activity of Spo14, the yeast homolog of classical mammalian PLD (Rose et al., 1995), but no inhibition of sporulation was observed (data not shown). Similarly, no inhibition was observed in an *in vitro* assay (Morris and Smyth, 2007) for autotaxin, a LysoPLD enzyme that hydrolyzes LysoPC to generate LysoPA but which is a member of an unrelated gene family (data not shown). Thus FIPI action appears restricted to PLD1 and PLD2, the classical family members of mammalian PLD.

Because of inherent limitations of the "exogenous substrate" *in vitro* PLD assay used in Fig. 1A, the mechanism by which FIPI inhibits PLD activity remains to be established. However, because FIPI inhibits both PLD1 and PLD2, the mechanism cannot involve interference with any of the selective activators of PLD1, and because the inhibition is selective for PLD1 and PLD2 over other PLD superfamily enzymes, a general effect on substrate accessibility can be discounted. These results suggest that FIPI is a direct inhibitor of the PC phosphodiesterase activity of PLD1 and PLD2.

FIPI blocks PLD activity within 15 min and its effect is partially reversible.

To examine the kinetics of inhibition, FIPI was added to PLD2-overexpressing cells for varying periods of time prior to beginning the *in vivo* PLD assay; 15 minutes was found to suffice to achieve complete inhibition (Fig. 3. 2A). Conversely, we examined the rate at which cells recover PLD activity after being exposed to FIPI (Fig. 3. 2B). PLD2-overexpressing cells were treated with cycloheximide to block new protein

production and then cultured with FIPI for 30 minutes at either the beginning or end of a 1 hour or 8 hour time period before being assayed. Cells exposed to FIPI that were then washed and cultured for 1 hour (dark bars) recovered 29% of their PLD2 activity, whereas cells that had an 8-hour post-exposure period of culture recovered 41% of their activity. Thus, FIPI is not an irreversible suicide inhibitor, but neither is it rapidly and completely reversed upon removal of the drug, suggesting that the FIPI binding site may be affected by PLD conformation in some unknown and potentially activity-dependent manner.

FIPI does not affect PLD subcellular localization, PIP_2 availability, or the actin stress fiber network.

Compounds that affect membrane properties and dislodge PLDs from the bilayer membrane surface, or that sequester PIP_2, the required co-factor for mammalian PLD, inhibit PLD activity indirectly. Changes in the actin cytoskeleton can also regulate PLD activity(Lee et al., 2001). We examined these possibilities for FIPI. PLD1's typical localization to peri-nuclear membrane vesicles and PLD2's typical localization to the plasma membrane were not affected by exposure to FIPI (Fig. 3. 3A), nor did FIPI decrease PIP_2 availability on the plasma membrane in PLD1- and PLD2-overexpressing cells as assessed using an EGFP-fused PIP_2 sensor (based on the PH domain of PLCδ, Fig. 3. 3B). Our data also showed that FIPI had no visible effect on cortical F-actin and stress fibers in quiescent cells (Fig. 3. 3C).

FIPI does not affect the upstream signaling of PLD.

PMA is commonly used stimulation to increase PLD activity and study the functions of PLD-generated PA. PLD1 was reported to translocate from peri-nuclear membrane to plasma membrane upon PMA stimulation. To check if FIPI affects the ability of PLD1 translocation upon stimulation, PLD1 overexpressed CHO cells were treated with FIPI and then stimulated with PMA. PLD1 were able to translocate to the plasma membrane in presence of FIPI (Fig. 3. 4A), suggesting that FIPI does not affect the downstream signaling of PMA and the ability of PLD1 in response to it.

PLD activation has been reported to lie downstream of AKT, p38, and / or ERK activation during signaling events (Brizuela et al., 2007; Kang et al., 2008; Varadharaj et al., 2006). nor did it inhibit AKT or ERK phosphorylation in the human breast cancer cell line MDA-MB-231 in response to serum stimulation (Fig. 3. 4B), or p38 or ERK phosphorylation in bone marrow-derived macrophages stimulated with lipopolysaccharide (LPS, Fig. 3. 4C). Taken together, we have not identified any mechanisms other than direct inhibition of the PLD protein catalytic activity that could account for FIPI's inhibitory actions *in vivo*.

Validation of FIPI as a specific and non-toxic PLD inhibitor through rescue of PLD2-driven suppression of membrane ruffling

PLD has been proposed to promote many cell biological processes including Golgi budding, Ras activation, and secretion. However, although demonstrating that FIPI inhibits these processes would be consistent with its action as a PLD inhibitor, off-target or non-specific toxicity would also constitute a possible explanation for the observed outcomes. To validate FIPI as a specific and non-toxic PLD inhibitor, we chose to test it

in a setting in which we could attempt to rescue a cell behavior that is normally suppressed by PLD action.

Stimulation of Cos-7 cells with PMA causes dramatic membrane ruffling, which is visualized as concentrated regions of F-actin at the edges and top surfaces of the cells (Fig. 3. 5A, top panel, arrows). Elevated expression of PLD2 suppresses this ruffling phenotype (Fig. 3. 5A, asterisk). However, culture of the PLD2-overexpressing cells in FIPI restored the ruffling phenotype, as shown in representative cells in the bottom panel of Fig. 3. 5A and in the quantitation provided in the bar graph.

We have also recently reported a role for PLD2 in early phases of cell spreading (Du and Frohman, 2008). Cell spreading is a critical process that occurs during inflammation and metastasis as cells cease traveling through the vasculature and undergo morphological changes required to adhere to extracellular matrix. We have shown that the PA generated by PLD2 at the plasma membrane in circulating cells inhibits the PA-binding and regulated enzyme myosin phosphatase, leading to increased myosin light chain phosphorylation, myosin activity, and myosin filament formation, which increases peripheral contractile force and hence cells having a spherical shape. Upon attachment, downregulation of PLD2 activity leads to myosin disassembly, decreased contractile force, and cell spreading. Overexpression of PLD2 prevents spreading, whereas PLD2 RNAi promotes accelerated spreading.

We performed a cell spreading assay in the presence and absence of FIPI. By 15 minutes after plating spherical CHO cells in suspension onto coverslips, the cells have started to spread but are still far from fully flattened (Fig. 3. 5B). In contrast, CHO cells pre-incubated in FIPI exhibit accelerated spreading (Fig. 3. 5B), phenocopying the result

observed for CHO cells stably expressing PLD2 RNAi (Du and Frohman, 2008). Similar results were observed at 7 minutes after plating, and treatment with FIPI additionally rescued PLD2 overexpression-mediated suppression of cell spreading (data not shown). Taken together, these data demonstrate that FIPI can be used to block actions of endogenous PLD2 in roles connected to cytoskeletal reorganization and cell trafficking.

Discordance between FIPI- and alcohol-mediated effects on glucose-stimulated insulin secretion

PLD has been linked to regulated exocytosis in many cell types based on the observation that the signaling-stimulated secretion is inhibited by 1-butanol (reviewed in Huang and Frohman, 2007; McDermott et al., 2004). The Min6 pancreatic β-cell line, which releases insulin in response to extracellular elevation of glucose, provides a typical example. Insulin release increases 4-5 fold with glucose stimulation (see Fig. 3. 6B), and the release is blocked efficiently in a dose-dependent manner by 1-butanol (Fig. 3. 6A). *tert*-butanol, the non-primary isomer of 1-butanol, is commonly used as a control in such assays to reveal potential non-specific or toxic side-effects, because *tert*-butanol is chemically similar to 1-butanol but can not be used as a substrate by PLD. As shown in Fig. 4A, *tert*-butanol has no effect or a much smaller effect on insulin release than 1-butanol does.

Surprisingly, no inhibition of glucose-stimulated insulin release was observed in the presence of FIPI (Fig. 3. 6B). Similarly, no effect of FIPI was observed on glucose-stimulated insulin release for pancreatic islets (not shown). To address whether FIPI was functioning effectively as a PLD inhibitor for the Min6 cells, we again employed the PA sensor (Fig. 3. 6C). In cells maintained under basal conditions, almost all of the sensor

localized to the nucleus rather than to the plasma membrane (arrowheads). Upon high glucose stimulation, the PA sensor became easily detected on the plasma membrane. However, no plasma membrane translocation of the PA sensor was detected in high glucose-stimulated cells pre-treated with FIPI, indicating that the PLD-mediated production of PA was inhibited ($p < 0.01$, Fig. 3. 6D). Again surprisingly, 1-butanol treatment did not block the glucose-stimulated plasma membrane translocation of the PA sensor. Taken together, these results suggest that eliminating all PLD activity in Min6 pancreatic β-cells does not affect glucose-stimulated insulin secretion, whereas although 1-butanol exposure does prevent insulin release, it does so through a mechanism other than inhibition of PA production.

FIPI inhibition of PLD blunts chemokine-stimulated neutrophil chemotaxis

HL60 cells differentiated into neutrophils respond to the chemokine fMLP through a signaling pathway involving p38 and ERK phosphorylation that directs them to undergo directional migration. 1-Butanol has been reported to inhibit both the signaling pathways involving p38 (Bechoua and Daniel, 2001) and ERK and the end result of chemotactic movement (Carrigan et al., 2007). Using this model system, we confirmed that 1-butanol does inhibit fMLP-triggered p38 and ERK phosphorylation (84% decrease, Fig. 3. 7A); however, consistent with the finding shown in Fig. 3. 4C for other cell types and stimulators, no inhibition of the phosphorylation was observed in the presence of FIPI. The quantitation of p38 phosphorylation is shown in Fig. 3. 7B. Nonetheless, FIPI inhibition of PLD did diminish fMLP-directed chemotaxis ($p<0.01$, Fig. 3. 7C), validating this role for PLD function and suggesting PLD regulates chemotaxis via mechanisms distinct from affecting MAKP signaling. Regulation of actin reorganization

is a possibility based on the results shown in Fig. 4, since ruffling and cell spreading connect to cell movement.

FIPI blocks the plasma membrane translocation of DOCK2 during chemotaxis

During chemotaxis, F-actin polymerizes asymmetrically at the leading edges of the cell, which is regulated by small GTPase Rac (Rickert et al., 2000; Ridley et al., 2003; Schmidt and Hall, 2002). Rac is preferentially activated at the leading edge, which is achieved by regulating the subcellular localization of guanine nucleotide exchange factors (GEFs). DOCK2, predominantly expressed in hematopoietic cells, is a major Rac GEF that controls polarity and motility during neutrophil chemotaxis (Kunisaki et al., 2006; Rickert et al., 2000). Upon chemokine stimulation, rapid translocation of DOCK2 to the plasma membrane depends on PIP_3. However, a functional leading edge is established even in neutrophils lacking PI3Kγ, the major generator of PIP_3 in the cell type, indicating that other factors may alternately suffice to DOCK2 at the leading edge during chemotaxis. Very recently, our collaborators found that PA is the other lipid to localize Rac activation during chemotaxis (Nishikimi et al., 2009). In response to C5α or fMLP, neutrophils treated with the vehicle control exhibited polarized morphology with focus distribution of DOCK2. However, treatment with FIPI significantly inhibited accumulation of DOCK2 and F-actin at the pseudopods (Fig.3.8A&B). Moreover, FIPI blocked the pseudopod localization of a fluorescent probe that detects activated Rac, the GFP-tagged Rac-binding domain (RBD) of p21-activated kinase (PAK) (Srinivasan et al., 2003)(Fig.3.8C). However, FIPI did not have any effect on the initial membrane translocation of DOCK2 (Fig.3.8A), which is proposed to be dependent on PIP_3 generation by PI3K. Thus, intracellular DOCK2 dynamics is sequentially regulated by

distinct phospholipids to localize Rac activation during neutrophil chemotaxis. The effect of FIPI on accumulation of DOCK2 provides a molecular mechanism to explain the phenotype we observed in chemotaxis assays.

3. 5 Discussion

Although primary alcohols have long been employed as probes to investigate the role of PLD in cellular processes, concerns have been raised both about potential off-target effects and about lack of complete inhibition of PA production (Huang et al., 2005a; Huang and Frohman, 2007; Skippen et al., 2002a). Our characterization of FIPI as a selective PLD1 and PLD2 inhibitor provides a novel tool to evaluate the selectivity of butanol for presumptively PLD-regulated processes. Our results support the idea that FIPI is an effective PLD inhibitor both *in vitro* and in cultured cells but raise and exacerbate concerns about the validity of results obtained using butanol as a probe of PLD function. We show that 1-butanol almost completely blocks glucose-stimulated insulin release (Fig. 4A), but does so without visibly inhibiting production of PA, whereas FIPI blocks PA production but has little effect on insulin release. These data raise the interesting possibility that Ptd-But does not function as an inert lipid, but rather exerts a potent inhibitory effect on the secretory pathway through a mechanism that remains to be defined. Alternately, the inhibition could ensue from other actions mediated by 1-butanol that are not adequately controlled for through comparison to the actions of *tert*-butanol.

PLD activity has been linked to regulatory exocytois using other approaches, such as RNAi-mediated downregulation of individual isoforms (Waselle et al., 2005). Our findings do not invalidate these reports, since FIPI inhibits both PLD1 and PLD2, and it may well be, for example, that PLD1 facilitates insulin secretion (Waselle et al., 2005), whereas PLD2 opposes it. Future studies on mice lacking the individual PLD isoforms or using as yet to be developed isoform-selective PLD inhibitors will provide clarification.

Nonetheless, our findings do suggest that FIPI is a useful tool for re-evaluating the many cell biological processes that have been linked to PLD using alcohol-mediated inhibition of PA production or other approaches that inhibit both classical isoforms. In addition to insulin secretion, we also found a lack of evidence that PLD plays roles in activation of ERK, AKT, and p38 in several signaling systems, counter to what has been reported previously. Moreover, we saw no effect on F-actin stress fibers, again counter to prior reports (Cross et al., 1996; Kam and Exton, 2001).

Thus far, we have not identified any other pathways directly inhibited by FIPI. FIPI inhibits the catalytic activity of classical PLD isoforms and appears to do so without causing changes in the localization of the proteins, access to the required co-factor PIP_2, or the actin cytoskeleton. Nonetheless, future studies will be required to establish the mechanism by which FIPI inhibits PLD1 and PLD2 activity and to further evaluate its specificity for other signaling pathways. It is intriguing that FIPI exhibits greater potency *in vivo* (as low as 0.5 nM IC_{50}) than it does the standard *in vitro* PLD assay (25 nM IC_{50}). It should be noted that the *in vitro* assay is performed using positively curved synthetic liposomes containing only a few types of lipids and no proteins, whereas PLD functions *in vivo* on a planar or slightly negatively-curved surface membrane surface composed of a complex set of lipids and proteins. The latter environment may be less hospitable for PLD enzymatic action, allowing the inhibitor to be visibly effective at a lower concentration. Further investigation using broken cell *in vitro* assays and other approaches may yield novel insights into PLD mechanisms of action in the cellular setting.

We also show here using FIPI that PLD inhibition blunts chemotaxis and blocks effects on cytoskeletal reorganization and elements of cell spreading that are regulated by PLD2. PLD has long been of interest in the context of immune responses (reviewed in Huang and Frohman, 2007), but these outcomes are particularly intriguing because PLD has been receiving increasing attention in the cancer field for the past several years. PLD1 and 2 gene expression, protein level, and activity are upregulated in numerous tumor types (reviewed in Huang and Frohman, 2007), and promote mTor activity and block cancer cell apoptosis (Chen et al., 2005). PLD1 facilitates MMP release (Williger et al., 1999), whereas PLD2 affects cell spreading (Du and Frohman, 2008), proliferation (Zhao et al., 2007), and migration, and PLD2 mutations have been identified in breast cancer (Wood et al., 2007). FIPI is derived from halopemide, a therapeutic for neuroscience applications, and FIPI pharmacokinetics suggest that it has a half-life and bioavailability *in vivo* that make it a usable candidate for animal studies on metastasis (Monovich et al., 2007). It is likely that FIPI analogs with greater potency or other beneficial characteristics can be generated, and this current study suggests that they will be of potential utility as *in vivo* agents to examine physiological roles for PLD and to determine whether inhibiting PLD could be useful in the cancer therapeutic setting.

Fig. 3. 1. FIPI is a potent in vitro and in vivo PLD inhibitor.
A) FIPI blocks PLD activity *in vitro*. An *in vitro* headgroup release assay was performed in the presence of increasing amounts of FIPI on PLD protein-containing membrane fractions prepared from Sf9 insect cells infected with baculoviral constructs expressing human PLD1 (Hammond et al., 1995) or mouse PLD2 (Colley et al., 1997). The FIPI was diluted from a 7.5 mM stock in DMSO, and control wells contained matching amounts of DMSO or no DMSO. PLD2 exhibits constitutive activity and was assayed directly. As shown, PLD1 requires a soluble stimulator to exhibit significant activity, and ARF was used for that purpose in this assay. The assay was performed in duplicate; values shown are means with a variance between duplicates of less than 5%. B) FIPI blocks PLD activity *in vivo*. CHO cell lines inducibly expressing PLD1 or PLD2 were assayed for *in vivo* PLD activity after pre-treatment with the indicated concentrations of FIPI or vehicle control (DMSO) for 1 hour. Activities are shown in comparison to basal activity (no PMA stimulation). Assays were performed in duplicate, and the figure shown represents cumulative results from three independent experiments. C) FIPI blocks translocation of a PA sensor to the plasma membrane. PLD2-inducible CHO cells were transfected with the PA sensor GFP-Spo20-PABD or the mutant GFP-Spo20-PABD-L67R that does not bind PA. PLD2 expression was induced using 24 hour of doxycycline treatment. Asterisk, nucleus; arrows, plasma membrane shown in expanded form in inset; arrowheads, endocytic vesicles. D) FIPI does not inhibit MitoPLD. FIPI was added prior to inducing MitoPLD, which causes mitochondria to aggregate peri-nuclearly in a PA-dependent manner (Choi et al., 2006). Arrow, mitochondrial cluster (green); F-actin, red. Scale bar, 10 mm.

Fig. 3. 1.

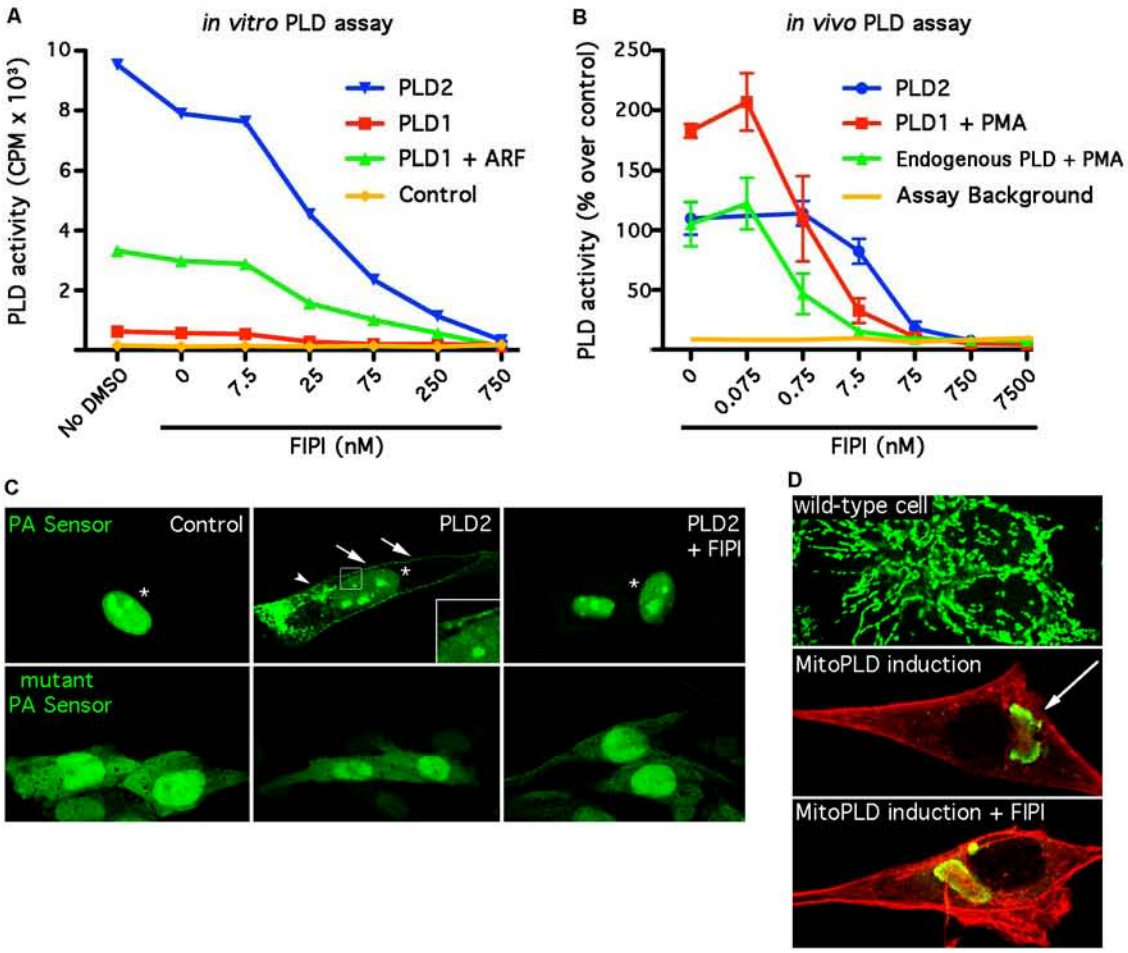
A
in vitro PLD assay
PLD activity (CPM x 10³)
PLD2
PLD1
PLD1 + ARF
Control
No DMSO
0
7.5
25
75
250
750
FIPI (nM)
B
in vivo PLD assay
PLD activity (% over control)
PLD2
PLD1 + PMA
Endogenous PLD + PMA
Assay Background
0
0.075
0.75
7.5
75
750
7500
FIPI (nM)
C
PA Sensor
Control
PLD2
PLD2 + FIPI
mutant PA Sensor
D
wild-type cell
MitoPLD induction
MitoPLD induction + FIPI

Fig. 3. 2. FIPI blocks PLD activity within 15 min and its effect is partially reversible.
A) Kinetics of FIPI action. PLD2 expressing CHO cells were pre-incubated with FIPI for varying lengths of time before being assayed using the *in vivo* PLD assay. B) FIPI is slowly reversible. PLD-expressing CHO cells were preincubated in cycloheximide to stop new protein synthesis, and cultured for an additional 1 or 8 hours before assaying in the *in vivo* assay. One set of cells for each time period was exposed to FIPI at the beginning of the culture period and then washed into fresh medium; the other was exposed at the end of the culture period.

Fig. 3. 2.

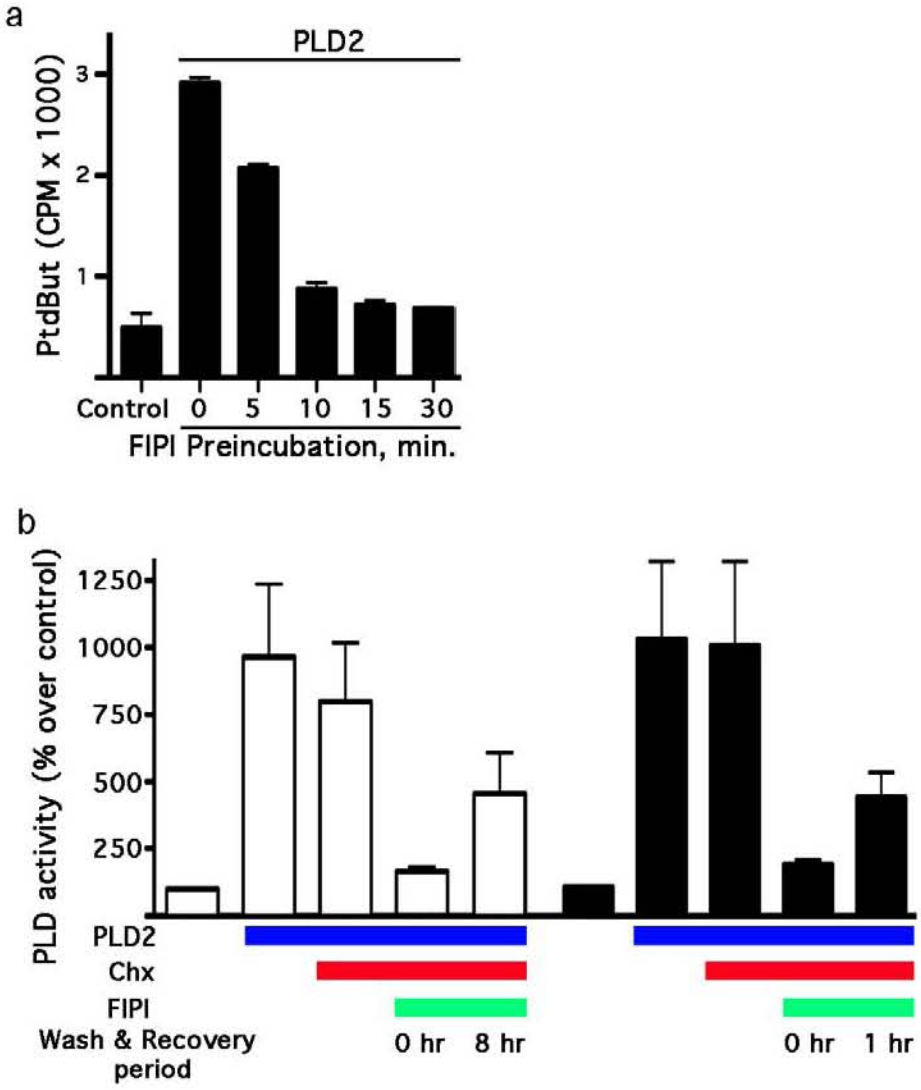
a
PLD2
PtdBut (CPM x 1000)
3
2
1
Control 0 5 10 15 30
FIPI Preincubation, min.
b
PLD activity (% over control)
1250
1000
750
500
250
PLD2
Chx
FIPI
Wash & Recovery period
0 hr 8 hr
0 hr 1 hr

Fig. 3. 3. FIPI does not alter PLD subcellular localization, access to PIP_2, or actin stress fibers.

A) FIPI does not change the subcellular distribution of PLD. Expression of PLD1 or PLD2 was induced by doxycyclin for 24 hours. Cells were treated with 750 nM FIPI for 4 hours, fixed, and immunostained for PLD isoforms. B) FIPI does not alter access to PIP_2. PLD-induced cells were transfected with the PIP_2 sensor PLCδ-PH-GFP, and 24 hour later, treated with FIPI for 4 hours, fixed, and imaged.

C) Stress fiber formation is not affected by FIPI. CHO cells were treated with FIPI for 4 hours, fixed, and stained with rhodamine-conjugated phalloidin to visualize F-actin. Representative cells are shown. Scale bar, 10 mm.

Fig. 3. 3.

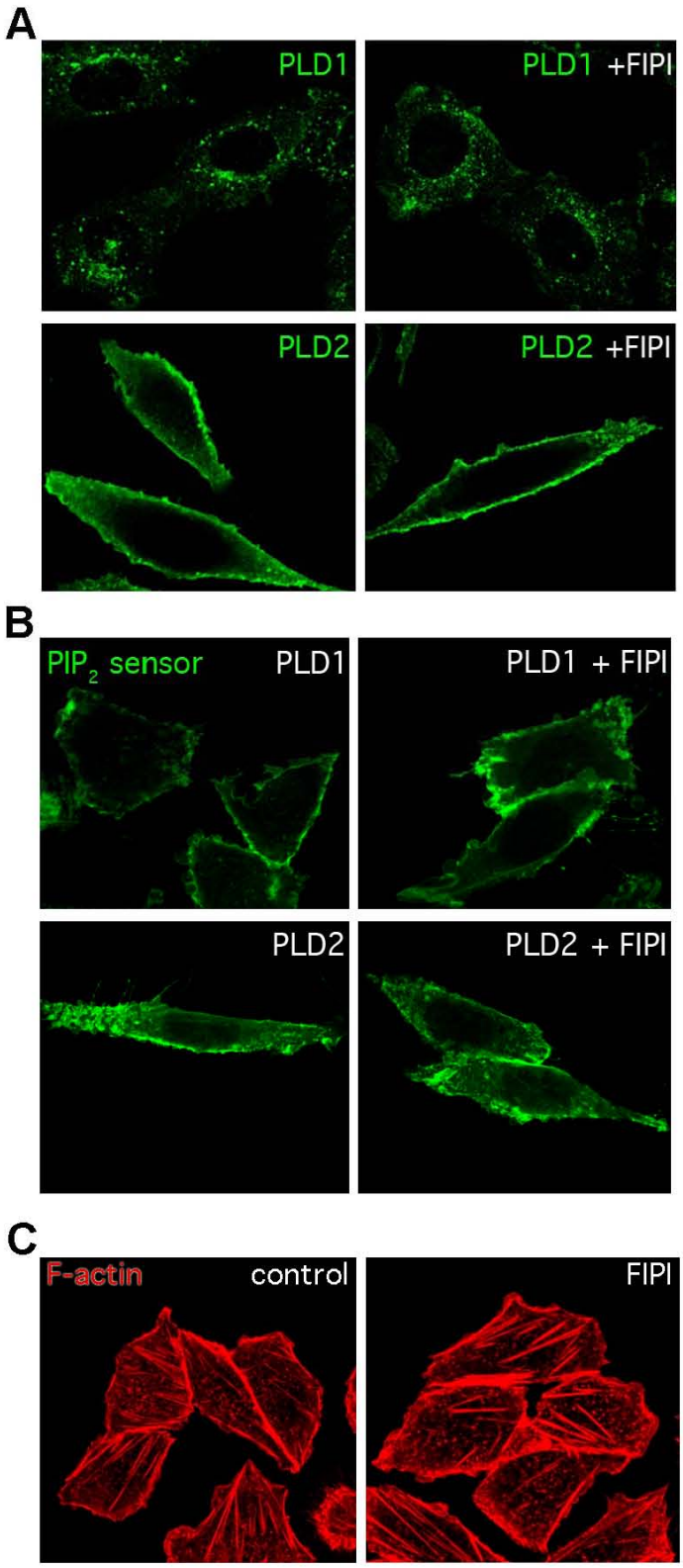
A
PLD1
PLD1 +FIPI
PLD2
PLD2 +FIPI
B
PIP2 sensor
PLD1
PLD1 + FIPI
PLD2
PLD2 + FIPI
C
F-actin
control
FIPI

Fig. 3. 4 FIPI does not affect upstream signaling of PLD.
A) FIPI does not affect PLD translocation upon PMA stimulation. Doxycyclin was used for induction of PLD1 expression. Cells were pre-treated with 750 nM FIPI for 4 hours, and then stimulated by 100 ng/ml PMA for 30 min (PLD1). PLD1 and F-actin were visualized by immunostaining and rhodamine-conjugated phalloidin. B) FIPI does not affect AKT phosphorylation upon serum stimulation. MDA-MB-231 cells were starved overnight before being pre-treated with 750 nM FIPI or vehicle (DMSO) for either 4 or 12 hours, and then stimulated with serum for 30 minutes. Cell lysates were analyzed by SDS-PAGE and Western blotting with antibodies against phosphorylated AKT, total AKT, phosphorlated ERK, or total ERK. C) LPS-induced MAPK activation is not blocked by FIPI. Bone marrow-derived macrophages were treated with FIPI or vehicle for 4 hours, and stimulated with LPS (100 ng/ml) for 10 or 30 min. Cell lysates were analyzed by Western blotting using antibodies against phosphorylated ERK or p38, and total ERK or p38. All results shown are representative of at least three experiments.

Fig. 3. 4.

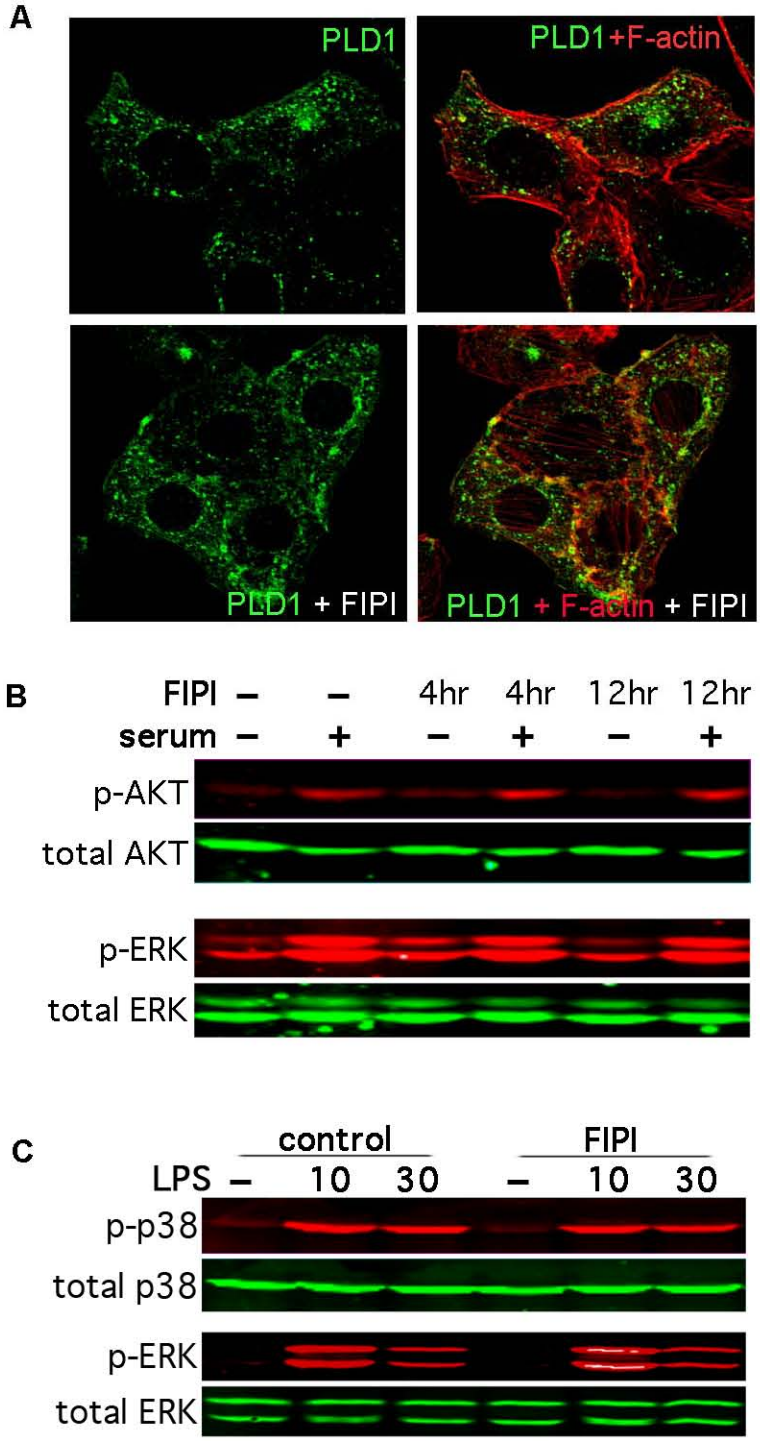
A
PLD1
PLD1+F-actin
PLD1 + FIPI
PLD1 + F-actin + FIPI
B
FIPI – – 4hr 4hr 12hr 12hr
serum – + – + – +
p-AKT
total AKT
p-ERK
total ERK
C
control
FIPI
LPS – 10 30 – 10 30
p-p38
total p38
p-ERK
total ERK

Fig. 3. 5. FIPI rescues PLD2-suppressed membrane ruffling and cell spreading.
A) HA-tagged PLD2 was introduced into Cos-7 cells by transient transfection. Cells were serum-starved for 18 hours and then treated with FIPI. 4 hours later, cells were stimulated with 100 ng/ml PMA for 10 min, and then fixed with 4% paraformaldehyde. F-actin was visualized using rhodamine-conjugated phalloidin. Asterisk, nucleus; arrows, membrane ruffles. 100 cells were counted for each condition and the percentage of cells with ruffling determined. B) CHO cells in suspension were plated on coverslips with or without a 30 minute pre-treatment with FIPI. 15 minutes after plating, the cells were fixed and stained to visualize F-actin (red) and DNA (green). Scale bar, 10 mm.

Fig. 3. 5.

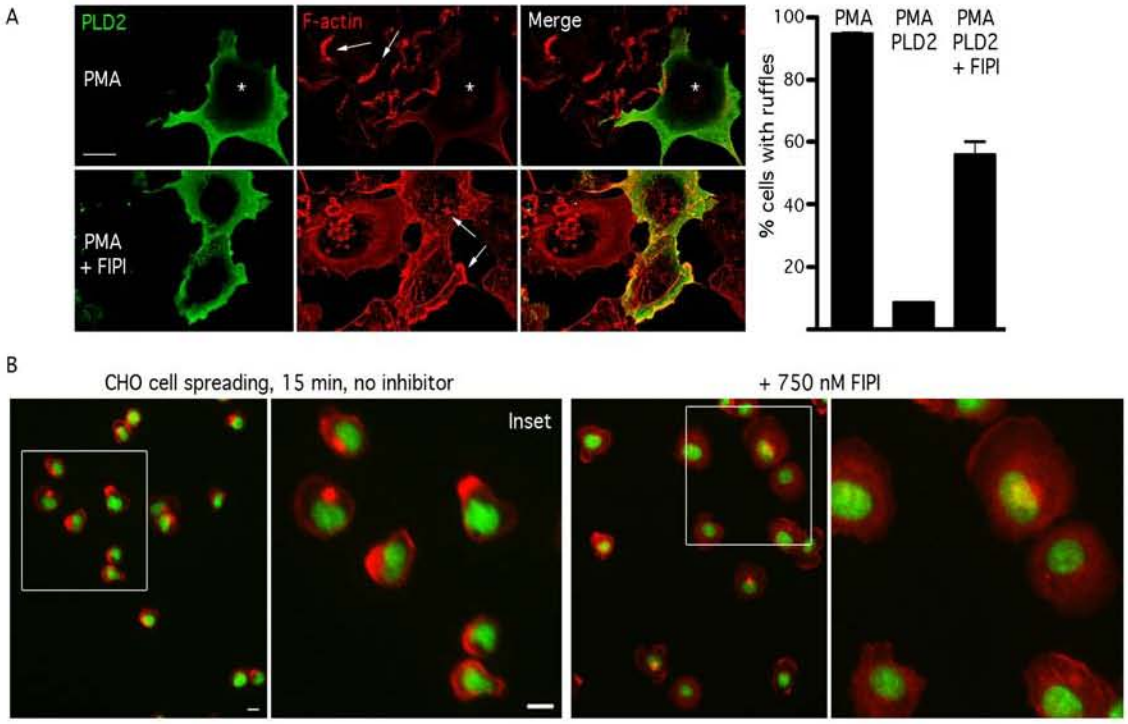
A
PLD2
PMA
F-actin
Merge
PMA
+ FIPI
100
80
60
40
20
% cells with ruffles
PMA
PMA
PLD2
PMA
PLD2
+ FIPI
B
CHO cell spreading, 15 min, no inhibitor
Inset
+ 750 nM FIPI

Fig. 3. 6. 1-Butanol inhibits glucose-stimulated insulin release without blocking production of PA, whereas FIPI blocks PA production but does not inhibit insulin release.

A) 1-Butanol blocks glucose-stimulated insulin release. Min6 cells were assayed for glucose-stimulated insulin release in the presence of increasing amounts of primary or *tert*-butanol. *, $p<0.05$ B) Min6 cells were assayed for glucose-stimulated insulin release in the presence of increasing amounts of FIPI added 30 minutes before the start of the assay. C) Min6 cells were transfected with the GFP-Spo20-PABD PA sensor and maintained in low glucose medium. 24 hours later, the cells were pretreated with 750 nM FIPI, 1-butanol, or vehicle for 1 hour, and then switched to high glucose medium and fixed after 1 hour. Two representative cells are shown for each condition. Arrowheads, plasma membrane. D) Quantitation of plasma membrane fluorescence ($n=21$, $p<0.001$). Scale bar, 10 mm.

Fig. 3. 6.

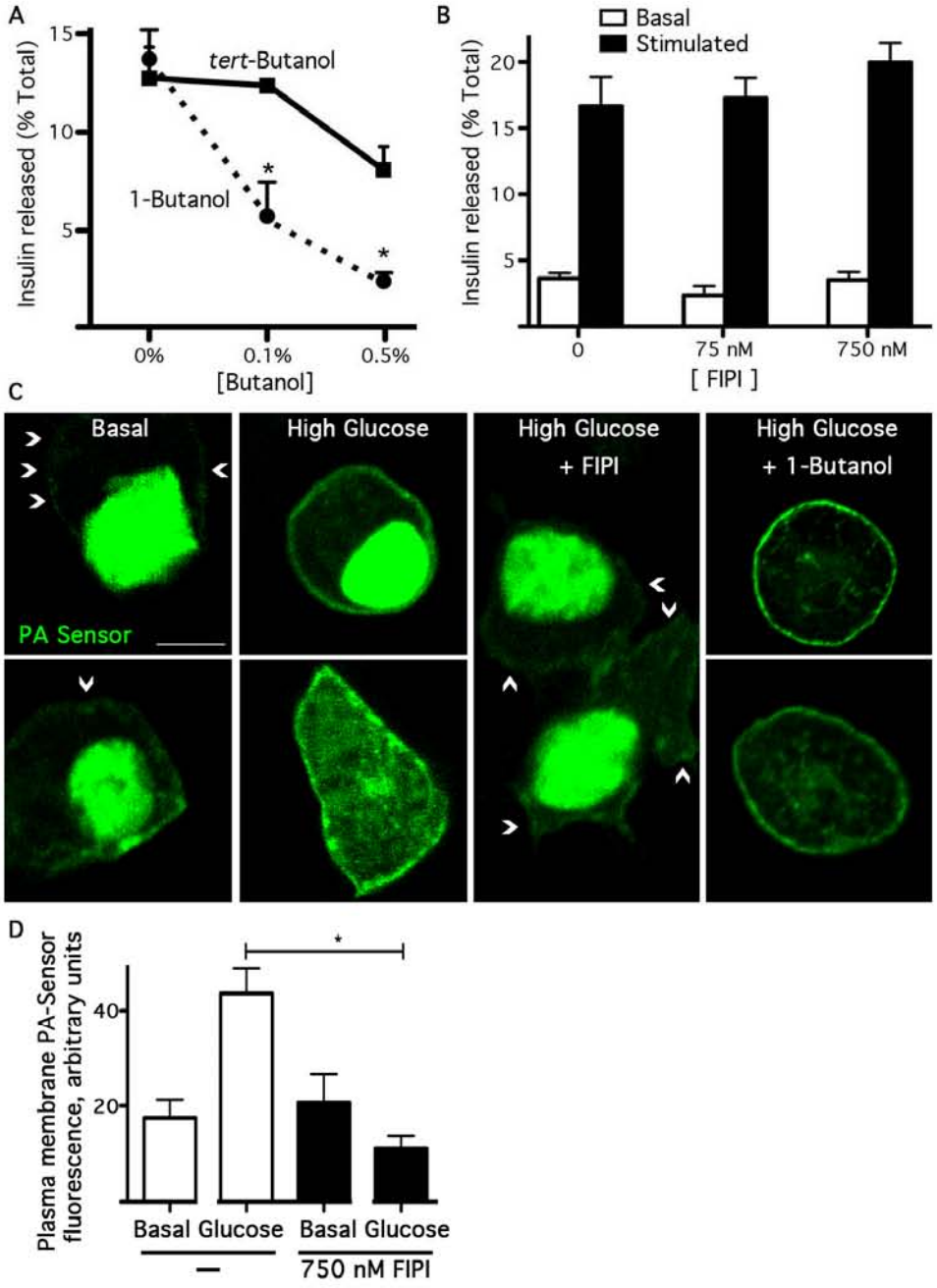
A
Insulin released (% Total)
15
10
5
tert-Butanol
1-Butanol
*
*
0%
0.1%
0.5%
[Butanol]
B
Basal
Stimulated
Insulin released (% Total)
20
15
10
5
0
75 nM
750 nM
[FIPI]
C
Basal
High Glucose
High Glucose
+ FIPI
High Glucose
+ 1-Butanol
PA Sensor
D
Plasma membrane PA-Sensor
fluorescence, arbitrary units
40
20
*
Basal Glucose Basal Glucose
—
750 nM FIPI

Fig. 3. 7. FIPI inhibits neutrophil chemotaxis.
A) Differentiated HL-60 cells were pre-incubated with 750 nM FIPI, 0.5% 1-butanol, or DMSO, and then stimulated with 1 μM fMLP for 2 min. Cell lysates were analyzed by SDS-PAGE and Western blotting using antibodies against p38, phosphorylated p38, ERK, or phosphorylated ERK. B) Quantitation of phosphorylation level of p38 using Odyssey imaging system. C) Differentiated HL-60 cells were treated with 750 nM of FIPI for 1 hour, resuspended in RPMI-based chemotaxis buffer with FIPI or DMSO, and placed in the upper chamber of 6.5-mm Transwell plates. Bottom wells contained either buffer or 10 nM fMLP. *, $p<0.05$, **, $p<0.01$.

Fig. 3. 7.

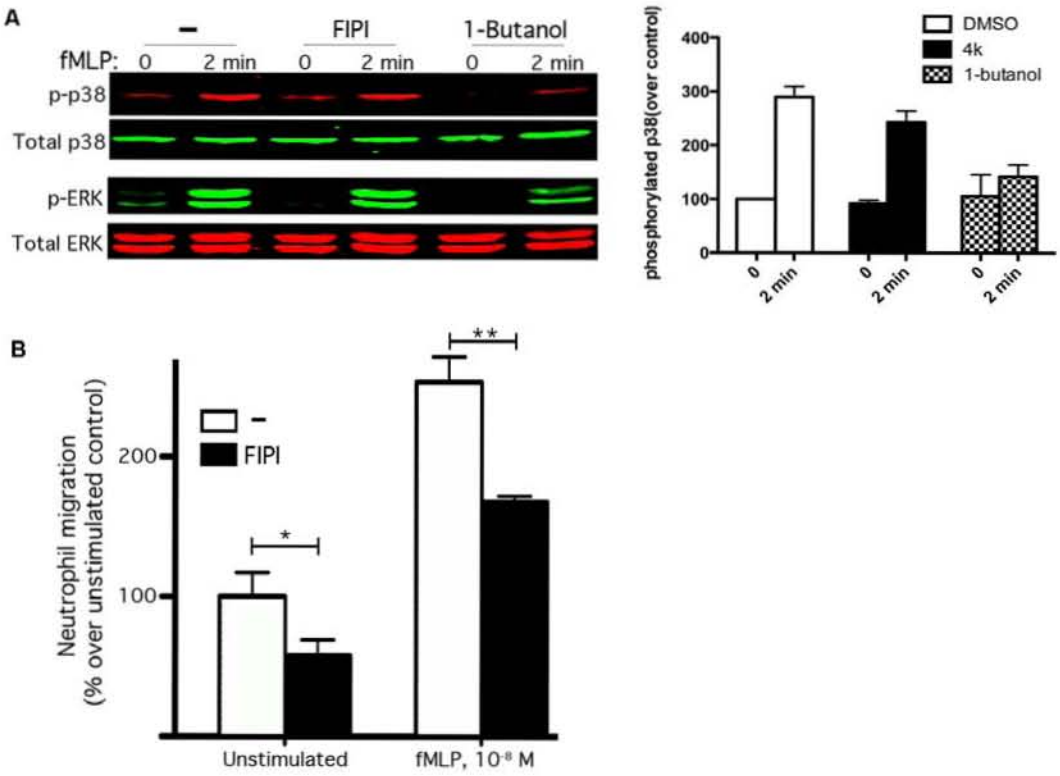
A
–
FIPI
1-Butanol
fMLP: 0 2 min 0 2 min 0 2 min
p-p38
Total p38
p-ERK
Total ERK
phosphorylated p38(over control)
400
300
200
100
0
DMSO
4k
1-butanol
0
2 min
0
2 min
0
2 min
B
Neutrophil migration
(% over unstimulated control)
200
100
–
FIPI
*
**
Unstimulated
fMLP, 10⁻⁸ M

Fig. 3. 8. FIPI inhibits DOCK2 accumulation at pseudopods during chemotaxis (Science. 2009 324: 384-7).

A). Effect of FIPI on DOCK2 localization was analyzed at 15s or 30s after stimulation with 25 nM C5α. B). Effect of FIPI on DOCK2 localization in neutrophils stimulated with a micropipette containing 10 μM fMLP. C). Effect of FIPI on localization of GFP-tagged PAK-RBD was analyzed at 30s after stimulation with 25 nM C5α. Data in (A) and (C) are the mean ± SD of triplicate experiments, in each of which at least 50 cells were analyzed.

Fig. 3.8.

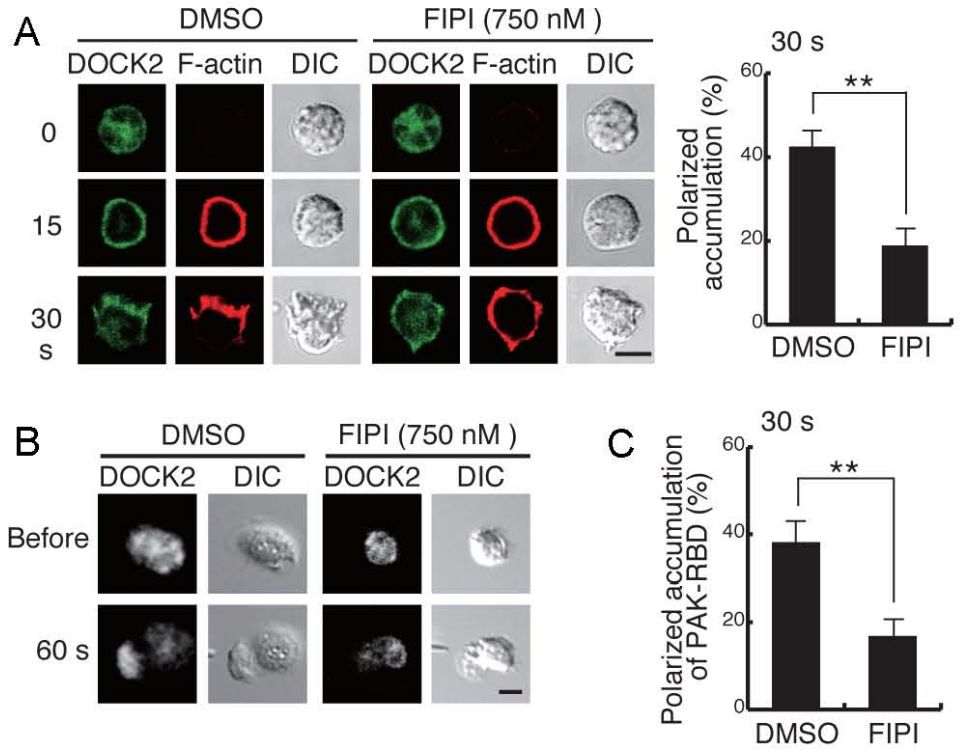
A
DMSO
FIPI (750 nM)
DOCK2 F-actin DIC
DOCK2 F-actin DIC
0
15
30 s
30 s
Polarized accumulation (%)
60
40
20
0
**
DMSO FIPI
B
DMSO
FIPI (750 nM)
DOCK2 DIC
DOCK2 DIC
Before
60 s
C
30 s
Polarized accumulation of PAK-RBD (%)
60
40
20
0
**
DMSO FIPI

Chapter 4

Conclusions and future directions

4.1 The role of PIP5Kα in host defense

4.1.1 Overall conclusions regarding the role of PIP5Kα in host defense against *Y. pseudotuberculosis*

PIP5Kα is one of three isoforms of PIP5K that are the major enzymes responsible for PIP_2 generation. As I mentioned before, PIP5Kα was proposed to be involved in FcγR-mediated and β1 integrin-mediated phagocytosis by using either overexpression or catalytically inactive mutant. At the start of my study in the role of PIP5Kα in *Y. pseudotuberculosis*, I speculated that PIP5Kα played a part in the phagocytosis. Besides this part, I also addressed the other potential functions of PIP5Kα in host defense including innate and adaptive immune responses. However, numerous additional roles of PIP5K still need to be defined.

PIP5Kα is required for efficient uptake of Y. pseudotuberculosis when Rac1 activity is inhibited by bacterial toxin YopE.

BMDMs derived from PIP5Kα$^{-/-}$ mice phagocytosed wt *Y. pseudotuberculosis* less efficiently than wt BMDMs did (Fig.2.1B), and the deficiency became more profound when the Yops were induced prior to infection (Fig.2.1C). In contrast, there was no difference in uptake of *Y. pseudotuberculosis* that did not carry the virulence plasmid (Fig.2.1B), or expressed a defective YopE protein (Fig.2.2A). YopE, a Rho GAP protein,

blocks phagocytosis mainly by inhibiting Rac1 activity. When treated with the Rac1 inhibitor NSC23766 (Fig.2.2B), PIP5K$\alpha^{-/-}$ macrophages uptook less bacteria than wt macrophages did even though bacteria did not express functional YopE. These indicate the unique role of PIP5Kα in the phagocytosis of *Y. pseudotuberculosis*, a key regulator against toxin YopE.

PIP5K$\alpha^{-/-}$ mice are more susceptible to Y. pseudotuberculosis infection than wt mice.

My *in vivo* data further confirm the significance of PIP5Kα in host defense against *Y. pseudotuberculosis.* When infected orogastrically with *Y. pseudotuberculosis*, PIP5K$\alpha^{-/-}$ mice exhibited greater susceptibility with 35% surviving to 21 days post infection, while 85% of wt mice survived during this observation period (Fig.2.5A). This suggests that PIP5Kα plays a protective role in *Y. pseudotuberculosis* infection, which is not compensated by other isoforms of PIP5K. Furthermore, 25-fold more bacteria were found in the spleens of PIP5K$\alpha^{-/-}$ mice than that of the wt (Fig.2.5B) on day6 after infection, which suggests that either more bacteria were disseminated to spleens or less bacteria were cleared in PIP5K$\alpha^{-/-}$ mice. However, colonization levels in MLNs of wt and PIP5K$\alpha^{-/-}$ mice were similar, which indicates that bacterial clearance, but not dissemination, may count for the phenotype of PIP5Kα-deficiency mice. TNFα and IFNγ are two key cytokines important for the clearance of *Y. pseudotuberculosis*. Indeed, lower IFNγ levels were found in PIP5K$\alpha^{-/-}$ mice at day6 post infection (Fig.2.6), which is consistent with the colonization data.

Diminished IFNγ level is due to lower levels of MHC class II on the surface of the antigen presenting cells (APCs) lacking PIP5Kα.

T cells are the major source of IFNγ at the late stage of *Y. pseudotuberculosis* infection. There are two possibilities leading to diminished IFNγ levels: lower T cell content; or T cell less primed. T cell content in the spleens of infected mice remained constant and similar from 3 to 6 days post infection in either the wt or PIP5Kα$^{-/-}$ mice (Fig.2.7). However, the levels of MHC class II molecules is lower on the surface of BMDMs induced by IFNγ. Furthermore, in contrast to 70% of wt CD11c+ BMDCs, only 44% of PIP5Kα$^{-/-}$ BMDCs expressed MHC class II (Fig.2.9). The lower levels of MHC class II results in the defect in T cell priming, which may count for less IFNγ in PIP5Kα$^{-/-}$ mice at the late stage of infection. Immunoflurorescence staining also showed that there was less MHC class II on the PIP5Kα$^{-/-}$ BMDMs than that on the wt after IFNγ treatment. However, no significant difference was observed in the cytosolic levels of MHC class II, suggesting that PIP5Kα may affect the translocation of MHC II from cytosol to plasma membrane in response to IFNγ. Using various markers to label different cytosolic compartments, MHC II in PIP5Kα$^{-/-}$ BMDMs was found to barely go to TGN where it can be further transported to plasma membrane in wt cells. This unexpected finding indicates that PIP5Kα may be involved in intra-Golgi trafficking.

4.1.2 Further considerations regarding the role of PIP5Kα in host defense

How does PIP5Kα regulate the phagocytosis of Y. pseudotuberculosis?

In previous studies, PIP5K was shown to be recruited to the nascent phagosome and generate PIP2 mediating actin rearrangement there in COS cells infected with *Y.*

pseudotuberculosis (Wong and Isberg, 2003). It is very possible that the deficiency in phagocytosis in PIP5K$\alpha^{-/-}$ BMDMs is due to the less PIP2 production on the phagosomal cup. However, based on the data from our collaborator, just 10% decreased in PIP2 level was observed by HPLC in bone marrow-derived mast cells (Sasaki et al., 2005). It might be impractical to image such small change of PIP2 level by using PLCδ-PH-GFP. Since PIP2 level affects actin polymerization, and eventually leads to F-actin reorganization, I decided to use F-actin change as readout. Unfortunately, in the course of my studies, I failed to observe obvious changes in the actin cytoskeleton of macrophages in the PIP5K$\alpha^{-/-}$ mice either at the resting stage or after infection. *Yersinia* is a small bacterium and phagocytosed by macrophage quickly, making it difficult to image actin accumulation during an individual uptake event. In this case, tracking F-actin change in real time could be helpful. However, the common used F-actin labeling reagent, phailloidin binds F-actin, strongly promoting actin polymerization and poisoning the cell. Additionally, it does not permeate cell membrane, making it difficult to be applied in living cell imaging. Recently, Wedlich-Soldner R. et al reported a new tool to visualize actin dynamics in vivo, which use a fluoro-labeled 17 amino acid peptide called F-Lifeact (Riedl et al., 2008). F-Lifeact can label live untransfectable cells such as neutrophils using 'scrape-loading' (McNeil et al., 1984). With this method, actin dynamic can be tracked in an individual uptake event.

Since both Arf6 and Rac1 can activate PIP5Ks *in vitro* and overexpression of Arf6 can bypass the inhibition of Rac1 during the phagocytosis of *Y. pseudotuberculosis*, I propose that Arf6-PIP5K may constitute a parallel pathway to Rac1. However, whether Arf6 is a key regulator of the uptake of *Y. pseudotuberculosis* has not been clearly

verified. Arf6 knockout mice were reported recently (Suzuki et al., 2006). Although they are embryonic lethal, the function of Arf6 in *Y. pseudotuberculosis* uptake can be tested using Arf6$^{-/-}$ cells.

Can IFNγ rescue the phenotype in PIP5Kα$^{-/-}$ mice?

As reported (Autenrieth et al., 1994; Parent et al., 2006), IFNγ is a key cytokine protecting host against *Yersinia* and recombinant IFNγ rendered susceptible mice the resistance. I proposed that lower level of IFNγ in PIP5Kα$^{-/-}$ mice was the major cause of animal death. To further confirm this, exogenous IFNγ will be daily injected into wt and PIP5Kα$^{-/-}$ mice from day 3 after oral infection to eliminate the difference in IFNγ levels between wt and PIP5Kα$^{-/-}$ mice, and the colonization in spleens will be determined at day 6. I expect that exogenous IFNγ will rescue the defect of colonization in PIP5Kα$^{-/-}$ mice after infection.

Which results in the susceptibility of PIP5Kα-deficient mice upon Y. pseudotuberculosis: defect in phagocytosis, or diminished MHC class II levels, or both?

In this study, PIP5Kα was found to be important in two key processes of immune responses: phagocytosis and MHC class II presentation. Any of them or both could contribute to the susceptibility of PIP5Kα$^{-/-}$ mice to *Y. pseudotuberculosis*. Due to defect in phagocytosis, macrophages could uptake and clear less bacteria in spleens, which leads to uncontrolled bacteria colonization and animal death eventually. On the other hand, lower levels of MHC II on the surface of macrophages and dendritic cells could count for less priming T cells because of the defect in antigen presentation, resulting in less IFNγ produced in PIP5Kα$^{-/-}$ mice upon infection. To clarify which is the key, YopE inactive

mutant is a unique tool because there is no difference in uptaking YopE mutant between wt and PIP5K$\alpha^{-/-}$ macrophages. However, *Yersinia* lacking YopE is much less virulent than wt strain, which make it difficult to study the immune responses in deep tissues using this mutant strain. Instead of oral inoculation, i.v. injection may be a route to avoid peripheral immune system and dissect the deep tissue problems. First, I will make the survival curve using different amounts of bacterial loads to determine ID_{50} of YopE mutant during i. v. infection. Then, I will use 10 folds of ID_{50} to infect wt and PIP5K$\alpha^{-/-}$ mice to check the colonization in spleens. If the colonization in spleen is similar between wt and PIP5K$\alpha^{-/-}$ mice, it suggests phagocytosis does play an irreplaceable role in host defense against *Y. pseudotuberculosis*. Although there is a defect on MHC II presentation, PIP5K$\alpha^{-/-}$ mice can handle the bacterial infection as well as wt mice when the phagocytosis defect has been removed by inactivating YopE. In contrast, if the colonization in PIP5K$\alpha^{-/-}$ spleens is more than that in wt, which mimics the phenotype using wt *Y. pseudotuberculosis* strain, it indicates that the role of PIP5Kα in T cell priming and MHC II presentation may be more critical in host defense.

How does PIP5Kα affect MHC II presentation?

The role of PIP5Kα in MHC II presentation is an unexpected finding. Based on my preliminary work, PIP5Kα may affect the surface expression level of MHC II by regulating the intracellular trafficking. Normally, MHC II is synthesized in the ER, and then translocate to *cis*-Golgi and TGN, eventually goes to plasma membrane through endocytic pathway. In wt macrophages, IFNγ-induced MHC II co-localizes with *cis*-Golgi marker GM130 and TGN maker TGN38. However, the majority of MHC II in PIP5K$\alpha^{-/-}$ macrophages co-localizes with GM130, but no TGN38, suggesting that

PIP5Kα may play a part in the translocation from *cis*-Golgi to TGN. Although the trafficking from *cis*-Golgi to TGN has not been well studied, PIP2 has been implicated in the regulation of Golgi structure and trafficking (De Matteis et al., 2002; Egea et al., 2006). Using the PH domain of PLCδ in immunoelectron microscopy, the presence of PIP2 has recently been visualized at the Golgi complex, mainly at the level of the stacks. Although none of PIP5K isoforms has been visualized at Golgi, a PIP5K activity and recombinant PIP5Kα associate with Golgi membranes, and both elevate PIP_2 levels *in vitro* (Godi et al., 1999; Jones et al., 2000; Siddhanta et al., 2000). PIP_2 has been proposed to play a role in ER-to-Golgi transport (Godi et al., 1998), in the formation/release of post-Golgi transport vesicles, and in maintaining the structural integrity and function of Golgi (Siddhanta et al., 2000; Sweeney et al., 2002). PIP_2 might play those roles by controlling the spectrin and actin machineries that are involved in the organization and function of Golgi (Egea et al., 2006; Lorra and Huttner, 1999), and by acting on the membrane fission processes through recruiting/activating dynamin (Kozlov, 2001). Similarly, PIP2 generated by PIP5K could affect the intra-Golgi trafficking by regulating those pathways since PIP2 mainly localize at the stacks.

Does PIP5Kα play other roles in host defense against Y. pseudotuberculosis?

MHC II level on the surface of PIP5K$\alpha^{-/-}$ APCs is lower than that on wt APCs, strongly arguing that there is an antigen presentation defect in PIP5K$\alpha^{-/-}$ mice. However, antigen presentation assay might be still needed to be carried out to really confirm it. To do so, T cells can be isolated from wt and PIP5K$\alpha^{-/-}$ mice immunized by *Y. pseudotuberculosis*, and then T cells are incubated with BMDCs or BMDMs infected

with *Y. pseudotuberculosis*. T cell recognition can be measured by the detection of IFNγ in culture supernatant using ELISA (Russmann et al., 2003).

Defect in T cell activation could be another possibility to cause the lower IFNγ levels in PIP5Kα$^{-/-}$ mice even thought no evidence points out the involvement of PIP5Kα in this process. One of the most common ways to assess T cell activation is to measure T cell proliferation upon in vitro stimulation of T cells via antigen or agonistic antibodies to TCR. T cells isolated from spleens can be activated by anti-CD3, and cellular proliferation can be measured by MTT assay or IFNγ level as readout (eBioscience protocol: T cell activation). Although I do not expect any difference between wt and PIP5Kα$^{-/-}$ T cells, it will be another interesting direction we may follow if any defect is found.

Do other PIP5Ks also play a part in Y. pseudotuberculosis infection?

There is no difference between wt and PIP5Kα$^{-/-}$ macrophages in terms of uptaking YopE inactive mutant strain. Moreover, the defect in phagocytosis of PIP5Kα$^{-/-}$ macrophages was not very dramatic, about 35% less in comparison to wt macrophages, indicating that other PIP5K isoforms may also be involved in phagocytosis of *Yersinia*. PIP5Kβ is highly homologous to PIP5Kα, and has been implicated in Fcγ-R mediated phagocytosis. Recently, PIP5Kβ$^{-/-}$ mice was reported and characterized by Wang Y *et al* (Wang et al., 2008). Using this tool, we can clarify the overlapping role of α and β isforms in the phagocytosis. Since both PIP5Kα and PIP5Kβ knockout mice are born and grow normally, it is possible to cross them to generate double knockout mice to evaluate the function of PIP5Kα/β that may be different from that of γ isoform in the bacterial uptake.

Is PIP5Kα a universal protective factor in host defense?

Here, I showed that PIP5Kα is an important protective factor against *Y. pseudotuberculosis* infection via regulating phagocytosis and MHC class II presentation. However, the preliminary data showed that PIP5Kα$^{-/-}$ mice survived a little better, but not significantly, in comparison to wt mice upon *Listeria* infection, suggesting that PIP5Kα plays different parts in host defense regarding different pathogens. In contrast to *Y. pseudotuberculosis*, *Listeria* is a gram-postive pathogen, and replicate intracellularly (Ramaswamy et al., 2007). Moreover, not like *Y. pseudotuberculosis,* the clearance of *Listeria* is not dependent on IFNγ. PIP_2 and PIP_3 have been implicated in the *Listeria* uptake (Cossart and Sansonetti, 2004), it would be interesting to test whether PIP5Kα or β is involved in the phagocytosis of *Listeria* using knockout BMDMs. If there is a defect in phagoyctosis in knockout cells, I'll propose that the defect in the *Listeria* phagocytosis leads to less bactereia proliferated intracellularly, which is the major way to spread the infection, eventually resulting in less susceptibility to *Listeria* in knockout mice. It will be an interesting finding that PIP5Kα, a host regulator, plays similar roles in phagocytosis, but leads to different outcomes.

4.2 FIPI and its potential applications

4.2.1 Overall conclusions regarding the characterization of FIPI

FIPI is here characterized as a small molecule inhibitor of PLD1 and PLD2 (Fig.3.1). It rapidly blocks in vivo PA production with sub-nM potency, and its inhibition is partially reversible (Fig3.2). It neither affects the activities of other PLD superfamily

members such as mitoPLD or lysoPLD, nor interferes with PLD localization or the upstream signaling pathways (Fig.3.3). Surprisingly, FPI does not block several biological processes that are inhibited by 1-butanol, such as insulin secretion upon glucose stimulation (Fig.3.6). However, FPI does inhibit PLD regulation of membrane ruffling, cell spreading (Fig.3.5), and chemotaxis (Fig.3.7), indicating its potential utility as a therapeutic.

4.2.2 Future considerations regarding the potential applications of FIPI

Why does FIPI not work in some biological processes blocked by 1-butanol?

PLD can use 1-butanol to generate Ptd-but, which is thought to be inert lipid unable to recruit or activate target proteins, or serve as a substrate to generate signaling lipid, or affect membrane structure. Thus, 1-butanol is widely used as a PLD inhibitor, and many involvements of PLD were discovered by using this tool. However, concerns have been raised since as little as 0.1% 1-butanol has been shown to inhibit a variety of the cell biological processes. As reviewed (Huang et al., 2005; Huang and Frohman, 2007), 1-butanol and Ptd-but do have other effects on the cells that extend beyond inhibiting PA production. Therefore, the so-called PLD functions found by using 1-butanol should be carefully re-evaluated. In this case, FIPI, the small molecule inhibitor, would be a good tool as well as RNAi or knockout animals.

Additionally, 1-butanol did not block PA generation in our experimental setting (Fig.3.6C) even though it blocked insulin secretion. In contrast, FIPI did block PA

production, but not inhibit insulin secretion. These suggest that 1-butanol affect insulin secretion may through other pathways instead of inhibiting PLD activity.

FIPI helps to synthesize isoform-specific inhibitor.

As I showed, FIPI is a potent inhibitor for both PLD1 and PLD2, which infers pos and cons. PLD1 and 2 are classic mammalian PLDs, which are intensively studied regarding their roles in cellular processes and diseases. With FIPI that eliminates the PA production by PLD, confusion caused by 1-butanol will be cleared up, and PA signaling pathway will be further dissected as discussed later. However, this pan-inhibition can not point out which isoform is involved in the particular process, and may cause troubles when the isoform-specific issues need to be addressed. For example, FIPI did not affect insulin secretion upon glucose stimulation. However, evidence showed that PLD1 was required for insulin release by using RNAi approach, and preliminary data from my lab mate indicated that PLD2 might inhibit insulin secretion by analyzing PLD2 knockout mice. Under this circumstance, PLD1 and 2 may play different roles that can not be distinguished by FIPI. Thus, isoform-specific inhibitors would be important advance in the field. Using FIPI as a leading compound, a variety of modification can be made, and isoform specificity will screened using in vitro PLD assay as described in the method. Very recently, Alex Brown reported such isoform-specific inhibitors designed based on FIPI. But they are not as efficient as FIPI in terms of IC_{50}, which may lead to many non-specific effects. However, this work at least supports the idea that FIPI is a good leading compound to design isoform-specific inhibitors.

FIPI may be a useful tool to dissect PA generation pathways.

Although FIPI is not perfect regarding its isoform specificity, it is a useful tool to dissect PA production pathways. PA can be formed in three ways: the hydrolysis of PC by PLD; the phosphorylation of DAG by DAG kinase; or the acylation of lysoPA by lysoPA-acyltransferase. With FIPI, PA production by PLD can be distinguished from other pathways, which helps us to clarify the complexity.

PA consists of a glycerol backbone with a saturated fatty acid to carbon1, an unsaturated fatty acid bonded to carbon2, and a phosphate bonded to carbon3. The length of fatty acid chain and the number of unsaturated bonds vary, which defines different PA species. Although the biological significance of each PA is largely unknown, dissecting PA specie production upon different stimulations may provide insight into it. Interestingly, our collaborator showed that blocking PLD activity by FIPI selectively diminished the production of some species of PA in response to PMA by lipid mass spectrometry, suggesting than PLD may be involved in those PA generation, but not for the others. These also provide the opportunity to distinguish the biological role of PLD-regulated PA from PLD-unrelated PA, and intrigue us to find out other regulators of PA production. Using similar approaches, PA generation upon other stimuli can certainly be studied in the future.

Is FIPI a potential anti-tumor drug?

Recently, the role of PLD in tumorigenesis has begun to draw more attentions, including acting as an alternate survival signal, promoting cell tansformation, and regulating metastasis (Zheng et al., 2006). Among them, metastasis is a key issue in cancer therapy, since it causes 90% of the deaths from solid tumors (Gupta and Massague, 2006). Metastasis is a complicated multi-step process in which cell

motility/migration is essential. Cytoskeleton networks play a crucial part in cell motility and have been studied extensively in tumor invasion. PLD has been recognized as a key regulator in cytoskeleton reorganization and cell movement. PLD activity is also implicated in tumor invasion: MDA-MB-231 human breast cancer cells with high levels of PLD activity migrate and invade in matrigel, whereas MCF-7 cells with relatively low PLD activity do not. Moreover, the ability of MDA-MB-231 to migrate and invade matrigel is dependent on PLD (Zheng et al., 2006). These suggest the contribution of PLD to cell migration and invasiveness, and therefore inhibiting PLD activity could be a potential target in metastatic cancer therapy.

I showed that FIPI inhibited fMLP-drived chemotaxis, which indicates FIPI may be a promising reagent to block tumor cell movement. Furthermore, the pharmacokinetic parameters of FIPI such as the 5.57 h half-life, indicating that FIPI could be used as a drug. To test the hypothesis, cell migration assay in culture and tumor metastasis mouse model can be performed. However, the mouse model is the way to evaluate its clinical potential. There are various ways to mimic metastasis in mice including genetically modification or tumor transplantation (Fantozzi and Christofori, 2006). The implantation of established cell lines derived from human breast cancer is relatively simple and allows the genetic or pharmacological manipulation of the implanted cells. Here, LM2 cells derived from MDA-MB-231 will be used not only because they have high PLD activities, but also because they showed aggressive lung metastasis when as few as 2×10^3 cells were injected into the tail vein of immunodeficient mice (Minn et al., 2005). Additionally, the LM2 cells express a triple-fusion protein reporter encoding herpes simplex virus thymidine kinase 1, green fluorescence protein (GFP) and firefly luciferase, which allow

to visualize the xenograft. With this model, FIPI will be given daily to transplanted nude mice, and the metastasis will be evaluated by bioluminescent imaging system. Once this system is established, the derivatives of FIPI can also be examined to find out the best drug candidates, which will be an advance in cancer therapeutic.

Although I have only expound one potential clinical application of FIPI, it is likely that FIPI could be applied to the treatment of other diseases, as PLD and its product PA have been implicated in a wide range of physiological processes and diseases.

References

Abbott, M., A. Galloway, and J.L. Cunningham. 1986. Haemochromatosis presenting with a double Yersinia infection. *J Infect*. 13:143-5.

Aepfelbacher, M., and J. Heesemann. 2001. Modulation of Rho GTPases and the actin cytoskeleton by Yersinia outer proteins (Yops). *Int J Med Microbiol*. 291:269-76.

Aikawa, Y., and T.F. Martin. 2003. ARF6 regulates a plasma membrane pool of phosphatidylinositol(4,5)bisphosphate required for regulated exocytosis. *J Cell Biol*. 162:647-59.

Alonso, A., N. Bottini, S. Bruckner, S. Rahmouni, S. Williams, S.P. Schoenberger, and T. Mustelin. 2004. Lck dephosphorylation at Tyr-394 and inhibition of T cell antigen receptor signaling by Yersinia phosphatase YopH. *J Biol Chem*. 279:4922-8.

Alrutz, M.A., A. Srivastava, K.W. Wong, C. D'Souza-Schorey, M. Tang, L.E. Ch'Ng, S.B. Snapper, and R.R. Isberg. 2001. Efficient uptake of Yersinia pseudotuberculosis via integrin receptors involves a Rac1-Arp 2/3 pathway that bypasses N-WASP function. *Mol Microbiol*. 42:689-703.

Andersson, K., N. Carballeira, K.E. Magnusson, C. Persson, O. Stendahl, H. Wolf-Watz, and M. Fallman. 1996. YopH of Yersinia pseudotuberculosis interrupts early phosphotyrosine signalling associated with phagocytosis. *Mol Microbiol*. 20:1057-69.

Aroor, A.R., G.W. Custer, Y.I. Weng, Y.J. Lee, and S.D. Shukla. 2002. Phosphotidylethanol mimics ethanol modulation of p42/44 mitogen-activated protein kinase signalling in hepatocytes. *Alcohol Alcohol*. 37:534-9.

Autenrieth, I.B., M. Beer, E. Bohn, S.H. Kaufmann, and J. Heesemann. 1994. Immune responses to Yersinia enterocolitica in susceptible BALB/c and resistant C57BL/6 mice: an essential role for gamma interferon. *Infect Immun*. 62:2590-9.

Autenrieth, I.B., and R. Firsching. 1996. Penetration of M cells and destruction of Peyer's patches by Yersinia enterocolitica: an ultrastructural and histological study. *J Med Microbiol*. 44:285-94.

Autenrieth, I.B., and J. Heesemann. 1992. In vivo neutralization of tumor necrosis factor-alpha and interferon-gamma abrogates resistance to Yersinia enterocolitica infection in mice. *Med Microbiol Immunol*. 181:333-8.

Autenrieth, I.B., A. Tingle, A. Reske-Kunz, and J. Heesemann. 1992. T lymphocytes mediate protection against Yersinia enterocolitica in mice: characterization of murine T-cell clones specific for Y. enterocolitica. *Infect Immun*. 60:1140-9.

Autenrieth, I.B., U. Vogel, S. Preger, B. Heymer, and J. Heesemann. 1993. Experimental Yersinia enterocolitica infection in euthymic and T-cell-deficient athymic nude C57BL/6 mice: comparison of time course, histomorphology, and immune response. *Infect Immun*. 61:2585-95.

Barnes, P.D., M.A. Bergman, J. Mecsas, and R.R. Isberg. 2006. Yersinia pseudotuberculosis disseminates directly from a replicating bacterial pool in the intestine. *J Exp Med*. 203:1591-601.

Bechoua, S., and L.W. Daniel. 2001. Phospholipase D is required in the signaling pathway leading to p38 MAPK activation in neutrophil-like HL-60 cells, stimulated by N-formyl-methionyl-leucyl-phenylalanine. *J Biol Chem*. 276:31752-9.

Besterman, J.M., V. Duronio, and P. Cuatrecasas. 1986. Rapid formation of diacylglycerol from phosphatidylcholine: a pathway for generation of a second messenger. *Proc Natl Acad Sci U S A*. 83:6785-9.

Black, D.S., and J.B. Bliska. 2000. The RhoGAP activity of the Yersinia pseudotuberculosis cytotoxin YopE is required for antiphagocytic function and virulence. *Mol Microbiol*. 37:515-27.

Black, D.S., L.G. Montagna, S. Zitsmann, and J.B. Bliska. 1998. Identification of an amino-terminal substrate-binding domain in the Yersinia tyrosine phosphatase that is required for efficient recognition of focal adhesion targets. *Mol Microbiol*. 29:1263-74.

Bliska, J.B., and D.S. Black. 1995. Inhibition of the Fc receptor-mediated oxidative burst in macrophages by the Yersinia pseudotuberculosis tyrosine phosphatase. *Infect Immun*. 63:681-5.

Bocckino, S.B., P.F. Blackmore, P.B. Wilson, and J.H. Exton. 1987. Phosphatidate accumulation in hormone-treated hepatocytes via a phospholipase D mechanism. *J Biol Chem*. 262:15309-15.

Boland, A., and G.R. Cornelis. 1998. Role of YopP in suppression of tumor necrosis factor alpha release by macrophages during Yersinia infection. *Infect Immun*. 66:1878-84.

Botelho, R.J., M. Teruel, R. Dierckman, R. Anderson, A. Wells, J.D. York, T. Meyer, and S. Grinstein. 2000. Localized biphasic changes in phosphatidylinositol-4,5-bisphosphate at sites of phagocytosis. *J Cell Biol*. 151:1353-68.

Brindley, D.N., and D.W. Waggoner. 1996. Phosphatidate phosphohydrolase and signal transduction. *Chem Phys Lipids*. 80:45-57.

Brizuela, L., M. Rabano, P. Gangoiti, N. Narbona, J.M. Macarulla, M. Trueba, and A. Gomez-Munoz. 2007. Sphingosine-1-phosphate stimulates aldosterone secretion through a mechanism involving the PI3K/PKB and MEK/ERK 1/2 pathways. *J Lipid Res*. 48:2264-74.

Brown, F.D., A.L. Rozelle, H.L. Yin, T. Balla, and J.G. Donaldson. 2001. Phosphatidylinositol 4,5-bisphosphate and Arf6-regulated membrane traffic. *J Cell Biol*. 154:1007-17.

Brown, H.A., S. Gutowski, R.A. Kahn, and P.C. Sternweis. 1995. Partial purification and characterization of Arf-sensitive phospholipase D from porcine brain. *J Biol Chem*. 270:14935-43.

Brown, H.A., S. Gutowski, C.R. Moomaw, C. Slaughter, and P.C. Sternweis. 1993. ADP-ribosylation factor, a small GTP-dependent regulatory protein, stimulates phospholipase D activity. *Cell*. 75:1137-44.

Brubaker, R.R. 2003. Interleukin-10 and inhibition of innate immunity to Yersiniae: roles of Yops and LcrV (V antigen). *Infect Immun*. 71:3673-81.

Carniel, E. 2002. Plasmids and pathogenicity islands of Yersinia. *Curr Top Microbiol Immunol*. 264:89-108.

Carrigan, S.O., D.B. Pink, and A.W. Stadnyk. 2007. Neutrophil transepithelial migration in response to the chemoattractant fMLP but not C5a is phospholipase D-dependent and related to the use of CD11b/CD18. *J Leukoc Biol*. 82:1575-84.

Carter, P.B. 1975. Pathogenecity of Yersinia enterocolitica for mice. *Infect Immun*. 11:164-70.

Carter, P.B., T.T. MacDonald, and F.M. Collins. 1979. Host responses to infection with Yersinia enterocolitica. *Contrib Microbiol Immunol*. 5:346-50.

Chatah, N.E., and C.S. Abrams. 2001. G-protein-coupled receptor activation induces the membrane translocation and activation of phosphatidylinositol-4-phosphate 5-kinase I alpha by a Rac- and Rho-dependent pathway. *J Biol Chem*. 276:34059-65.

Chen, Y., V. Rodrik, and D.A. Foster. 2005. Alternative phospholipase D/mTOR survival signal in human breast cancer cells. *Oncogene*. 24:672-9.

Chen, Y., Y. Zheng, and D.A. Foster. 2003. Phospholipase D confers rapamycin resistance in human breast cancer cells. *Oncogene*. 22:3937-42.

Chen, Y.G., A. Siddhanta, C.D. Austin, S.M. Hammond, T.C. Sung, M.A. Frohman, A.J. Morris, and D. Shields. 1997. Phospholipase D stimulates release of nascent secretory vesicles from the trans-Golgi network. *J Cell Biol*. 138:495-504.

Choi, S.Y., P. Huang, G.M. Jenkins, D.C. Chan, J. Schiller, and M.A. Frohman. 2006a. A common lipid links Mfn-mediated mitochondrial fusion and SNARE-regulated exocytosis. *Nat Cell Biol*. 8:1255-62.

Choi, S.Y., P. Huang, G.M. Jenkins, D.C. Chan, J. Schiller, and M.A. Frohman. 2006b. A common lipid links Mfn-mediated mitochondrial fusion and SNARE-regulated exocytosis. *Nature Cell Biology*. 8:1255-62.

Colley, W.C., T.C. Sung, R. Roll, J. Jenco, S.M. Hammond, Y. Altshuller, D. Bar-Sagi, A.J. Morris, and M.A. Frohman. 1997. Phospholipase D2, a distinct phospholipase D isoform with novel regulatory properties that provokes cytoskeletal reorganization. *Curr Biol*. 7:191-201.

Coppolino, M.G., R. Dierckman, J. Loijens, R.F. Collins, M. Pouladi, J. Jongstra-Bilen, A.D. Schreiber, W.S. Trimble, R. Anderson, and S. Grinstein. 2002. Inhibition of phosphatidylinositol-4-phosphate 5-kinase Ialpha impairs localized actin remodeling and suppresses phagocytosis. *J Biol Chem*. 277:43849-57.

Cossart, P., and P.J. Sansonetti. 2004. Bacterial invasion: the paradigms of enteroinvasive pathogens. *Science*. 304:242-8.

Critchley, D.R. 2005. Genetic, biochemical and structural approaches to talin function. *Biochem Soc Trans*. 33:1308-12.

Cross, M.J., S. Roberts, A.J. Ridley, M.N. Hodgkin, A. Stewart, L. Claesson-Welsh, and M.J.O. Wakelam. 1996. Stimulation of actin stress fibre formation mediated by activation of phospholipase D. *Curr. Biol.* 6:588-597.

Daniel, L.W., M. Waite, and R.L. Wykle. 1986. A novel mechanism of diglyceride formation. 12-O-tetradecanoylphorbol-13-acetate stimulates the cyclic breakdown and resynthesis of phosphatidylcholine. *J Biol Chem*. 261:9128-32.

De Matteis, M., A. Godi, and D. Corda. 2002. Phosphoinositides and the golgi complex. *Curr Opin Cell Biol*. 14:434-47.

Denecker, G., W. Declercq, C.A. Geuijen, A. Boland, R. Benabdillah, M. van Gurp, M.P. Sory, P. Vandenabeele, and G.R. Cornelis. 2001. Yersinia enterocolitica YopP-induced apoptosis of macrophages involves the apoptotic signaling cascade upstream of bid. *J Biol Chem*. 276:19706-14.

Denecker, G., S. Totemeyer, L.J. Mota, P. Troisfontaines, I. Lambermont, C. Youta, I. Stainier, M. Ackermann, and G.R. Cornelis. 2002. Effect of low- and high-

virulence Yersinia enterocolitica strains on the inflammatory response of human umbilical vein endothelial cells. *Infect Immun*. 70:3510-20.

Di Paolo, G., and P. De Camilli. 2006. Phosphoinositides in cell regulation and membrane dynamics. *Nature*. 443:651-7.

Di Paolo, G., H.S. Moskowitz, K. Gipson, M.R. Wenk, S. Voronov, M. Obayashi, R. Flavell, R.M. Fitzsimond, T.A. Ryan, and P. De Camilli. 2004. Impaired PtdIns(4,5)P2 synthesis in nerve terminals produces defects in synaptic vesicle trafficking. *Nature*. 431:415 - 422.

Di Paolo, G., L. Pellegrini, K. Letinic, G. Cestra, R. Zoncu, S. Voronov, S. Chang, J. Guo, M.R. Wenk, and P. De Camilli. 2002. Recruitment and regulation of phosphatidylinositol phosphate kinase type 1 gamma by the FERM domain of talin. *Nature*. 420:85-9.

Doughman, R.L., A.J. Firestone, and R.A. Anderson. 2003a. Phosphatidylinositol phosphate kinases put PI4,5P(2) in its place. *J Membr Biol*. 194:77-89.

Doughman, R.L., A.J. Firestone, M.L. Wojtasiak, M.W. Bunce, and R.A. Anderson. 2003b. Membrane ruffling requires coordination between type Ialpha phosphatidylinositol phosphate kinase and Rac signaling. *J Biol Chem*. 278:23036-45.

Downes, C.P., A. Gray, and J.M. Lucocq. 2005. Probing phosphoinositide functions in signaling and membrane trafficking. *Trends Cell Biol*. 15:259-68.

Du, G., Y.M. Altshuller, N. Vitale, P. Huang, S. Chasserot-Golaz, A.J. Morris, M.F. Bader, and M.A. Frohman. 2003. Regulation of phospholipase D1 subcellular cycling through coordination of multiple membrane association motifs. *J Cell Biol*. 162:305-15.

Du, G., and M.A. Frohman. 2008. A lipid-signaled myosin phosphatase surge disperses cortical contractile force early in cell spreading. *Mol. Biol. Cell*. in press.

Du, G., P. Huang, B.T. Liang, and M.A. Frohman. 2004. Phospholipase D2 localizes to the plasma membrane and regulates angiotensin II receptor endocytosis. *Mol Biol Cell*. 15:1024-30.

Egea, G., F. Lazaro-Dieguez, and M. Vilella. 2006. Actin dynamics at the Golgi complex in mammalian cells. *Curr Opin Cell Biol*. 18:168-78.

El-Maraghi, N.R., and N.S. Mair. 1979. The histopathology of enteric infection with Yersinia pseudotuberculosis. *Am J Clin Pathol*. 71:631-9.

Emoto, M., J. Klarlund, S. Waters, V. Hu, J. Buxton, A. Chawla, and M. Czech. 2000. A role for phospholipase D in GLUT4 glucose transporter translocation. *J Biol Chem*. 275:7144-51.

Erfurth, S.E., S. Grobner, U. Kramer, D.S. Gunst, I. Soldanova, M. Schaller, I.B. Autenrieth, and S. Borgmann. 2004. Yersinia enterocolitica induces apoptosis and inhibits surface molecule expression and cytokine production in murine dendritic cells. *Infect Immun*. 72:7045-54.

Falgarone, G., H.S. Blanchard, B. Riot, M. Simonet, and M. Breban. 1999. Cytotoxic T-cell-mediated response against Yersinia pseudotuberculosis in HLA-B27 transgenic rat. *Infect Immun*. 67:3773-9.

Fallman, M., K. Andersson, S. Hakansson, K.E. Magnusson, O. Stendahl, and H. Wolf-Watz. 1995. Yersinia pseudotuberculosis inhibits Fc receptor-mediated phagocytosis in J774 cells. *Infect Immun*. 63:3117-24.

Fantozzi, A., and G. Christofori. 2006. Mouse models of breast cancer metastasis. *Breast Cancer Res*. 8:212.

Frohman, M.A., T.C. Sung, and A.J. Morris. 1999. Mammalian phospholipase D structure and regulation. *Biochim Biophys Acta*. 1439:175-86.

Galyov, E.E., S. Hakansson, and H. Wolf-Watz. 1994. Characterization of the operon encoding the YpkA Ser/Thr protein kinase and the YopJ protein of Yersinia pseudotuberculosis. *J Bacteriol*. 176:4543-8.

Garcia, A., Y. Zheng, C. Zhao, A. Toschi, J. Fan, N. Shraibman, H.A. Brown, D. Bar-Sagi, D.A. Foster, and J.L. Arbiser. 2008. Honokiol suppresses survival signals mediated by Ras-dependent phospholipase D activity in human cancer cells. *Clin Cancer Res*. 14:4267-74.

Giudici, M.L., P.C. Emson, and R.F. Irvine. 2004. A novel neuronal-specific splice variant of Type I phosphatidylinositol 4-phosphate 5-kinase isoform gamma. *Biochem J*. 379:489-96.

Godi, A., P. Pertile, R. Meyers, P. Marra, G. Di Tullio, C. Iurisci, A. Luini, D. Corda, and M.A. De Matteis. 1999. ARF mediates recruitment of PtdIns-4-OH kinase-beta and stimulates synthesis of PtdIns(4,5)P2 on the Golgi complex. *Nat Cell Biol*. 1:280-7.

Godi, A., I. Santone, P. Pertile, P. Devarajan, P.R. Stabach, J.S. Morrow, G. Di Tullio, R. Polishchuk, T.C. Petrucci, A. Luini, and M.A. De Matteis. 1998. ADP ribosylation factor regulates spectrin binding to the Golgi complex. *Proc Natl Acad Sci U S A*. 95:8607-12.

Golub, T., and P. Caroni. 2005. PI(4,5)P2-dependent microdomain assemblies capture microtubules to promote and control leading edge motility. *J Cell Biol*. 169:151-65.

Gong, L.W., G. Di Paolo, E. Diaz, G. Cestra, M.E. Diaz, M. Lindau, P. De Camilli, and D. Toomre. 2005. Phosphatidylinositol phosphate kinase type I gamma regulates dynamics of large dense-core vesicle fusion. *Proc Natl Acad Sci U S A*. 102:5204-9.

Gupta, G.P., and J. Massague. 2006. Cancer metastasis: building a framework. *Cell*. 127:679-95.

Halstead, J.R., J. van Rheenen, M.H. Snel, S. Meeuws, S. Mohammed, C.S. D'Santos, A.J. Heck, K. Jalink, and N. Divecha. 2006. A role for PtdIns(4,5)P2 and PIP5Kalpha in regulating stress-induced apoptosis. *Curr Biol*. 16:1850-6.

Hamid, N., A. Gustavsson, K. Andersson, K. McGee, C. Persson, C.E. Rudd, and M. Fallman. 1999. YopH dephosphorylates Cas and Fyn-binding protein in macrophages. *Microb Pathog*. 27:231-42.

Hammond, S.M., Y.M. Altshuller, T.C. Sung, S.A. Rudge, K. Rose, J. Engebrecht, A.J. Morris, and M.A. Frohman. 1995. Human ADP-ribosylation factor-activated phosphatidylcholine-specific phospholipase D defines a new and highly conserved gene family. *J Biol Chem*. 270:29640-3.

Hammond, S.M., J.M. Jenco, S. Nakashima, K. Cadwallader, Q. Gu, S. Cook, Y. Nozawa, G.D. Prestwich, M.A. Frohman, and A.J. Morris. 1997. Characterization of two alternately spliced forms of phospholipase D1. Activation of the purified enzymes by phosphatidylinositol 4,5-bisphosphate, ADP-ribosylation factor, and

Rho family monomeric GTP-binding proteins and protein kinase C-alpha. *J Biol Chem*. 272:3860-8.

Haucke, V., and G. Di Paolo. 2007. Lipids and lipid modifications in the regulation of membrane traffic. *Current Opinion in Cell Biology*. 19:426-435.

Heesemann, J., A. Sing, and K. Trulzsch. 2006. Yersinia's stratagem: targeting innate and adaptive immune defense. *Curr Opin Microbiol*. 9:55-61.

Hilgemann, D.W., and R. Ball. 1996. Regulation of cardiac Na+,Ca2+ exchange and KATP potassium channels by PIP2. *Science*. 273:956-9.

Honda, A., M. Nogami, T. Yokozeki, M. Yamazaki, H. Nakamura, H. Watanabe, K. Kawamoto, K. Nakayama, A.J. Morris, M.A. Frohman, and Y. Kanaho. 1999. Phosphatidylinositol 4-phosphate 5-kinase alpha is a downstream effector of the small G protein ARF6 in membrane ruffle formation. *Cell*. 99:521-32.

Huang, P., Y.M. Altshuller, J. Chunqiu Hou, J.E. Pessin, and M.A. Frohman. 2005. Insulin-stimulated Plasma Membrane Fusion of Glut4 Glucose Transporter-containing Vesicles Is Regulated by Phospholipase D1. *Mol Biol Cell*. 16:2614-23.

Huang, P., and M.A. Frohman. 2007. The potential for phospholipase D as a new therapeutic target. *Expert Opin Ther Targets*. 11:707-16.

Huang, Y., I.A. Qureshi, and H. Chen. 1999. Effects of phosphatidylinositol 4,5-bisphosphate and neomycin on phospholipase D: kinetic studies. *Mol Cell Biochem*. 197:195-201.

Igwe, E.I., H. Russmann, A. Roggenkamp, A. Noll, I.B. Autenrieth, and J. Heesemann. 1999. Rational live oral carrier vaccine design by mutating virulence-associated genes of Yersinia enterocolitica. *Infect Immun*. 67:5500-7.

Insall, R.H., and O.D. Weiner. 2001. PIP3, PIP2, and cell movement--similar messages, different meanings? *Dev Cell*. 1:743-7.

Interthal, H., J.J. Pouliot, and J.J. Champoux. 2001. The tyrosyl-DNA phosphodiesterase Tdp1 is a member of the phospholipase D superfamily. *Proc Natl Acad Sci U S A*. 98:12009-14.

Jenkins, G.M., and M.A. Frohman. 2005. Phospholipase D: a lipid centric review. *Cell Mol Life Sci*. 62:2305-16.

Jones, D.H., J.B. Morris, C.P. Morgan, H. Kondo, R.F. Irvine, and S. Cockcroft. 2000. Type I phosphatidylinositol 4-phosphate 5-kinase directly interacts with ADP-ribosylation factor 1 and is responsible for phosphatidylinositol 4,5-bisphosphate synthesis in the golgi compartment. *J Biol Chem*. 275:13962-6.

Kagan, J.C., and R. Medzhitov. 2006. Phosphoinositide-mediated adaptor recruitment controls Toll-like receptor signaling. *Cell*. 125:943-55.

Kam, Y., and J.H. Exton. 2001. Phospholipase D activity is required for actin stress fiber formation in fibroblasts. *Mol Cell Biol*. 21:4055-66.

Kang, D.W., M.H. Park, Y.J. Lee, H.S. Kim, T.K. Kwon, W.S. Park, and S. Min do. 2008. Phorbol ester up-regulates phospholipase D1 but not phospholipase D2 expression through a PKC/Ras/ERK/NFkappaB-dependent pathway and enhances matrix metalloproteinase-9 secretion in colon cancer cells. *J Biol Chem*. 283:4094-104.

Kerschen, E.J., D.A. Cohen, A.M. Kaplan, and S.C. Straley. 2004. The plague virulence protein YopM targets the innate immune response by causing a global depletion of NK cells. *Infect Immun*. 72:4589-602.

Koonin, E.V. 1996. A duplicated catalytic motif in a new superfamily of phosphohydrolases and phospholipid synthases that includes poxvirus envelope proteins. *Trends Biochem Sci*. 21:242-3.

Kozlov, M.M. 2001. Fission of biological membranes: interplay between dynamin and lipids. *Traffic*. 2:51-65.

Kunisaki, Y., A. Nishikimi, Y. Tanaka, R. Takii, M. Noda, A. Inayoshi, K. Watanabe, F. Sanematsu, T. Sasazuki, T. Sasaki, and Y. Fukui. 2006. DOCK2 is a Rac activator that regulates motility and polarity during neutrophil chemotaxis. *J Cell Biol*. 174:647-52.

Lee, C.S., I.S. Kim, J.B. Park, M.N. Lee, H.Y. Lee, P.G. Suh, and S.H. Ryu. 2006. The phox homology domain of phospholipase D activates dynamin GTPase activity and accelerates EGFR endocytosis. *Nat Cell Biol*. 8:477-84.

Lee, S., J.B. Park, J.H. Kim, Y. Kim, J.H. Kim, K.J. Shin, J.S. Lee, S.H. Ha, P.G. Suh, and S.H. Ryu. 2001. Actin directly interacts with phospholipase D, inhibiting its activity. *J Biol Chem*. 276:28252-60.

Lehman, N., M. Di Fulvio, N. McCray, I. Campos, F. Tabatabaian, and J. Gomez-Cambronero. 2006. Phagocyte cell migration is mediated by phospholipases PLD1 and PLD2. *Blood*. 108:3564-72.

Lian, C.J., W.S. Hwang, and C.H. Pai. 1987. Plasmid-mediated resistance to phagocytosis in Yersinia enterocolitica. *Infect Immun*. 55:1176-83.

Ling, K., R.L. Doughman, A.J. Firestone, M.W. Bunce, and R.A. Anderson. 2002. Type I gamma phosphatidylinositol phosphate kinase targets and regulates focal adhesions. *Nature*. 420:89-93.

Liscovitch, M., A. Freese, J.K. Blusztajn, and R.J. Wurtman. 1985. High-performance liquid chromatography of water-soluble choline metabolites. *Anal Biochem*. 151:182-7.

Logsdon, L.K., and J. Mecsas. 2003. Requirement of the Yersinia pseudotuberculosis effectors YopH and YopE in colonization and persistence in intestinal and lymph tissues. *Infect Immun*. 71:4595-607.

Lorra, C., and W.B. Huttner. 1999. The mesh hypothesis of Golgi dynamics. *Nat Cell Biol*. 1:E113-5.

Lutz, M.B., N. Kukutsch, A.L. Ogilvie, S. Rossner, F. Koch, N. Romani, and G. Schuler. 1999. An advanced culture method for generating large quantities of highly pure dendritic cells from mouse bone marrow. *J Immunol Methods*. 223:77-92.

McDermott, M., M.J. Wakelam, and A.J. Morris. 2004. Phospholipase D. *Biochem Cell Biol*. 82:225-53.

McNeil, P.L., R.F. Murphy, F. Lanni, and D.L. Taylor. 1984. A method for incorporating macromolecules into adherent cells. *J Cell Biol*. 98:1556-64.

Mejillano, M., M. Yamamoto, A.L. Rozelle, H.Q. Sun, X. Wang, and H.L. Yin. 2001. Regulation of apoptosis by phosphatidylinositol 4,5-bisphosphate inhibition of caspases, and caspase inactivation of phosphatidylinositol phosphate 5-kinases. *J Biol Chem*. 276:1865-72.

Mills, S.D., A. Boland, M.P. Sory, P. van der Smissen, C. Kerbourch, B.B. Finlay, and G.R. Cornelis. 1997. Yersinia enterocolitica induces apoptosis in macrophages by a process requiring functional type III secretion and translocation mechanisms and involving YopP, presumably acting as an effector protein. *Proc Natl Acad Sci U S A*. 94:12638-43.

Minn, A.J., G.P. Gupta, P.M. Siegel, P.D. Bos, W. Shu, D.D. Giri, A. Viale, A.B. Olshen, W.L. Gerald, and J. Massague. 2005. Genes that mediate breast cancer metastasis to lung. *Nature*. 436:518-24.

Monack, D.M., J. Mecsas, D. Bouley, and S. Falkow. 1998. Yersinia-induced apoptosis in vivo aids in the establishment of a systemic infection of mice. *J Exp Med*. 188:2127-37.

Monovich, L., B. Mugrage, E. Quadros, K. Toscano, R. Tommasi, S. LaVoie, E. Liu, Z. Du, D. LaSala, W. Boyar, and P. Steed. 2007. Optimization of halopemide for phospholipase D2 inhibition. *Bioorg Med Chem Lett*. 17:2310-11.

Mor, A., G. Campi, G. Du, Y. Zheng, D.A. Foster, M.L. Dustin, and M.R. Philips. 2007. The lymphocyte function-associated antigen-1 receptor costimulates plasma membrane Ras via phospholipase D2. *Nat Cell Biol*. 9:712-719.

Morris, A.J. 2007. Regulation of phospholipase D activity, membrane targeting and intracellular trafficking by phosphoinositides. *Biochem Soc Symp*:247-57.

Morris, A.J., M.A. Frohman, and J. Engebrecht. 1997. Measurement of phospholipase D activity. *Anal Biochem*. 252:1-9.

Morris, A.J., and S.S. Smyth. 2007. Measurement of autotaxin/lysophospholipase D activity. *Methods Enzymol*. 434:89-104.

Naktin, J., and K.G. Beavis. 1999. Yersinia enterocolitica and Yersinia pseudotuberculosis. *Clin Lab Med*. 19:523-36, vi.

Niggli, V. 2005. Regulation of protein activities by phosphoinositide phosphates. *Annu Rev Cell Dev Biol*. 21:57-79.

Nishikimi, A., H. Fukuhara, W. Su, T. Hongu, S. Takasuga, H. Mihara, Q. Cao, F. Sanematsu, M. Kanai, H. Hasegawa, Y. Tanaka, M. Shibasaki, Y. Kanaho, T. Sasaki, M.A. Frohman, and Y. Fukui. 2009. Sequential Regulation of DOCK2 Dynamics by Two Phospholipids during Neutrophil Chemotaxis. *Science*.

Orth, K., L.E. Palmer, Z.Q. Bao, S. Stewart, A.E. Rudolph, J.B. Bliska, and J.E. Dixon. 1999. Inhibition of the mitogen-activated protein kinase kinase superfamily by a Yersinia effector. *Science*. 285:1920-3.

Oude Weernink, P.A., L. Han, K.H. Jakobs, and M. Schmidt. 2007. Dynamic phospholipid signaling by G protein-coupled receptors. *Biochim Biophys Acta*. 1768:888-900.

Padron, D., Y.J. Wang, M. Yamamoto, H. Yin, and M.G. Roth. 2003. Phosphatidylinositol phosphate 5-kinase Ibeta recruits AP-2 to the plasma membrane and regulates rates of constitutive endocytosis. *J Cell Biol*. 162:693-701.

Pai, J.K., M.I. Siegel, R.W. Egan, and M.M. Billah. 1988. Activation of phospholipase D by chemotactic peptide in HL-60 granulocytes. *Biochem Biophys Res Commun*. 150:355-64.

Palmer, L.E., S. Hobbie, J.E. Galan, and J.B. Bliska. 1998. YopJ of Yersinia pseudotuberculosis is required for the inhibition of macrophage TNF-alpha

production and downregulation of the MAP kinases p38 and JNK. *Mol Microbiol*. 27:953-65.

Pannequin, J., N. Delaunay, C. Darido, T. Maurice, P. Crespy, M.A. Frohman, M.S. Balda, K. Matter, D. Joubert, J.F. Bourgaux, J.P. Bali, and F. Hollande. 2007. Phosphatidylethanol accumulation promotes intestinal hyperplasia by inducing ZONAB-mediated cell density increase in response to chronic ethanol exposure. *Mol Cancer Res*. 5:1147-57.

Parent, M.A., L.B. Wilhelm, L.W. Kummer, F.M. Szaba, I.K. Mullarky, and S.T. Smiley. 2006. Gamma interferon, tumor necrosis factor alpha, and nitric oxide synthase 2, key elements of cellular immunity, perform critical protective functions during humoral defense against lethal pulmonary Yersinia pestis infection. *Infect Immun*. 74:3381-6.

Persson, C., N. Carballeira, H. Wolf-Watz, and M. Fallman. 1997. The PTPase YopH inhibits uptake of Yersinia, tyrosine phosphorylation of p130Cas and FAK, and the associated accumulation of these proteins in peripheral focal adhesions. *EMBO J*. 16:2307-18.

Persson, C., R. Nordfelth, K. Andersson, A. Forsberg, H. Wolf-Watz, and M. Fallman. 1999. Localization of the Yersinia PTPase to focal complexes is an important virulence mechanism. *Mol Microbiol*. 33:828-38.

Pizarro-Cerda, J., and P. Cossart. 2004. Subversion of phosphoinositide metabolism by intracellular bacterial pathogens. *Nat Cell Biol*. 6:1026-33.

Ponting, C.P., and I.D. Kerr. 1996. A novel family of phospholipase D homologues that includes phospholipid synthases and putative endonucleases: identification of duplicated repeats and potential active site residues. *Protein Sci*. 5:914-22.

Preininger, A.M., L.G. Henage, W.M. Oldham, E.J. Yoon, H.E. Hamm, and H.A. Brown. 2006. Direct modulation of phospholipase D activity by Gbetagamma. *Mol Pharmacol*. 70:311-8.

Pujol, C., and J.B. Bliska. 2003. The ability to replicate in macrophages is conserved between Yersinia pestis and Yersinia pseudotuberculosis. *Infect Immun*. 71:5892-9.

Ramaswamy, V., V.M. Cresence, J.S. Rejitha, M.U. Lekshmi, K.S. Dharsana, S.P. Prasad, and H.M. Vijila. 2007. Listeria--review of epidemiology and pathogenesis. *J Microbiol Immunol Infect*. 40:4-13.

Rickert, P., O.D. Weiner, F. Wang, H.R. Bourne, and G. Servant. 2000. Leukocytes navigate by compass: roles of PI3Kgamma and its lipid products. *Trends Cell Biol*. 10:466-73.

Ridley, A.J., M.A. Schwartz, K. Burridge, R.A. Firtel, M.H. Ginsberg, G. Borisy, J.T. Parsons, and A.R. Horwitz. 2003. Cell migration: integrating signals from front to back. *Science*. 302:1704-9.

Riedl, J., A.H. Crevenna, K. Kessenbrock, J.H. Yu, D. Neukirchen, M. Bista, F. Bradke, D. Jenne, T.A. Holak, Z. Werb, M. Sixt, and R. Wedlich-Soldner. 2008. Lifeact: a versatile marker to visualize F-actin. *Nat Methods*. 5:605-7.

Rose, K., S.A. Rudge, M.A. Frohman, A.J. Morris, and J. Engebrecht. 1995. Phospholipase D signaling is essential for meiosis. *Proc Natl Acad Sci U S A*. 92:12151-5.

Rosqvist, R., A. Forsberg, M. Rimpilainen, T. Bergman, and H. Wolf-Watz. 1990. The cytotoxic protein YopE of Yersinia obstructs the primary host defence. *Mol Microbiol*. 4:657-67.

Rosqvist, R., A. Forsberg, and H. Wolf-Watz. 1991. Intracellular targeting of the Yersinia YopE cytotoxin in mammalian cells induces actin microfilament disruption. *Infect Immun*. 59:4562-9.

Roth, M.G. 2004. Phosphoinositides in constitutive membrane traffic. *Physiol Rev*. 84:699-730.

Rozelle, A.L., L.M. Machesky, M. Yamamoto, M.H. Driessens, R.H. Insall, M.G. Roth, K. Luby-Phelps, G. Marriott, A. Hall, and H.L. Yin. 2000. Phosphatidylinositol 4,5-bisphosphate induces actin-based movement of raft-enriched vesicles through WASP-Arp2/3. *Curr Biol*. 10:311-20.

Russmann, H., U. Gerdemann, E.I. Igwe, K. Panthel, J. Heesemann, S. Garbom, H. Wolf-Watz, and G. Geginat. 2003. Attenuated Yersinia pseudotuberculosis carrier vaccine for simultaneous antigen-specific CD4 and CD8 T-cell induction. *Infect Immun*. 71:3463-72.

Santarius, M., C.H. Lee, and R.A. Anderson. 2006. Supervised membrane swimming: small G-protein lifeguards regulate PIPK signalling and monitor intracellular PtdIns(4,5)P2 pools. *Biochem J*. 398:1-13.

Sasaki, J., T. Sasaki, M. Yamazaki, K. Matsuoka, C. Taya, H. Shitara, S. Takasuga, M. Nishio, K. Mizuno, T. Wada, H. Miyazaki, H. Watanabe, R. Iizuka, S. Kubo, S. Murata, T. Chiba, T. Maehama, K. Hamada, H. Kishimoto, M.A. Frohman, K. Tanaka, J.M. Penninger, H. Yonekawa, A. Suzuki, and Y. Kanaho. 2005. Regulation of anaphylactic responses by phosphatidylinositol phosphate kinase type I {alpha}. *J Exp Med*. 201:859-70.

Schesser, K., A.K. Spiik, J.M. Dukuzumuremyi, M.F. Neurath, S. Pettersson, and H. Wolf-Watz. 1998. The yopJ locus is required for Yersinia-mediated inhibition of NF-kappaB activation and cytokine expression: YopJ contains a eukaryotic SH2-like domain that is essential for its repressive activity. *Mol Microbiol*. 28:1067-79.

Schmidt, A., and A. Hall. 2002. Guanine nucleotide exchange factors for Rho GTPases: turning on the switch. *Genes Dev*. 16:1587-609.

Schotte, P., G. Denecker, A. Van Den Broeke, P. Vandenabeele, G.R. Cornelis, and R. Beyaert. 2004. Targeting Rac1 by the Yersinia effector protein YopE inhibits caspase-1-mediated maturation and release of interleukin-1beta. *J Biol Chem*. 279:25134-42.

Sciorra, V.A., and A.J. Morris. 1999. Sequential actions of phospholipase D and phosphatidic acid phosphohydrolase 2b generate diglyceride in mammalian cells. *Mol Biol Cell*. 10:3863-76.

Scott, C.C., W. Dobson, R.J. Botelho, N. Coady-Osberg, P. Chavrier, D.A. Knecht, C. Heath, P. Stahl, and S. Grinstein. 2005. Phosphatidylinositol-4,5-bisphosphate hydrolysis directs actin remodeling during phagocytosis. *J Cell Biol*. 169:139-49.

Shao, F., P.M. Merritt, Z. Bao, R.W. Innes, and J.E. Dixon. 2002. A Yersinia effector and a Pseudomonas avirulence protein define a family of cysteine proteases functioning in bacterial pathogenesis. *Cell*. 109:575-88.

Siddhanta, A., J.M. Backer, and D. Shields. 2000. Inhibition of phosphatidic acid synthesis alters the structure of the Golgi apparatus and inhibits secretion in endocrine cells. *J Biol Chem*. 275:12023-31.

Simonet, M., and S. Falkow. 1992. Invasin expression in Yersinia pseudotuberculosis. *Infect Immun*. 60:4414-7.

Skippen, A., D.H. Jones, C.P. Morgan, M. Li, and S. Cockcroft. 2002a. Mechanism of ADP ribosylation factor-stimulated phosphatidylinositol 4,5-bisphosphate synthesis in HL60 cells. *J Biol Chem*. 277:5823-31.

Skippen, A., D.H. Jones, C.P. Morgan, M. Li, and S. Cockcroft. 2002b. Mechanism of ADP ribosylation factor-stimulated phosphatidylinositol 4,5-bisphosphate synthesis in HL60 cells. *J Biol Chem*. 277:5823-31.

Srinivasan, S., F. Wang, S. Glavas, A. Ott, F. Hofmann, K. Aktories, D. Kalman, and H.R. Bourne. 2003. Rac and Cdc42 play distinct roles in regulating PI(3,4,5)P3 and polarity during neutrophil chemotaxis. *J Cell Biol*. 160:375-85.

Stace, C.L., and N.T. Ktistakis. 2006. Phosphatidic acid- and phosphatidylserine-binding proteins. *Biochim Biophys Acta*. 1761:913-26.

Stephens, L.R., K.T. Hughes, and R.F. Irvine. 1991. Pathway of phosphatidylinositol(3,4,5)-trisphosphate synthesis in activated neutrophils. *Nature*. 351:33-9.

Su, W., P. Chardin, M. Yamazaki, Y. Kanaho, and G. Du. 2006. RhoA-mediated Phospholipase D1 signaling is not required for the formation of stress fibers and focal adhesions. *Cell Signal*. 18:469-78.

Suh, B.C., and B. Hille. 2005. Regulation of ion channels by phosphatidylinositol 4,5-bisphosphate. *Curr Opin Neurobiol*. 15:370-8.

Sung, T.C., Y.M. Altshuller, A.J. Morris, and M.A. Frohman. 1999a. Molecular analysis of mammalian phospholipase D2. *J Biol Chem*. 274:494-502.

Sung, T.C., R.L. Roper, Y. Zhang, S.A. Rudge, R. Temel, S.M. Hammond, A.J. Morris, B. Moss, J. Engebrecht, and M.A. Frohman. 1997a. Mutagenesis of phospholipase D defines a superfamily including a trans- Golgi viral protein required for poxvirus pathogenicity. *EMBO J*. 16:4519-30.

Sung, T.C., R.L. Roper, Y. Zhang, S.A. Rudge, R. Temel, S.M. Hammond, A.J. Morris, B. Moss, J. Engebrecht, and M.A. Frohman. 1997b. Mutagenesis of phospholipase D defines a superfamily including a trans-Golgi viral protein required for poxvirus pathogenicity. *EMBO J*. 16:4519-30.

Sung, T.C., Y. Zhang, A.J. Morris, and M.A. Frohman. 1999b. Structural analysis of human phospholipase D1. *J Biol Chem*. 274:3659-66.

Suzuki, T., Y. Kanai, T. Hara, J. Sasaki, T. Sasaki, M. Kohara, T. Maehama, C. Taya, H. Shitara, H. Yonekawa, M.A. Frohman, T. Yokozeki, and Y. Kanaho. 2006. Crucial role of the small GTPase ARF6 in hepatic cord formation during liver development. *Mol Cell Biol*. 26:6149-56.

Sweeney, D.A., A. Siddhanta, and D. Shields. 2002. Fragmentation and re-assembly of the Golgi apparatus in vitro. A requirement for phosphatidic acid and phosphatidylinositol 4,5-bisphosphate synthesis. *J Biol Chem*. 277:3030-9.

Toker, A., and L.C. Cantley. 1997. Signalling through the lipid products of phosphoinositide-3-OH kinase. *Nature*. 387:673-6.

Varadharaj, S., E. Steinhour, M.G. Hunter, T. Watkins, C.P. Baran, U. Magalang, P. Kuppusamy, J.L. Zweier, C.B. Marsh, V. Natarajan, and N.L. Parinandi. 2006. Vitamin C-induced activation of phospholipase D in lung microvascular endothelial cells: regulation by MAP kinases. *Cell Signal*. 18:1396-407.

Viboud, G.I., and J.B. Bliska. 2005. Yersinia outer proteins: role in modulation of host cell signaling responses and pathogenesis. *Annu Rev Microbiol*. 59:69-89.

Viboud, G.I., E. Mejia, and J.B. Bliska. 2006. Comparison of YopE and YopT activities in counteracting host signalling responses to Yersinia pseudotuberculosis infection. *Cell Microbiol*. 8:1504-15.

Vitale, N., A.S. Caumont, S. Chasserot-Golaz, G. Du, S. Wu, V.A. Sciorra, A.J. Morris, M.A. Frohman, and M.F. Bader. 2001. Phospholipase D1: a key factor for the exocytotic machinery in neuroendocrine cells. *Embo J*. 20:2424-34.

Vogel, U., I.B. Autenrieth, R. Berner, and J. Heesemann. 1993. Role of plasmid-encoded antigens of Yersinia enterocolitica in humoral immunity against secondary Y. enterocolitica infection in mice. *Microb Pathog*. 15:23-36.

Wang, Y., X. Chen, L. Lian, T. Tang, T.J. Stalker, T. Sasaki, Y. Kanaho, L.F. Brass, J.K. Choi, J.H. Hartwig, and C.S. Abrams. 2008. Loss of PIP5KIbeta demonstrates that PIP5KI isoform-specific PIP2 synthesis is required for IP3 formation. *Proc Natl Acad Sci U S A*. 105:14064-9.

Waselle, L., R.R. Gerona, N. Vitale, T.F. Martin, M.F. Bader, and R. Regazzi. 2005. Role of phosphoinositide signaling in the control of insulin exocytosis. *Mol Endocrinol*. 19:3097-106.

Watt, S.A., G. Kular, I.N. Fleming, C.P. Downes, and J.M. Lucocq. 2002. Subcellular localization of phosphatidylinositol 4,5-bisphosphate using the pleckstrin homology domain of phospholipase C delta1. *Biochem J*. 363:657-66.

Williger, B.T., W.T. Ho, and J.H. Exton. 1999. Phospholipase D mediates matrix metalloproteinase-9 secretion in phorbol ester-stimulated human fibrosarcoma cells. *J Biol Chem*. 274:735-8.

Wong, K.W., and R.R. Isberg. 2003. Arf6 and phosphoinositol-4-phosphate-5-kinase activities permit bypass of the Rac1 requirement for beta1 integrin-mediated bacterial uptake. *J Exp Med*. 198:603-14.

Wong, K.W., and R.R. Isberg. 2005a. Emerging views on integrin signaling via Rac1 during invasin-promoted bacterial uptake. *Curr Opin Microbiol*. 8:4-9.

Wong, K.W., and R.R. Isberg. 2005b. Yersinia pseudotuberculosis spatially controls activation and misregulation of host cell Rac1. *PLoS Pathog*. 1:e16.

Wood, L.D., D.W. Parsons, S. Jones, J. Lin, T. Sjoblom, R.J. Leary, D. Shen, S.M. Boca, T. Barber, J. Ptak, N. Silliman, S. Szabo, Z. Dezso, V. Ustyanksky, T. Nikolskaya, Y. Nikolsky, R. Karchin, P.A. Wilson, J.S. Kaminker, Z. Zhang, R. Croshaw, J. Willis, D. Dawson, M. Shipitsin, J.K. Willson, S. Sukumar, K. Polyak, B.H. Park, C.L. Pethiyagoda, P.V. Pant, D.G. Ballinger, A.B. Sparks, J. Hartigan, D.R. Smith, E. Suh, N. Papadopoulos, P. Buckhaults, S.D. Markowitz, G. Parmigiani, K.W. Kinzler, V.E. Velculescu, and B. Vogelstein. 2007. The genomic landscapes of human breast and colorectal cancers. *Science*. 318:1108-13.

Xu, Y., L.F. Seet, B. Hanson, and W. Hong. 2001. The Phox homology (PX) domain, a new player in phosphoinositide signalling. *Biochem J*. 360:513-30.

Yang, J.-S., H. Gad, S. Lee, A. Mironov, L. Zhang, G.V. Beznoussenko, C. Valente, G. Turacchio, A.N. Bonsra, G. Du, G. Baldanzi, A. Graziani, S. Bourgoin, M.A. Frohman, A. Luini, and V.W. Hsu. 2008. COPI vesicle fission: a role for phosphatidic acid and insight into Golgi maintenance. *Nature Cell Biology*. 10:1146-53.

Yang, S.A., C.L. Carpenter, and C.S. Abrams. 2004. Rho and Rho-kinase mediate thrombin-induced phosphatidylinositol 4-phosphate 5-kinase trafficking in platelets. *J Biol Chem*. 279:42331-6.

Yao, T., J. Mecsas, J.I. Healy, S. Falkow, and Y. Chien. 1999. Suppression of T and B lymphocyte activation by a Yersinia pseudotuberculosis virulence factor, yopH. *J Exp Med*. 190:1343-50.

Zeniou-Meyer, M., N. Zabari, U. Ashery, S. Chasserot-Golaz, A.M. Haeberle, V. Demais, Y. Bailly, I. Gottfried, H. Nakanishi, A.M. Neiman, G. Du, M.A. Frohman, M.F. Bader, and N. Vitale. 2007. Phospholipase D1 production of phosphatidic acid at the plasma membrane promotes exocytosis of large dense-core granules at a late stage. *J Biol Chem*. 282:21746-57.

Zhang, Y., J. Murtha, M.A. Roberts, R.M. Siegel, and J.B. Bliska. 2008. Type III secretion decreases bacterial and host survival following phagocytosis of Yersinia pseudotuberculosis by macrophages. *Infect Immun*. 76:4299-310.

Zhang, Y., A.T. Ting, K.B. Marcu, and J.B. Bliska. 2005. Inhibition of MAPK and NF-kappa B pathways is necessary for rapid apoptosis in macrophages infected with Yersinia. *J Immunol*. 174:7939-49.

Zhang, Z.Y., J.C. Clemens, H.L. Schubert, J.A. Stuckey, M.W. Fischer, D.M. Hume, M.A. Saper, and J.E. Dixon. 1992. Expression, purification, and physicochemical characterization of a recombinant Yersinia protein tyrosine phosphatase. *J Biol Chem*. 267:23759-66.

Zhao, C., G. Du, K. Skowronek, M.A. Frohman, and D. Bar-Sagi. 2007. Phospholipase D2-generated phosphatidic acid couples EGFR stimulation to Ras activation by Sos. *Nat Cell Biol*. 9:707-712.

Zhao, Y., J.A. Stuckey, D.L. Lohse, and J.E. Dixon. 1997. Expression, characterization, and crystallization of a member of the novel phospholipase D family of phosphodiesterases. *Protein Sci*. 6:2655-8.

Zheng, Y., V. Rodrik, A. Toschi, M. Shi, L. Hui, Y. Shen, and D.A. Foster. 2006. Phospholipase D couples survival and migration signals in stress response of human cancer cells. *J Biol Chem*. 281:15862-8.

Zumbihl, R., M. Aepfelbacher, A. Andor, C.A. Jacobi, K. Ruckdeschel, B. Rouot, and J. Heesemann. 1999. The cytotoxin YopT of Yersinia enterocolitica induces modification and cellular redistribution of the small GTP-binding protein RhoA. *J Biol Chem*. 274:29289-93.